Synthesis, *in vitro* Cytotoxicity and Trypanocidal Evaluation of Novel 1,3,6-Substituted Non-fluoroquinolones

Richard M. Beteck[a,*§], Michelle Isaacs[c], Heinrich C. Hoppe[b,c] and Setshaba D. Khanye[a,c,d,*]

[a]*Department of Chemistry, Rhodes University, Grahamstown, 6140, South Africa.*

[b]*Department of Biochemistry and Microbiology, Rhodes University, Grahamstown, 6140, South Africa.*

[c]*Centre for Chemico- and Biomedical Research, Rhodes University, Grahamstown, 6140, South Africa.*

[d]*Faculty of Pharmacy, Rhodes University, Grahamstown, 6140, South Africa.*

Received 7 March 2018, revised 13 November 2018, accepted 15 November 2018.

ABSTRACT

Sleeping sickness (trypanosomiasis) is a neglected tropical disease that affects mostly the poorest communities in sub-Saharan Africa. Toxic side effects associated with the use of current anti-trypanosomal drugs, which in some cases kill faster than the disease itself, necessitate the search for new drugs with better safety margins. To this effect, a small library bearing different substituents at position -1, -3, and -6 of the quinolone nucleus were synthesized and evaluated *in vitro* against HeLa cell lines and *Trypanosoma brucei brucei* for cytotoxicity and trypanocidal potentials, respectively. While most of these compounds showed no cytotoxic effect, they exhibited moderate to weak anti-trypanosomal activities. The SAR studies of this series provide new information worth considering in future exploration of the quinolone scaffold in search of more potent and safe trypanocidal agents.

KEYWORDS

Sleeping sickness, trypanosomiasis, quinolones, non-fluoroquinolones.

1. Introduction

Human African trypanosomiasis (HAT), also referred to as sleeping sickness,[1] is among the WHO's list of neglected tropical diseases (NTDs).[2] It mostly affects people living in rural areas of sub-Saharan Africa,[3] where medical facilities are scarce and drug purchasing power of inhabitants is very low.[4] At least 2184 new cases of the disease were reported in 2016,[5] and approximately 60 million people living in 36 different countries are presently at risk of contracting the disease.[6]

HAT takes two forms caused by two different subspecies of *Trypanosoma brucei*.[7] *T. b. gambiense* is the pathogenic subspecies causing the form of HAT commonly found in central and western Africa,[8,9] whereas *T. b. rhodesiense* is the subspecies responsible for the form of HAT prevalent in eastern and southern Africa.[10] It has been noted that the two sub-pathogenic species coexist in Uganda.[11] These pathogens are transmitted between humans following the bite of an infected *tsetse* fly.[12] The disease exists in two stages:[13,14] haemolymphatic stage – wherein the parasites are localized in blood and lymphatic systems,[15] and an encephalitic stage – wherein the parasites have invaded the central nervous system.[16,17]

Current treatment options are limited to just four drugs.[18] In any case of HAT, the drug to be used is dictated by the form and stage of the disease. Pentamidine is the drug of choice for treating the haemolymphatic stage of HAT caused by *T. b. gambiense*,[19] while a combination of nifurtimox and eflornithine is used to treat the encephalitic stage.[20] In cases of *T. b. rhodesiense*, suramin is the recommended drug for treating the haemolymphatic stage,[21] while malarsoprol is used to treat the encephalitic stage.[22] Besides limited treatment options, the foregoing drugs are far from ideal. They all have poor oral bioavailability (and hence are administered intravenously), and considerable toxic side effects.[23] For example, pentamidine causes hyper or hypoglycaemia and hypotension,[24] suramin causes renal failure, eflornithine causes alopecia and seizures,[25] while at least 5.9 % of patients on malarsoprol die from its toxicity,[26] creating a scenario wherein patients either die from an acute illness or die faster from a pill.

The overwhelming life-threatening side effects of existing drugs used to treat sleeping sickness create a dire need for new compounds with better drug properties such as high oral bioavailability, and a high safety margin. The therapeutic potentials of quinolones cannot be over emphasized. Compounds containing this scaffold are currently in use as drugs to treat bacterial and viral infections as well as other conditions such as cancers.[27] Fluoroquinolones (Fig. 1a) in clinical use have been extensively screened against trypanosomes and their activity profiles established as moderate to poor.[28,29,30] A hit optimization study by Hiltensperger and co-workers generated a potent library of fluoroquinolones characterized by benzylamides, (a)cyclic amines, and aliphatic chains at positions -3, -7, and -1 of the quinolone nucleus. However, the lead compound (Fig. 1b) in this series suffers from poor solubility,[31] necessitating further work on this class of compounds. Unlike fluoroquinolones, the anti-trypanosomal potentials of non-fluorinated quinolones have not been extensively investigated, with just one study on non-fluorinated quinolones bearing substituents at position -1 and -2, respectively, being reported[32] (Fig. 1c). To further expand the SAR around the non-fluoquinolone scaffold, we conceptualized and synthesized a library of 18 non-fluorinated quinolones bearing unique concurrent substituents at position -1, -3, and -6. Target compounds were subjected to *in vitro* cytotoxicity and anti-trypanosomal evaluation. At 20 μM concentration, most of the compounds exhibited less than 50 % parasite viability while having little effect on the viability of HeLa cell lines (see Supplementary information). This suggests that the quinolone scaffold

* To whom correspondence should be addressed.
E-mail: r.beteck@ru.ac.za / s.khanye@ru.ac.za

ISSN 0379-4350 Online / ©2018 South African Chemical Institute / http://saci.co.za/journal
DOI: https://doi.org/10.17159/0379-4350/2018/v71a25

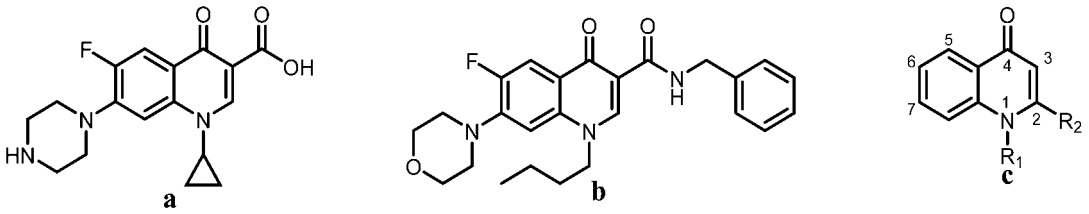

Figure 1 Representative structures of fluoroquinolones (**a** and **b**) and non-fluoroquinolones (**c**) investigated for anti-trypanosomal activities.

can be tailored *via* chemical synthesis to generate safe and potent drug substrates to treat trypanosomiasis.

2. Results and Discussion

We conceptualized and synthesized a set of 18 novel compounds that bear different substituents at positions -1, -3 and -6 of the quinolone scaffold. Conceptualized compounds were synthesized as depicted in Scheme 1. Briefly, 4′-nitroacetophenone was reduced to 4′-aminoacetophenone using reduced iron powder and acetic acid.[33] 4′-Aminoacetophenone and 4-chloroaniline were each treated with diethyl ethoxymethylenemalonate in refluxing acetonitrile to form condensed methylenemalonate esters, which underwent cyclization in boiling diphenylether at 245–250 °C for 5 min to form compound **2**. Deprotonation of **2** using K_2CO_3, followed by *N*-alkylation with alkylhalides afforded target compounds **3a–h** in yields ranging between 40 and 70 %. Ester functionality in compounds **3d–h** underwent selective aminolysis in the presence of a ketone to afford target compounds **4a–j** in 30–50 % yields. This transformation was realized using DBU as a base. All targeted compounds were characterized using proton and carbon NMR, HRMS and IR. The carbon NMR spectra of all compounds show a peak at *c.* 174 ppm, which is indicative of an oxo carbon within the quinolone nucleus (C-4) and the peak at *c.* 164 ppm is assigned to ester or amide carbonyl carbon (C-3a). With the exception of compounds **3a–c**, the proton NMR spectra of all compounds show a singlet signal at ~2.3–2.6 ppm, which is assigned to a methyl attached to a carbonyl carbon ($CH_3C{=}O$). The carbonyl carbon is also evident in the respective carbon spectra at ~197ppm. The presence of a triplet peak (J = 5.9 Hz) at *c.* 9.9 ppm in the proton NMR spectra of compounds **4a–j**, which is absent in compounds **3d–h**, suggests the successful conver-

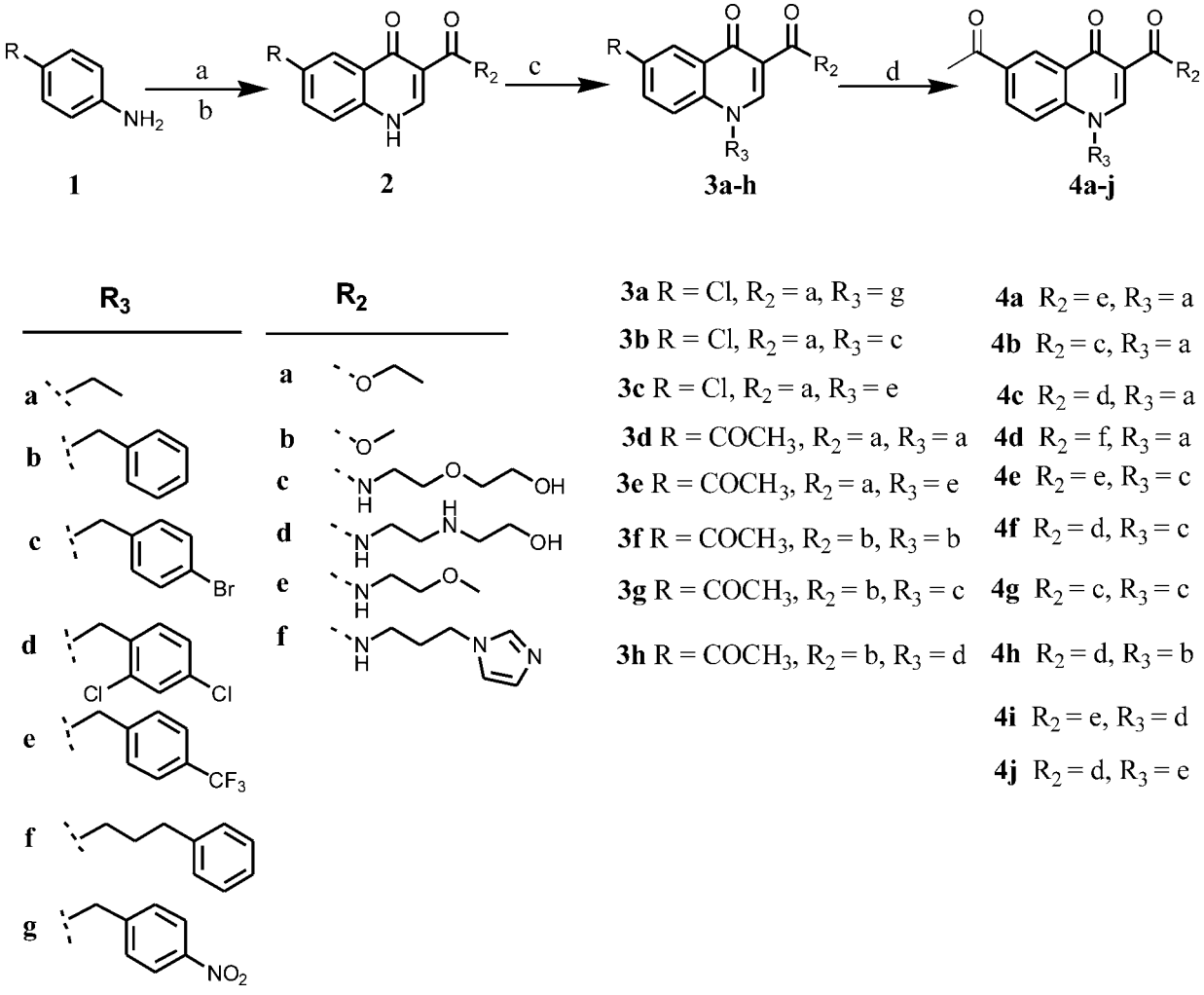

Scheme 1
Synthesis of target compounds
Reagents and conditions: (a) Acetonitrile, diethyl ethoxymethylenemalonate, reflux 12 h, (b) Diphenyl ether, 250 °C, 5 min, (c) K_2CO_3, DMF, alkylhalide (1.2 eqv), 12 h, (d) Amine (5 eqv), DBU (1.2 eqv), $CHCl_3$, reflux 12 h.

sion of ester to amide. It is also worth noting that the acquisition of NMR spectroscopic data was at times hindered by compounds crystallizing out of the solutions. This sometimes necessitated the use of hot solvents to encourage compounds to remain in solution long enough to obtain 1H and 13C NMR spectroscopic data (see Supplementary information). The absorption band at 1654/cm on the IR spectrum further confirms the presence of amide.

This focused library was screened *in vitro* against human cervix adenocarcinoma (HeLa) cell lines to investigate potential cytotoxicity effects. The compounds were incubated at 20 μM in 96-well plates containing HeLa cells for 48 h. The numbers of cells surviving upon drug exposure were determined using resazurin reduction to resorufin by live cells and reading resorufin fluorescence in a multiwell plate reader. Compounds were tested in duplicate, and a standard deviation (S.D.) calculated. Results are expressed as % viability based on fluorescence readings in treated wells *versus* untreated control wells. Emetine (which induces cell apoptosis) was used as positive control. With the exception of compound **4f** (% viability, –19 %), and **4j** (% viability, –13 %), which strongly inhibited HeLa cell lines, the rest of the series had little to no effect on HeLa cell viability. This observation suggests that this series with necessary optimization could serve as templates for the development of non-toxic anti-trypanosomal agents.

The compounds were further evaluated *in vitro* for anti-trypanosomal activities by screening against the 427 strain of *T. b. brucei*. Compounds were added to *in vitro* cultures of *T. b. brucei* in 96-well plates at a 20 μM concentration. After an incubation period of 48 h, the numbers of parasites surviving drug exposure were determined by adding resazurin. As in HeLa cells, resazurin is reduced to resorufin by living parasites. Resorufin is a fluorophore (Exc_{560}/Em_{590}) and can thus be quantified in a multiwell fluorescence plate reader. Compounds were tested in duplicate wells, and a standard deviation (S.D.) calculated. Results are expressed as % viability – the resorufin fluorescence in compound-treated wells relative to untreated controls. Pentamidine (an existing drug for treatment of trypanosomiasis) was used as a positive control. At 20 μM concentration, 11 compounds inhibited parasite growth below 50 % (Table 1); however, only compounds inhibiting parasite viability below 25 % with little or no effect on HeLa cell line were considered for IC_{50} determination. The IC50 values for the selected compounds are summarized in Fig. 2.

Structure–activity relationship analysis across this series suggests that modifications at position -1, -3, and -6 of the quinolone scaffold influence anti-trypanosomal activities. For example, comparing the activity profiles of compounds **3b** (IC_{50}, 19 μM) and **3g** (IC_{50}, 24 μM), all having the same substituents at position -1 and -3 and differing in substitution pattern only at position -6 suggests that a chloride substituent at this position leads to increase anti-trypanosomal activity than a ketone. Also, comparing compounds **3d** (IC_{50}, 32 μM) bearing an alkyl chain at position -1 and **3g** (IC_{50}, 24 μM) bearing a substituted-benzyl moiety at position -1, indicates that the presence of a substi-

Table 1 *In vitro* cytotoxicities and anti-trypanosomal activities of target compounds expressed as percentage viabilities.

Comp.	% Viability ± S.D.	
	T. b. brucei	HeLa cells
3a	**21.2 ± 4.0**	97.6 ± 5.6
3b	**4.0 ± 0.7**	100.2 ± 6.2
3c	97.3±3.3	102.7 ± 7.6
3d	**21.0 ± 3.7**	77.0 ± 0.7
3e	43.8 ± 3.2	96.7 ± 3.7
3f	87.3 ± 7.0	107.2 ± 1.6
3g	**5.5 ± 5.2**	103.6 ± 3.7
3h	42.3 ± 8.4	108.6 ± 5.3
4a	95.4 ± 10	92.6 ± 3.6
4b	**4.8 ± 0.1**	86.1 ± 2.4
4c	105.8 ± 1.6	110.7 ± 6.7
4d	31.2 ± 12.2	88.9 ± 5.8
4e	100.0 ± 2.7	102.6 ± 5.7
4f	**-1.3 ± 0.3**	**-19.2 ± 0.04**
4g	**24.7 ± 7.6**	102.1 ± 5.8
4i	64.5 ± 7.8	91.0 ± 4.9
4j	50.3 ± 4.4	-14.0 ± 0.6
PE[a]	0.0	N.D
EMT[b]	N.D[c]	0.0

[a]PE = pentamidine, [b]EMT = ematine, [c]N.D = not determined.

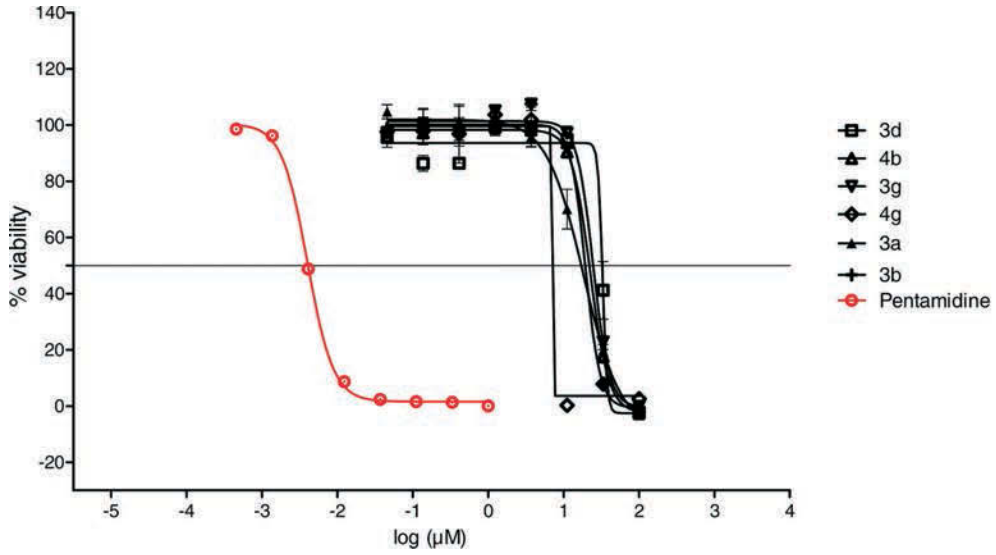

Compound	IC_{50}(μM)
3a	18.4
3b	19.4
3d	32.9
3g	24.6
4b	22.4
4g	7.14
PE*	0.0062

Figure 2 Plot of percentage viability against log concentration for compound **3a**, **3b**, **3d**, **3g**, **4b** and **4g** as well as the standard (PE = pentamidine) and their corresponding IC_{50} values.

tuted-benzyl moiety at position -1 seems to promote anti-trypanosomal activities over alkyl chains. We also observed that the substituent on the benzyl moiety at position -1 also influences anti-trypanosomal activities. This is evident when comparing the effects of compounds **3a, 3b** and **3c** on parasite viability at a concentration of 20 μM. Compounds **3a** and **3b** bearing -NO_2, and -Br, respectively, exhibited more than 75 % parasite growth inhibition, while compound **3c** having -CF_3 substituent exhibited less than 5 % parasite growth inhibition. These results suggest that electron-withdrawing units promote activity while electron-donating unit leads to poor activity. The substitution pattern at position -3 also seems to greatly influence activity. Comparing the activity of compounds **3g** (IC_{50}, 24 μM) and **4g** (IC_{50}, 7 μM), both of which differ only in the substituent at position -3, suggests that an amide moiety at position -3 seems to enhance activity over ethyl ester.

3. Conclusion

We have synthesized a series of novel quinolones with varied substituents at position -1, -3 and -6 of the quinolone scaffold. While most compounds in this series showed no promising cytotoxicity potentials, compounds **4g** emerged as potent anti-trypanosomal hit with IC_{50} value of 7 μM. Although this series exhibited moderate to weak activities profiles, the comprehensive structure–activity relationship analyses of this series will undoubtedly serve as a resource for further optimization of the quinolone scaffold in search of new and potent anti-trypanosomal agents.

4. Experimental

4.1. General Method

All the chemicals and solvents used were purchased from various chemical suppliers and were used without further purification. Melting points were determined using a Reichert hot stage microscope and are uncorrected. The progress of the reactions was monitored by thin layer chromatography (TLC) using Merck F254 silica gel plates supported on aluminium. The crude products were purified by a silica gel column chromatography using Merck Kieselgel 60 Å: 70–230 (0.068–0.2 mm) silica gel mesh. ^{1}H and ^{13}C NMR spectra were recorded on Bruker Biospin 300 MHz, or 400 MHz spectrometers, and the chemical shifts are given in δ values referenced to solvents and are reported in parts per million (ppm). The high-resolution mass spectrometric data of final compounds was recorded on a Waters Synapt G2 quadrupole time-of-flight (QTOF) mass spectrometer operated with an electrospray ionization probe in the positive mode (University of Stellenbosch). The instrument was operated with an electrospray ionization probe in the positive mode. The starting quinolones **2** were synthesized from the synthetically accessible compounds **1** as previously described in literature.[34]

4.2. Synthesis of Compounds

4.2.1. *General Method for the Preparation of N-alkylated Compounds* **3a–h**

A mixture of **2** (3.86 mmol, 1 g, 1 eq), K_2CO_3 (5.0 mmol, 0.53 g), alkyl halide (5 eq.) in acetone (50 mL) was refluxed for 15 h. Upon reaction completion as indicated by TLC, the mixture was filtered, and the filtrate evaporated to dryness to obtain a crude *N*-alkylated product which was purified through silica gel column chromatography using CH_2Cl_2/MeOH (10:1) as the mobile phase. Compounds **3a–h** were obtained in 40–70 % yield following this procedure.

Methyl 6-chloro-1-(4-nitrobenzyl)-4-oxo-1,4-dihydroquinoline-3-carboxylate, **3a**

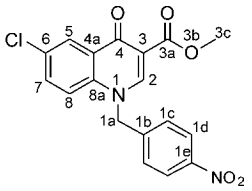

Brown powder, 0.515 g (48 %), R_f = 0.81 (DCM/MeOH 10:1) m.p. 153–155 °C; ^{1}H NMR (300 MHz, DMSO) δ 9.00 (s, 1H, H-2), 8.16 (d, J = 2.5 Hz, 1H, H-5), 7.89–7.57 (m, 3H, H-1c, H-8), 7.48 –7.05 (m, 3H, H-7, H-1d), 5.82 (s, 2H, H-1a), 4.24 (s, 3H, H-3c). ^{13}C NMR (75 MHz, DMSO) δ 172.2 (C-4), 164.1 (C-3a), 151.3 (C-2), 141.1 (C-3), 138.2 (C-6), 133.2 (C-1d), 131.3 (C-1c), 130.5 (C-5), 130.1 (C-7), 127.6 (C-1b), 126.3 (C-4a), 125.9 (C-8), 120.7 (C-8a), 110.9 (C-1e), 57.3 (C-3c), 55.7 (C-1a). IR (neat, cm^{-1}): 3093, 2972, 2931, 1702, 1686; ESI-HRMS m/z [M+H]$^+$ calcd for $C_{18}H_{14}ClN_2O_5$ 373.0586, found 373.0594.

Ethyl 1-(4-bromobenzyl)-6-chloro-4-oxo-1,4-dihydroquinoline-3-carboxylate, **3b**

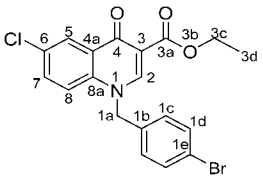

White powder, 0.015 g (46 %), R_f = 0.8 (DCM/MeOH 10:1), m.p. 196–198 °C; ^{1}H NMR (400 MHz, DMSO) δ 8.94 (s, 1H, H-2), 8.16 (d, J = 2.5 Hz, 1H, H-5), 7.81–7.48 (m, 4H, H-7, H-8, H-1c), 7.21 (d, J = 8.4 Hz, 2H, H-1d), 5.68 (s, 2H, H-1a), 4.25 (q, J = 7.1 Hz, 2H, H-3c), 1.30 (t, J = 7.1 Hz, 3H, H-3d). ^{13}C NMR (101 MHz, DMSO) δ 172.0 (C-4), 165.0 (C-3a), 151.0 (C-2), 138.5 (C-3), 135.5 (C-6), 132.9 (C-5), 132.2 (C-1d), 130.6 (C-1b), 129.9 (C-1c), 128.9 (C-4a), 125.9 (C-7), 121.8 (C-1e), 120.6 (C-8), 111.1 (C-8a), 60.3 (C-3c), 55.6 (C-1a), 14.2 (C-3d). IR (neat, cm^{-1}): 3096, 2978, 2941, 1702, 1680. ESI-HRMS m/z [M+H]$^+$ calcd for $C_{19}H_{16}BrClNO_3$ 419.997, found 419.9998.

Ethyl 6-chloro-4-oxo-1-(4-(trifluoromethyl)benzyl)-1,4-dihydroquinoline-3-carboxylate, **3c**

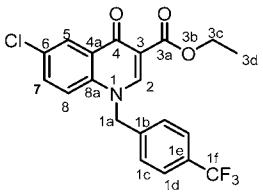

Brown powder, 0.5 g (70 %), R_f = 0.81 (DCM/MeOH 10:1), m.p. 203–205 °C; ^{1}H NMR (400 MHz, Pyridine) δ 9.19 (s, 1H, H-2), 7.65 (d, J = 8.4 Hz, 2H, H-1c), 7.56–7.49 (m, 3H, H-5, H-7, H-8), 7.43 (d, J = 8.4 Hz, 2H, H-1d), 5.00 (s, 2H, H-1a), 4.36 (q, J = 6.9 Hz, 2H, H-3c), 1.23 (t, J = 6.9 Hz, 3H, H-3d). ^{13}C NMR (101 MHz, Pyridine) δ 173.0 (C-4), 164.7 (C-3a), 150.64 (C-2), 140.6 (C-3), 140.2 (C-1b), 137.9 (C-6), 135.5 (C-1d), 132.9 (C-1c), 130.9 (C-5), 130.2 (C-7), 127.2 (C-1e), 126.4 (C-4a), 125.9 (C-8), 120.7 (C-8a), 119.5 (C-1f), 112.2 (C-1f), 60.3 (C-3c), 56.0 (C-1a), 14.2 (C-3d). IR (neat, cm^{-1}): 3003, 2962, 2921, 1705, 1684, ESI-HRMS m/z [M+H]$^+$ calcd for $C_{20}H_{16}ClF_3NO_3$ 410.0765, found 410.0766.

Ethyl 6-acetyl-1-ethyl-4-oxo-1,4-dihydroquinoline-3-carboxylate, **3d**

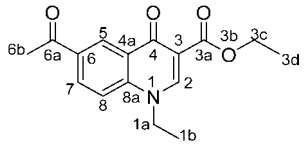

Red powder, 0.65 g (70 %), R_f = 0.71 (DCM/MeOH 10:1); m.p. 143–147 °C; ^{1}H NMR (300 MHz, $CDCl_3$) δ 8.97 (s, 1H, H-2), 8.44 (d, J = 2.1 Hz, 1H, H-5), 8.22 (dd, J = 8.9, 2.1 Hz, 1H, H-7), 7.46 (d, J = 9.0 Hz, 1H, H-8), 4.39–4.31 (m, 2H, H-1a), 4.23 (q, J = 7.2 Hz, 2H, H-3c), 2.63 (s, 3H, H-6b), 1.50 (t, J = 7.3 Hz, 3H, H-3d), 1.37–1.20 (m, 3H, H-1b). ^{13}C NMR (75 MHz, $CDCl_3$) δ 196.9 (6a), 173.9 (4), 165.4 (3a), 149.1 (2), 141.6 (3), 133.3 (6), 131.4 (5), 129.5 (7), 128.7 (4a), 116.2 (8), 112.4 (8a), 61.1 (3c), 49.1 (1a), 26.6 (6b), 14.5 (1b), 14.4 (3d). IR (neat, cm^{-1}): 3053, 2982, 2921, 1712, 1685, ESI-HRMS m/z [M+H]$^+$ calcd for $C_{16}H_{18}NO_4$ 288.1230, found 288.1234.

Methyl 6-acetyl-4-oxo-1-(4-(trifluoromethyl)benzyl)-1,4-dihydroquinoline-3-carboxylate, **3e**

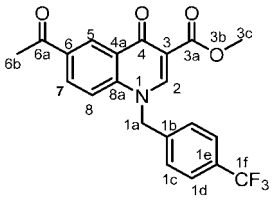

Brown powder, 0.680 g (68 %), R_f = 0.81 (DCM/MeOH 10:1), m.p. 133–136 °C; ^{1}H NMR (300 MHz, DMSO) δ 9.02 (s, 1H, H-2), 8.76 (d, J = 3.4 Hz, 1H, H-5) 8.15 (dd, J = 9.1, 3.4 Hz, 1H, H-7) , 7.73 (d, J = 8.0, Hz, 2H, H-1c), 7.60 (d, J = 7.1 Hz, 2H, H-1d) , 7.43 (d, J = 9.1 Hz, 1H, H-8), 5.82 (s, 2H, H-1a), 3.89 (s, 3H, H-3c), 2.49 (s, 3H, H-6b). ^{13}C NMR (75 MHz, DMSO) δ 197.1 (C-6a), 173.9 (4), 164.4 (3a), 151.4 (C-2), 142.2 (C-3), 140.2 (C-1b), 135.7 (C-1d), 133.3 (C-6), 132.3 (C-1c), 132.0 (C-5), 129.2 (C-7), 128.2 (C-1e), 127.6 (C-4a), 121.5 (C-8), 118.8 (C-8a), 111.6 (C-1f), 55.3 (C-3c), 53.7 (C-1a), 26.6 (6b). IR (neat, cm^{-1}): 3100, 2970, 2921, 1700, 1680. ESI-HRMS m/z [M+H]$^+$ calcd for $C_{21}H_{16}F_3NO_4$ 404.1104, found 404.1107.

Ethyl 6-acetyl-1-benzyl-4-oxo-1,4-dihydroquinoline-3-carboxylate, **3f**

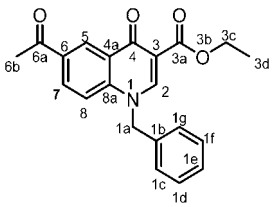

White powder, 0.80 g (58 %), R_f = 0.81 (DCM/MeOH 10:1) m.p. 142–144 °C; ^{1}H NMR (300 MHz, DMSO) δ 9.00 (s, 1H, H-2), 8.81 (s, 1H, H-5), 8.19 (d, J = 8.8 Hz, 1H, H-8), 7.77 (d, J = 8.9 Hz, 1H, H-7), 7.49–7.21 (m, 5H, H-1c/H-1g), 5.77 (s, 2H, H-1a), 4.31 (q, J = 7.0 Hz, 2H, H-3c), 2.55 (s, 3H, H-6b), 1.40–1.26 (m, 3H, H-3d). ^{13}C NMR (75 MHz, DMSO) δ 197.1 (C-6a), 173.3 (C-4), 164.7 (C-3a), 151.1 (C-2), 142.4 (C-3), 136.2 (C-1b), 133.2 (C-6), 131.8 (C-5), 129.4 (C-1g), 128.4 (C-4a), 128.3 (C-1f), 127.7 (C-7), 126.9 (C-1e), 118.8 (C-8), 111.9 (C-8a), 60.5 (C-3c), 56.2 (C-1a), 27.2 (C-6a), 14.7 (C-3d). IR (neat, cm^{-1}): 3083, 2970, 2921, 1705, 1681, ESI-HRMS m/z [M+H]$^+$ calcd for $C_{21}H_{20}NO_4$ 350.1387, found 350.1391.

Methyl 6-acetyl-1-(4-bromobenzyl)-4-oxo-1,4-dihydroquinoline-3-carboxylate, **3g**

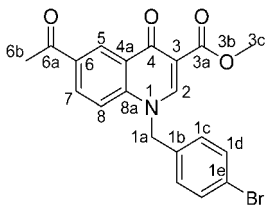

Brown powder, 0.58 g (62 %), R_f = 0.81 (DCM/MeOH 10:1), m.p. 173–175 °C; ^{1}H NMR (300 MHz, DMSO) δ 8.99 (s, 1H, H-2), 8.75 (s, 1H, H-5), 8.16 (d, J = 8.6 Hz, 1H, H-7), 7.81–7.52 (m, 3H, H-1c, H-8), 7.19 (d, J = 7.6 Hz, 2H, H-1d), 5.72 (s, 2H, H-1a), 3.79 (s, 3H, H-3c), 2.50 (s, 3H, H-6b). ^{13}C NMR (75 MHz, DMSO) δ 197.4 (C-6a), 173.1 (C-4), 166.4 (C-3a), 151.4 (C-2), 142.2 (C-3), 135.7 (C-1d), 133.3 (C-6), 132.3 (C-1c), 132.0 (C-5), 129.2 (C-7), 128.3 (C-1b), 127.6 (C-4a), 127.5 (C-8), 119.8 (C-8a), 111.6 (C-1e), 55.3 (C-3c), 53.7 (C-1a), 26.6 (6b). IR (neat, cm^{-1}): 3048, 2972, 2931, 1702, 1682. ESI-HRMS m/z [M+H]$^+$ calcd for $C_{20}H_{17}BrNO_4$ 414.0335, found 414.0333.

Methyl 6-acetyl-1-(2,4-dichlorobenzyl)-4-oxo-1,4-dihydroquinoline-3-carboxylate, **3h**

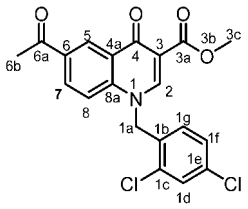

Brown powder, 0.28 g (48 %), R_f = 0.81 (DCM/MeOH 10:1), m.p. 197–1199 °C; ^{1}H NMR (300 MHz, DMSO) δ 9.16 (s, 1H, H-2), 8.92 (d, J = 2.2 Hz, 1H, H-5), 8.26 (dd, J = 8.9, 2.2 Hz, 1H, H-7), 7.85 (d, J = 9.0 Hz, 1H, H-8), 7.72–7.59 (m, 2H, H-1d, H-1g), 7.21 (dd, J = 8.3, 2.2 Hz, 1H, H-1f), 5.87 (s, 2H, H-1a), 3.77 (s, 3H, H-3c), 2.70 (s, 3H, H-6b). ^{13}C NMR (75 MHz, DMSO) δ 197.1 (C-6a), 176.3 (C-4), 164.0 (C-3a), 150.2 (C-2), 142.1 (C-3), 137.4 (C-6), 133.4 (C-1b), 132.1 (C-5), 131.9 (C-1g), 131.6 (C-1c), 131.1 (C-1e), 129.4 (C-1d), 127.7 (C-7), 127.4 (C-1f), 127.2 (C-4a), 118.7 (C-8), 112.8 (C-8a), 55.5 (C-1a), 52.3 (C-3c), 27.2 (C-6b). IR (neat, cm^{-1}): 3073, 2972, 2941, 1702, 1683. ESI-HRMS m/z [M+H]$^+$ calcd for $C_{20}H_{16}Cl_2NO_4$ 404.0451, found 404.0452.

4.2.2. *General Method for the Preparation of Amides* **4a–j**

A mixture of **3** (1 g, 1 eq.), DBU (320 μL, 0.33 g, 2.1 mmol), an appropriate amine (5 eq.), and chloroform (15 mL) in a 100 mL round-bottom flask was stirred under reflux for 24–30 h.[34] Upon reaction completion as indicated by TLC, the mixture was evaporated to dryness and resultant crude subjected to silica gel column chromatography eluting with CH_2Cl_2/MeOH (10:1). Fractions containing the desired product were combined, evaporated to dryness and recrystallized from ethanol. Compounds **4a–j** were obtained in 30–50 % yield following this procedure.

6-Acetyl-1-ethyl-N-(2-methoxyethyl)-4-oxo-1,4-dihydroquinoline-3-carboxamide, **4a**

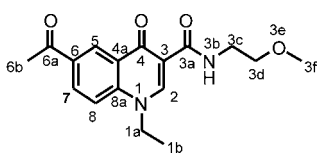

Orange powder, 0.028 g (32 %), R_f = 0.48 (DCM/MeOH 10:1), m.p. 163–165 °C; ^{1}H NMR (300 MHz, DMSO) δ 9.93 (s, 1H, NH), 8.88 (s, 1H, H-2), 8.83 (d, J = 1.5 Hz, 1H, H-5), 8.32–8.22 (m, 1H, H-7), 7.97 (d, J = 9.0 Hz, 1H, H-8), 4.55 (q, J = 7.0 Hz, 2H, H-1a), 3.49 (s, 3H, H-3f), 3.42–3.04 (m, 4H, H-3c, H-3d), 2.68 (s, 3H, H-6b), 1.39 (t, J = 7.0 Hz, 3H, H-1b). ^{13}C NMR (75 MHz, DMSO) δ 197.6 (C-6a), 175.9 (C-4), 164.2 (C-3a), 148.8 (C-2), 142.1 (C-3), 132.9 (C-6), 132.1 (C-5), 127.9 (C-7), 127.1 (C-4a), 118.4 (C-8), 112.6 (C-8a), 71.3 (C-3d), 58.3 (C-3f), 49.1 (C-1a), 38.8 (C-3c), 27.5 (C-6b), 14.9 (C-1b). IR (neat, cm^{-1}): 3393, 3041, 2970, 2929, 1682, 1656. ESI-HRMS m/z [M+H]$^+$ calcd for $C_{17}H_{21}N_2O_4$ 317.1496, found 317.1497.

6-Acetyl-1-ethyl-N-(2-(2-hydroxyethoxy)ethyl)-4-oxo-1,4-dihydroquinoline-3-carboxamide, **4b**

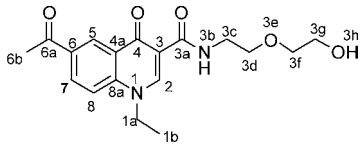

White powder, 0.235 g (33 %), R_f = 0.39 (DCM/MeOH 10:1), m.p. 127–129 °C; ^{1}H NMR (400 MHz, $CDCl_3$) δ 10.12 (s, 1H, NH), 8.97 (s, 1H, H-2), 8.75 (s, 1H, H-5), 8.27 (d, J = 7.9 Hz, 1H, H-7), 7.54 (d, J = 7.9 Hz, 1H, H-8), 4.31 (q, J = 7.1 Hz, 2H, H-1a), 3.74-3.61 (m, 8H, H-3c, H-3d, H-3f, H-3g), 2.67 (s, 3H, H-6b), 1.53 (t, J = 7.2 Hz, 3H, H-1b). ^{13}C NMR (101 MHz, $CDCl_3$) δ 196.8 (C-6a), 176.7 (C-4), 164.7 (C-3a), 147.9 (C-2), 141.5 (C-3), 133.6 (C-6), 131.9 (C-5), 129.2 (C-7), 127.9 (C-4a), 116.2 (C-8), 113.5 (C-8a), 72.7 (C-3g), 69.7 (C-3f), 61.7 (C-3d), 49.3 (C-1a), 39.0 (C-3c), 26.6 (C-6b), 14.6 (C-1b). IR (neat, cm^{-1}): 3333, 3252, 3001, 2970, 2929, 1682, 1654. ESI-HRMS m/z [M+H]$^+$ calcd for $C_{18}H_{23}N_2O_5$ 347.1601, found 347.1604.

6-Acetyl-1-ethyl-N-(2-((2-hydroxyethyl)amino)ethyl)-4-oxo-1,4-dihydroquinoline-3-carboxamide, **4c**

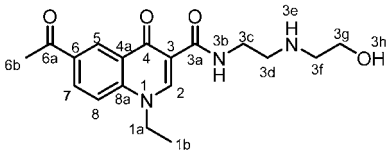

White powder, 0.475 g (48 %), R_f = 0.11 (DCM/MeOH 10:1), m.p. 157–159 °C; ^{1}H NMR (300 MHz, DMSO) δ 9.97 (t, J = 5.9 Hz, 1H, NH-3b), 8.91 (s, 1H, H-2), 8.84 (d, J = 2.2 Hz, 1H, H-5), 8.30 (dd, J = 9.0, 2.2 Hz, 1H, H-7), 8.01 (d, J = 9.0 Hz, 1H, H-8), 5.27 (s, 1H, H-3h), 4.56 (q, J = 7.1 Hz, 2H, H-1a), 3.67 (t, J = 6.3 Hz, 4H, H-3d, H-3f), 3.15 (t, J = 8.8 Hz, 2H, H-3g), 3.03 (t, J = 5.4 Hz, 2H, H-3c), 2.68 (s, 3H, H-6b), 1.39 (t, J = 7.1 Hz, 3H, H-1b). ^{13}C NMR (75 MHz, DMSO) δ 197.2 (C-6a), 175.8 (C-4), 165.1 (C-3a), 149.2 (C-2), 141.8 (C-3), 133.2 (C-6), 132.2 (C-5), 127.6 (C-7), 127.2 (C-4a), 118.5 (C-8), 112.3 (C-8a), 56.9 (C-3g), 49.7 (C-1a), 49.0 (C-3c), 47.1 (C-3f), 35.9 (C-3d), 27.2 (C-6b), 14.9 (C-1b). IR (neat, cm^{-1}): 3313, 3243, 3081, 2879, 2819, 1687, 1656. ESI-HRMS m/z [M+H]$^+$ calcd for $C_{18}H_{24}N_3O_4$ 346.1761, found 346.1762.

N-(3-(1H-imidazol-1-yl)propyl)-6-acetyl-1-ethyl-4-oxo-1,4-dihydroquinoline-3-carboxamide, **4d**

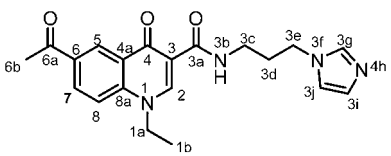

White powder, 0.521 g (57 %), R_f = 0.4 (DCM/MeOH 10:1), m.p. 207–209 °C; ^{1}H NMR (300 MHz, $CDCl_3$) δ 9.98 (s, 1H, NH), 8.99 (s, 1H, H-2), 8.76 (d, J = 0.9 Hz, 1H, H-5), 8.28 (dd, J = 9.0, 0.9 Hz, 1H, H-7), 7.57 (d, J = 9.0 Hz, 1H, H-8), 7.49 (s, 1H, H-3g), 6.99 (d, J = 9.2 Hz, 1H, H-3j), 6.93 (d, J = 9.2 Hz, 1H, H-3i), 4.32 (q, J = 7.2 Hz, 2H, H-1a), 4.01 (t, J = 7.0 Hz, 2H, H-3e), 3.43 (q, J = 6.3 Hz, 2H, H-3c), 2.66 (s, 3H, H-6b), 2.05 (dt, J = 6.8, 6.3 Hz, 2H, H-3d), 1.54–1.49 (t, J = 7.2 Hz, 3H, H-1b). ^{13}C NMR (75 MHz, $CDCl_3$) δ 196.6 (C-6a), 176.5 (C-4), 164.8 (C-3a), 147.9 (C-2), 141.6 (C-3), 137.2 (C-3g), 133.4 (C-6), 131.7 (C-5), 129.5 (C-3j), 128.9 (C-7), 127.4 (C-4a), 118.9 (C-3i), 116.4 (C-8), 112.9 (C-8a), 49.4 (C-1a), 44.5 (C-3c), 36.1 (C-3e), 31.3 (C-3d), 26.6 (C-6b), 14.6 (C-1b). IR (neat, cm^{-1}): 3303, 3087, 2960, 2912, 1687, 1655. ESI-HRMS m/z [M+H]$^+$ calcd for $C_{20}H_{23}N_4O_3$ 367.1765, found 367.1767.

6-Acetyl-1-(4-bromobenzyl)-N-(2-methoxyethyl)-4-oxo-1,4-dihydroquinoline-3-carboxamide, **4e**

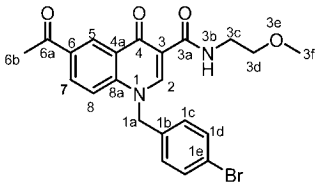

White powder, 0.432 g (43 %), R_f = 0.4 (DCM/MeOH 10:1), m.p. 136–138 °C; ^{1}H NMR (300 MHz, DMSO) δ 9.94 (t, J = 5.0 Hz, 1H, NH), 9.10 (s, 1H, H-2), 8.86 (d, J = 2.1 Hz, 1H, H-5), 8.19 (dd, J = 9.0, 2.2 Hz, 1H, H-7), 7.79 (d, J = 9.0 Hz, 1H, H-8), 7.62–7.45 (m, 2H, H-1d), 7.29–7.16 (m, 2H, H-1c), 5.79 (s, 2H, H-1a), 3.51 (t, J = 4.6 Hz, 2H, H-3c), 3.48–3.06 (m, 5H, H-3d, H-3f), 2.65 (s, 3H, H-6b). ^{13}C NMR (75 MHz, DMSO) δ 197.1 (C-6a), 176.2 (C-4), 164.1 (C-3a), 150.2 (C-2), 142.2 (C-3), 135.7 (C-1b), 133.3 (C-6), 132.3 (C-5), 132.0 (C-1c), 129.2 (C-1d), 127.7 (C-7), 127.3 (C-1e), 121.5 (C-4a), 118.9 (C-8), 112.7 (C-8a), 71.2 (C-3d), 58.5 (C-3f), 55.8 (C-1a), 38.8 (C-3c), 27.2 (C-6b). IR (neat, cm^{-1}): 3317, 3051, 2960, 2900, 1686, 1657. ESI-HRMS m/z [M+H]$^+$ calcd for $C_{22}H_{22}BrN_2O_4$ 459.0763, found 459.0751.

6-Acetyl-1-(4-bromobenzyl)-N-(2-((2-hydroxyethyl)amino)ethyl)-4-oxo-1,4-dihydroquinoline-3-carboxamide, **4f**

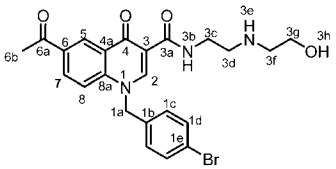

White powder, 0.20 g (48 %), R_f = 0.11 (DCM/MeOH 10:1), m.p. 178–180 °C; ^{1}H NMR (300 MHz, DMSO) δ 9.93 (t, J = 4.8 Hz, 1H, NH), 9.10 (s, 1H, H-2), 8.85 (d, J = 1.7 Hz, 1H, H-5), 8.19 (dd, J = 8.9, 1.7 Hz, 1H, H-7), 7.79 (d, J = 9.0 Hz, 1H, H-8), 7.54 (d, J = 8.3 Hz, 2H, H-1d), 7.20 (d, J = 8.3 Hz, 2H, H-1c), 5.79 (s, 2H, H-1a), 4.62 (t, J = 5.2 Hz, 2H, H-3c), 3.60–3.49 (m, 6H, H-3d, H-3f, H-3g), 2.43 (s, 3H, H-6b). ^{13}C NMR (75 MHz, DMSO) δ 197.1 (C-6a), 176.2 (C-4), 164.1 (C-3a), 150.2 (C-2), 142.2 (C-3), 135.7 (C-1d), 133.4 (C-6), 132.2 (C-1c), 132.0 (C-5), 129.3 (C-7), 127.4 (C-1b), 121.6 (C-4a), 118.9 (C-8), 112.7 (C-8a), 111.9 (C-1e), 58.7 (C-3g), 55.8 (C-1a), 49.4 (C-3f), 48.9 (C-3d), 36.9 (C-3c), 27.2 (C-6b). IR (neat, cm^{-1}): 3320, 3202, 3000, 2970, 2929, 1682, 1657. ESI-HRMS m/z [M+H]$^+$ calcd for $C_{23}H_{25}BrN_3O_4$ 486.1023, found 486.1021.

6-Acetyl-1-(4-bromobenzyl)-N-[2-(2-hydroxyethoxy)ethyl]-4-oxo-1,4-dihydroquinoline-3-carboxamide, **4g**

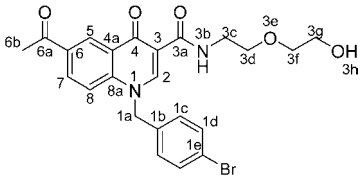

White powder, 0.20 g (48 %), R_f = 0.4 (DCM/MeOH 10:1), m.p. 183–185 °C; ^{1}H NMR (300 MHz, DMSO) δ 9.93 (t, J = 4.8 Hz, 1H, NH), 9.10 (s, 1H, H-2), 8.85 (d, J = 1.7 Hz, 1H, H-5), 8.19 (dd, J = 8.9, 1.7 Hz, 1H, H-7), 7.79 (d, J = 9.0 Hz, 1H, H-8), 7.54 (d, J = 8.3 Hz, 2H, H-1d), 7.20 (d, J = 8.3 Hz, 2H, H-1c), 5.79 (s, 2H, H-1a), 4.62 (t, J = 5.2 Hz, 2H, H-3c), 3.60–3.49 (m, 6H, H-3d, H-3f, H-3g), 2.43 (s, 3H, H-6b). ^{13}C NMR (75 MHz, DMSO) δ 197.1 (C-6a), 176.2 (C-4), 1- 64.1 (C-3a), 150.2 (C-2), 142.2 (C-3), 135.7 (C-1d), 133.4 (C-6), 132.2 (C-1c), 132.0 (C-5), 129.3 (C-7), 127.4 (C-1b), 121.6 (C-4a), 118.9 (C-8), 112.7 (C-8a), 111.9 (C-1e), 72.7 (C-3d), 69.7 (C-3f), 60.7 (C-3g), 55.0 (C-1a), 39.7 (C-3c), 27.2 (C-6b). IR (neat, cm^{-1}): 3397, 3252, 3041, 2950, 2861, 1686, 1654. ESI-HRMS *m/z* calcd for $C_{23}H_{24}BrN_2O_5$ 487.0863, found 487.0665 $[M+H]^+$. HPLC purity > 96 %, retention time = 9.89 min.

6-Acetyl-1-benzyl-N-(2-((2-hydroxyethyl)amino)ethyl)-4-oxo-1,4-dihydroquinoline-3-carboxamide, **4h**

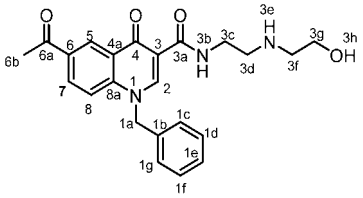

Orange powder, 0.320 g (48 %), R_f = 0.11 (DCM/MeOH 10:1), m.p. 169–171 °C; ^{1}H NMR (300 MHz, DMSO) δ 9.93 (t, J = 4.8 Hz, 1H, NH), 9.10 (s, 1H, H-2), 8.85 (d, J = 1.7 Hz, 1H, H-5), 8.19 (dd, J = 8.9, 1.7 Hz, 1H, H-7), 7.79 (d, J = 9.0 Hz, 1H, H-8), 7.54-7.20 (m, 5H, H-1c, H-1d, H-1f, H-1g), 5.79 (s, 2H, H-1a), 4.62 (t, J = 5.2 Hz, 2H, H-3c), 3.60–3.49 (m, 6H, H-3d, H-3f, H-3g), 2.43 (s, 3H, H-6b). ^{13}C NMR (75 MHz, DMSO) δ 197.1 (C-6a), 176.2 (C-4), 164.1 (C-3a), 150.2 (C-2), 142.2 (C-3), 135.7 (C-1d), 133.4 (C-6), 132.2 (C-1c), 132.0 (C-5), 129.3 (C-7), 127.4 (C-1b), 121.6 (C-4a), 118.9 (C-8), 112.7 (C-8a), 111.9 (C-1e), 72.7 (C-3d), 69.7 (C-3f), 60.7 (C-3g), 55.02 (C-1a), 39.7 (C-3c), 27.2 (C-6b). IR (neat, cm^{-1}): 3328, 3212, 3038, 2971, 2921, 1682, 1659. ESI-HRMS *m/z* $[M+H]^+$ calcd for $C_{23}H_{26}N_3O_4$ 408.1918, found 408.1923.

6-Acetyl-1-(2,4-dichlorobenzyl)-N-(2-methoxyethyl)-4-oxo-1,4-dihydroquinoline-3-carboxamide, **4i**

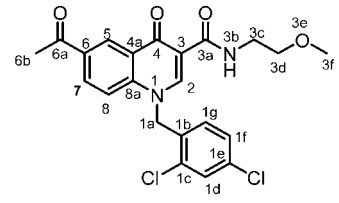

Brown powder, 0.370 g (44 %), R_f = 0.4 (DCM/MeOH 10:1). m.p. 203–205 °C; ^{1}H NMR (300 MHz, DMSO-d_6) δ 9.99 (t, J = 5.1 Hz, 1H, NH), 9.16 (s, 1H, H-2), 8.92 (d, J = 2.2 Hz, 1H, H-5), 8.26 (dd, J = 8.9, 2.2 Hz, 1H, H-7), 7.85 (d, J = 9.0 Hz, 1H, H-8), 7.72–7.59 (m, 2H, H-1d, H-1f), 7.21 (d, J = 8.3, Hz, 1H, H-1g), 5.87 (s, 2H, H-1a), 3.56–3.13 (m, 4H, H-3c, H-3d), 3.37 (s, 3H, H-3f), 2.70 (s, 3H, H-6b). ^{13}C NMR (75 MHz, DMSO) δ 197.1 (C-6a), 176.3 (C-4), 164.0 (C-3a), 150.2 (C-2), 142.1 (C-3), 137.4 (C-6), 133.4 (C-1b), 132.1 (C-5), 131.9 (C-1g), 131.6 (C-1c), 131.1 (C-1e), 129.4 (C-1d), 127.7 (C-7), 127.4 (C-1f), 127.2 (C-4a), 118.7 (C-8), 112.8 (C-8a), 71.2 (C-3d), 58.5 (C-3f), 55.3 (C-1a), 39.0 (C-3c), 27.2 (C-6b). IR (neat, cm^{-1}): 3298, 3071, 2971, 2929, 1682, 1655. ESI-HRMS *m/z* $[M+H]^+$ calcd for $C_{22}H_{21}Cl_2N_2O_4$ 447.0873, found 447.0878.

6-Acetyl-N-(2-((2-hydroxyethyl)amino)ethyl)-4-oxo-1-(4-(trifluoromethyl)benzyl)-1,4-dihydroquinoline-3-carboxamide, **4j**

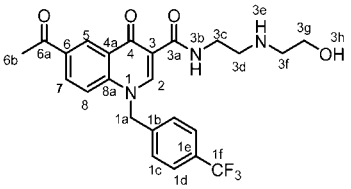

Orange powder, 0.367 g (44 %), R_f = 0.11 (DCM/MeOH 10:1), m.p. 193–195 °C; ^{1}H NMR (300 MHz, DMSO) δ 10.03 (t, J = 5.9 Hz, 1H, NH), 9.22 (s, 1H, H-2), 8.92 (d, J = 2.1 Hz, 1H, H-5), 8.28 (dd, J = 8.9, 2.2 Hz, 1H, H-7), 7.87 (d, J = 9.0 Hz, 1H, H-8), 7.79 (d, J = 8.1 Hz, 2H, H-1c), 7.51 (d, J = 8.0 Hz, 2H, H-1d), 6.03 (s, 2H, H-1a), 5.36 (t, J = 5.1 Hz, 1H, OH), 3.83–3.70 (m, 4H, H-3d, H-3f), 3.22 (t, J = 6.3 Hz, 2H, H-3c), 3.11 (t, J = 5.3 Hz, 2H, H-3g), 2.70 (s, 3H, H-6b). ^{13}C NMR (75 MHz, DMSO) δ 197.1 (C-6a), 176.1 (C-4), 165.0 (C-3a), 150.4 (C-2), 142.2 (C-3), 141.1 (C-1b), 133.5 (C-6), 132.4 (C-5), 129.1 (C-1e), 127.7 (C-7), 127.4 (C-1c), 127.3 (C-1d), 126.3 (C-1f), 126.3 (C-4a), 118.9 (C-8), 112.6 (C-8a), 56.9 (C-3g), 55.9 (C-1a), 49.6 (C-3f), 47.0 (C-3d), 35.9 (C-3c), 27.2 (C-6b). IR (neat, cm^{-1}): 3293, 3252, 3081, 2974, 2926, 1682, 1654. ESI-HRMS *m/z* $[M+H]^+$ calcd for $C_{24}H_{25}F_3N_3O_4$ 476.1792, found 476.1797.

4.3. *In vitro* Anti-trypanosomal Assay

Trypanosoma brucei brucei 427 trypomastigotes were cultured in Iscove's Modified Dulbecco's Medium (IMDM; Lonza) supplemented with 10 % fetal calf serum,[35] HMI-9 supplement, hypoxanthine and penicillin/streptomycin at 37 °C in a 5 % CO_2 incubator. Serial dilutions of test compounds were incubated with the parasites in 96-well plates for 24 h and residual parasite viability in the wells determined by adding 20 μL of 0.54 mM resazurin in phosphate buffered saline (PBS) and incubating for an additional 2–4 h. Reduction of resazurin to resorufin by viable parasites was assessed by fluorescence readings (excitation 560 nm, emission 590 nm) in a Spectramax M3 plate reader. Fluorescence readings were converted to % parasite viability relative to the average readings obtained from untreated control wells. IC_{50} values were determined by plotting % viability *vs.* log[compound] and performing non-linear regression using GraphPad Prism (v. 5.02) software.

4.4. *In vitro* Cytotoxicity Assay

HeLa cells (Cellonex) were cultured in Dulbecco's modified Eagle's medium (DMEM; Lonza) supplemented with 10 % fetal calf serum and antibiotics (penicillin/streptomycin/amphotericin B) at 37 ºC in a 5 % CO_2 incubator. Cells were plated in 96-well plates at a cell density of 2×10^4 cells per well and grown overnight. Serial dilutions of test compounds were incubated with the cells for an additional 24 h, and cell viability in the wells assessed by adding 20 μL 0.54 mM resazurin in PBS for an additional 2–4 h. Fluorescence readings (excitation 560 nm, emission 590 nm) obtained for the individual wells were converted to % cell viability relative to the average readings obtained from

untreated control wells. Plots of % cell viability *vs*. log[compound] were used to determine IC_{50} values by non-linear regression using GraphPad Prism (v. 5.02).

Supplementary Material

Supplementary information is provided in the online supplement.

Acknowledgements

The authors acknowledge the financial support by the National Research Foundation (SDK), Rhodes University for a Postdoctoral fellowship (RMB) and Rhodes University Sandisa Imbewu (SDK) towards this research. The bioassay component of the project was funded by the South African Medical Research Council (MRC) with funds from National Treasury under its Economic Competitiveness and Support Package awarded to HCH.

[§]ORCID iDs

S.D. Khanye: orcid.org/0000-0003-0725-5738
R.M. Beteck: orcid.org/0000-0002-6282-043X

References

1 R. Brun, R. Schumacher, C. Schmid, C. Kunz and C. Burri, The phenomenon of treatment failures in human African trypanosomiasis, *Trop. Med. Int. Health.*, 2001, **6**, 906–914.

2 WHO. Neglected tropical diseases http://www.who.int/neglected_diseases/diseases/en/ accessed on 14 August 2017.

3 M. Kaiser, M. Bray, M. Cal, B. Trunz, E. Torreele and R. Brun, Antitrypanosomal activity of fexinidazole, a new oral nitroimidazole drug candidate for treatment of sleeping sickness, *Antimicrob. Agents Chemother.*, 2011, **55**, 5602–5608.

4 M. Berninger, I. Schmidt, A. Ponte-Sucreb and U. Holzgrabe, Novel lead compounds in pre clinical development against African sleeping sickness, *Med. Chem. Commun.*, 2017, **8**, 1872–1890.

5 WHO. Trypanosomiasis, human African (Sleeping sickness), http://www.who.int/mediacentre/factsheets/fs259/en/ accessed on 14 August 2017.

6 H.-H. Tran, Z. Zheng, X. Wen, S. Manivannan, A. Pastor, M. Kaiser, R. Brun, F. Snyder and T. Back, Synthesis and activity of nucleoside-based antiprotozoan compounds, *Bioorg. Med. Chem.*, 2017, **25**, 2091–2104.

7 X. Wang, D. Inaoka, T. Shiba, E. Balogun, S. Allmann, Y. Watanabe, M. Boshart, K. Kita and S. Harada, Expression, purification, and crystallization of type 1 isocitrate dehydrogenase from *Trypanosoma brucei brucei*, *Protein Expr. Purif.*, 2017, **138**, 56–62.

8 H. Gordhan, S. Patrick, M. Swasy, A. Hackler, M. Anayee, J. Golden, J. Morris and D. Whitehead, Evaluation of substituted ebselen derivatives as potential trypanocidal agents, *Bioorg. Med. Chem. Lett.*, 2017, **27**, 537–541.

9 M. Beig, F. Oellien, L. Garoff, S. Noack, L. Krauth-Siegel and P. Selzer, Trypanothione reductase: a target protein for a combined *in vitro* and *in silico* screening approach, *PLOS Negl. Trop.*, 2015, **9**, e0003773.

10 I. Kuepfer, E. Hhary, M. Allan, A. Edielu, C. Burri and J. Blum, Clinical presentation of *T. b. rhodesiense* sleeping sickness in second stage patients from Tanzania and Uganda, *PLOS Negl. Trop. Dis.*, 2011, **5**, e968.

11 F. Wamwiri and R. Changasi, Tsetse flies (*Glossina*) as vectors of human African trypanosomiasis: a review, *BioMed. Res. Int.*, 2016, **2016**, 1–8.

12 D. Steverding, The history of African trypanosomiasis, *Parasites & Vectors*, 2008, **1**, 3.

13 M. Banerjee, D. Paraia, P. Dhar, M. Roy, R. Barik, S. Chattopadhyay and S. Mukherje, Andrographolide induces oxidative stress-dependent cell death in unicellular protozoan parasite *Trypanosoma brucei*, *Acta Trop.*, 2017, **176**, 58–67.

14 F. Ranjbarian, M. Vodnala, K. Alzahrani, G. Ebiloma, H. Koning and A. Hofer, 9-(2′-Deoxy-2′-fluoro-β-D-Arabinofuransosyl)adenine is a potent antitrypanosomal adenosine analogue that circumvents transport-related drug resistance, *Antimicrob. Agents Chemother.*, 2017, **61**, e02719–16.

15 L. MacLean, H. Reiber, P. Kennedy and J. Sternberg, Stage progression and neurological symptoms in *Trypanosoma brucei rhodesience* sleeping sickness: role of the CNS inflammatory response, *PLOS Negl. Trop. Dis.*, 2012, **6**, e1857.

16 P. Kennedy, The continuing problem of human African trypanosomiasis (sleeping sickness), *Ann. Neurol.*, 2008, **64**, 116–126.

17 N. Tiberti, A, Hainard and J.-C. Sanchez, Translation of human African trypanosomiasis biomarkers towards field application, *Transl. Prot.*, 2013, **12**, 12–24.

18 P. Babokhov, A. Sanyaolu, W. Oyibo, A. Fagbenro-Beyioku and N. Iriemenam, A current analysis of chemotherapy strategies for the treatment of human African trypanosomiasis, *Pathog. Glob. Health*, 2013, **107**, 242–252.

19 J. Song, N. Baker, M. Rothert, B. Henke, L. Jeacock, D. Horn and E. Beitz, Pentamidine is not a permeant but a nanomolar inhibitor of the *Trypanosoma brucei* aquaglyceroporin-2, *PLOS Pathog.*, 2016, **12**, e1005436.

20 E. Alirol, D. Schrumpf, J. Amici Heradi, A. Riedel, C. de Patoul, M. Quere and F. Chappuis, Nifurtimox-eflornithine combination therapy for second-stage gambiense human African trypanosomiasis: Médecins San Frontières experience in the Democratic Republic of Congo, *Clin. Infect. Dis.*, 2013, **56**, 195–203.

21 R. Jacobs, B. Nare and M. Phillips, State of the art in African trypanosome drug discovery, *Curr. Top. Med. Chem.*, 2011, **11**, 1255–1274.

22 M. Barrett, D. Boykin, R. Brun and R. Tidwe, Human African trypanosomiasis: pharmacological re-engagement with a neglected disease, *Br. J. Pharmacol.*, 2007, **152**, 1155–1171.

23 D. Malvy and F. Chappuis, Sleeping sickness, *Clin. Microbiol. Infect.*, 2011, **17**, 986–995.

24 G. Pohlig, S.C. Bernhard, J. Blum, C. Burri, A. Mpanya, J.-P. Fina Lubaki, A. Mpoto, B. Munungu, M. Bilenge, V. Mesu, J. Franco, N. Dituvanga, R. Tidwell and C. Olson, Efficacy and safety of pafuramidine versus pentamidine maleate for treatment of first stage sleeping sickness in a randomized, comparator-controlled, international phase 3 clinical trial, *PLOS Negl. Trop. Dis.*, 2016, **10**, e0004363.

25 P. Kennedy, Clinical features, diagnosis, and treatment of human African tripanosomiasis (sleeping sickness), *Lancet Neurol.*, 2013, **12**, 186–194.

26 C. Burri, Chemotherapy against human African tripanosomiasis: Is there a road to success?, *Parasitol.*, 2010, **137**, 1987–1994.

27 R. Beteck, F. Smit, R. Haynes and D. N'Da, Recent progress in the development of anti-malarial quinolones, *Mal. J.*, 2014, **13**, 339.

28 E. Nenortas, C. Burri and T. Shapiro, Antitrypanosomal activity of fluoroquinolones, *Antimicrob. Agents Chemother.*, 1999, **43**, 2066–2068.

29 J. Keiser and C. Burri, Antitrypanosomal activities of fluoroquinolones with pyrrolidinyl substitutions, *Trop. Med. Inter. Health.*, 2001, **6**, 369–389.

30 E. Nenortas, C. Burri, T. Kulikowicz and T. Shapiro, Antitrypanosomal activities of fluoroquinolones with pyrrolidinyl substitutions, *Antimicrob. Agents Chemother.*, 2003, **47**, 3015–3017.

31 G. Hiltensperger, N. Jones, S. Niedermeier, A. Stich, M. Kaiser, J. Jung, S. Puhl, A. Damme, H. Braunschweig, L. Meinel, M. Engstler and U. Holzgrabe, Synthesis and structure-activity relationships of new quinolone-type molecules against *Trypanosoma brucei*, *J. Med. Chem.*, 2012, **55**, 2538–2548.

32 A. Wube, A. Hüfner, W. Seebacher, M. Kaiser, R. Brun, R. Bauer and F. Bucar, 1,2-Substituted 4-(1*H*)-quinolones: synthesis, antimalarial and antitrypanosomal activities *in vitro*, *Molecules*, 2014, **19**, 14204–142020.

33 A. Gamble, J. Garner, C. Gordon, S. Conner and P. Keller, Aryl nitro reduction with iron powder or stannous chloride under ultrasonic irradiation, *Syn. Comm.*, 2007, **37**, 2777–2786.

34 Richard M. Beteck, D. Coertzen, F.J. Smit, L.-M. Birkholtz, R.K. Haynes and D.D. N'Da, Straightforward conversion of decoquinate into inexpensive tractable new derivatives with significant antimalarial activities, *Boorg. Med. Chem. Lett.*, 2016, **26**, 3006–3009.

35 H. Hirumi and K. Hirumi, Continous cultivation of *Trypanosoma brucei* blood stream forms in a medium containing a low concentration of serum protein without feeder cell layers, *J. Parasitol.*, 1989, **75**, 985–989.

Supplementary material to:

R.M. Beteck, M. Isaacs, H.C. Hoppe and S.D. Khanye,

Synthesis, *in vitro* Cytotoxicity and Trypanocidal Evaluation of Novel 1,3,6-Substituted Non-fluoroquinolones

S. Afr. J. Chem., 2018, **71**, 188–195.

Synthesis, *in vitro* cytotoxicity and trypanocidal evaluation of novel 1,3,6-substituted non-fluoroquinolones.

Richard M. Beteck[a,], Michelle Isaacs[c], Heinrich C. Hoppe[b,c], Setshaba D. Khanye[a,c,d,*]*

[a]Department of Chemistry, Rhodes University, Grahamstown 6140, South Africa

[b]Department of Biochemistry and Microbiology, Rhodes University, Grahamstown 6140, South Africa

[c]Centre for Chemico- and Biomedical Research, Rhodes University, Grahamstown 6140, South Africa

[d]Faculty of Pharmacy, Rhodes University, Grahamstown 6140, South Africa

* Corresponding Author. Tel.: +27 46 603 8397; fax: +27 46 603 7506.

E-mail: R.Beteck@ru.ac.za

* Corresponding Author. Tel.: +27 46 603 8397; fax: +27 46 603 7506.

E-mail: s.khanye@ru.ac.za

NMR (^{1}H, ^{13}C, DEPT135) AND MS SPECTRA AND BIOLOGICAL DATA OF COMPOUNDS

Compound 3a

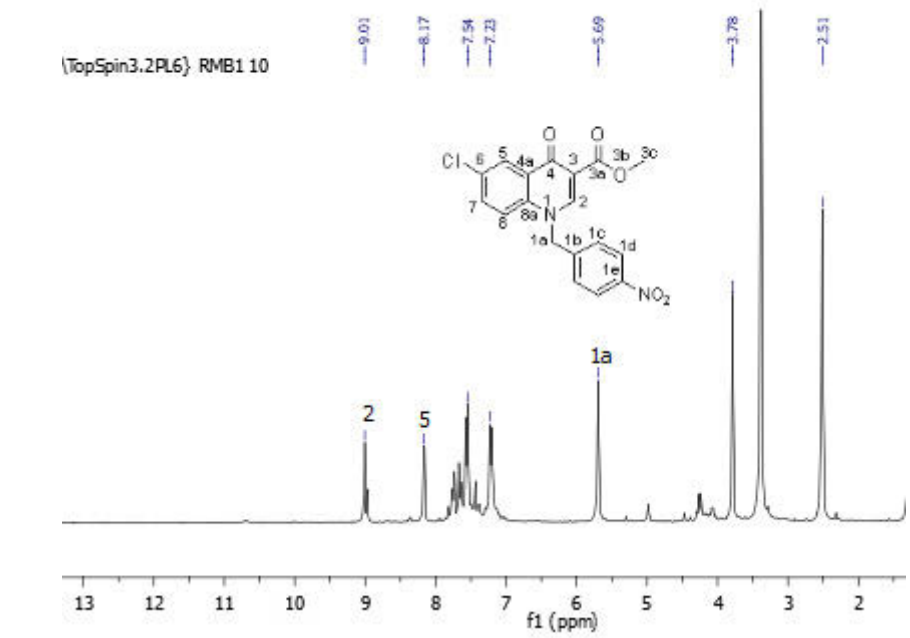

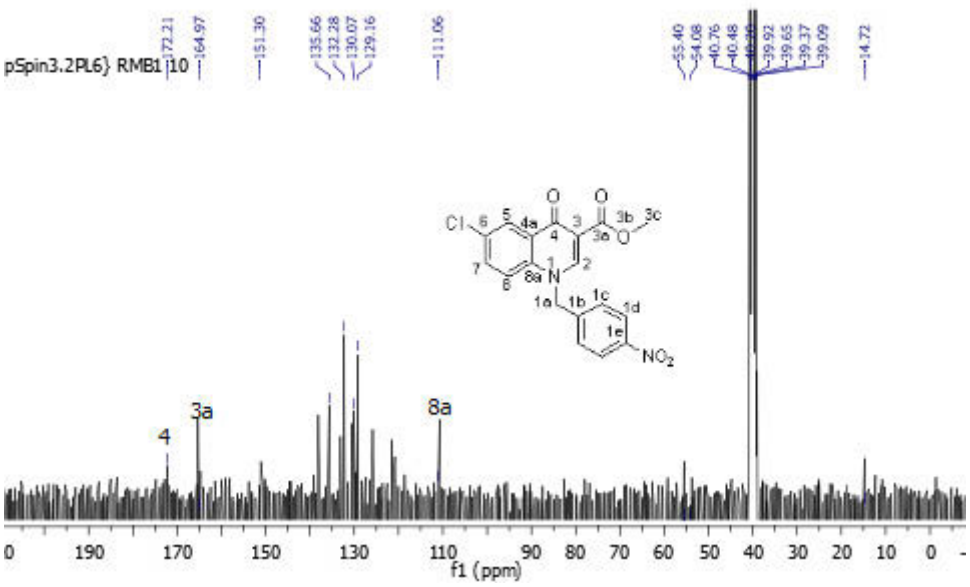

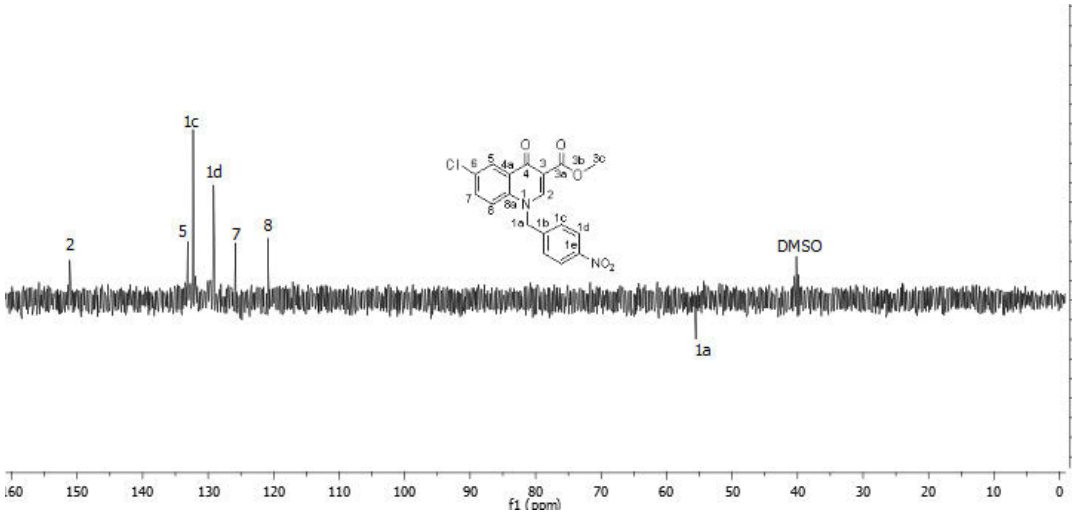
1c
1d
2
5
7
8
DMSO
1a
f1 (ppm)

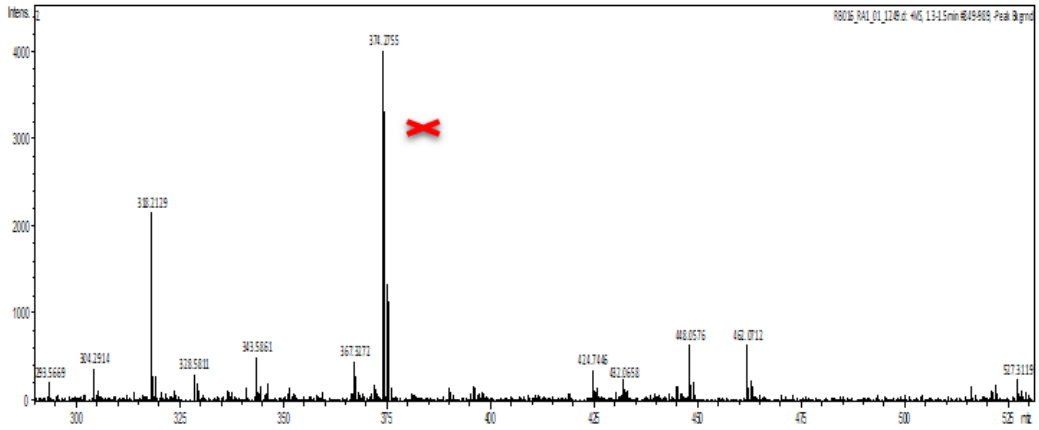
374.1755
318.2129
304.2914
328.5811
343.5861
367.3272
414.7446
432.0658
460.0576
462.0712
527.3119
m/z

Compound 3b

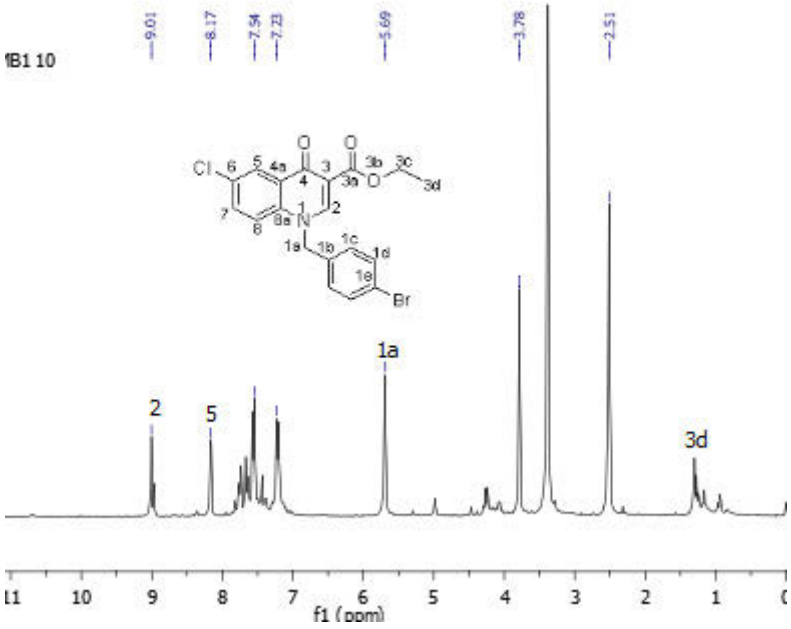
9.01
8.17
7.54
7.23
5.69
3.78
2.51
1a
2
5
3d
f1 (ppm)

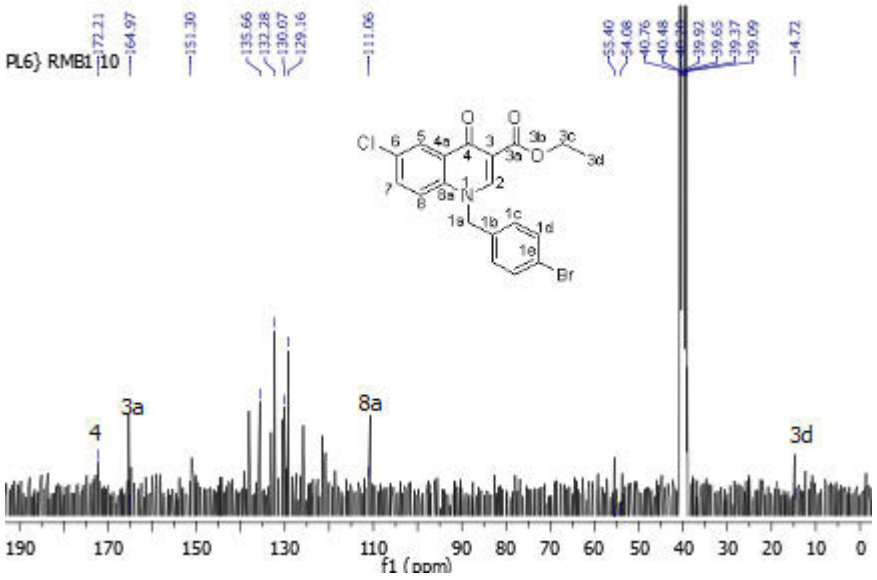

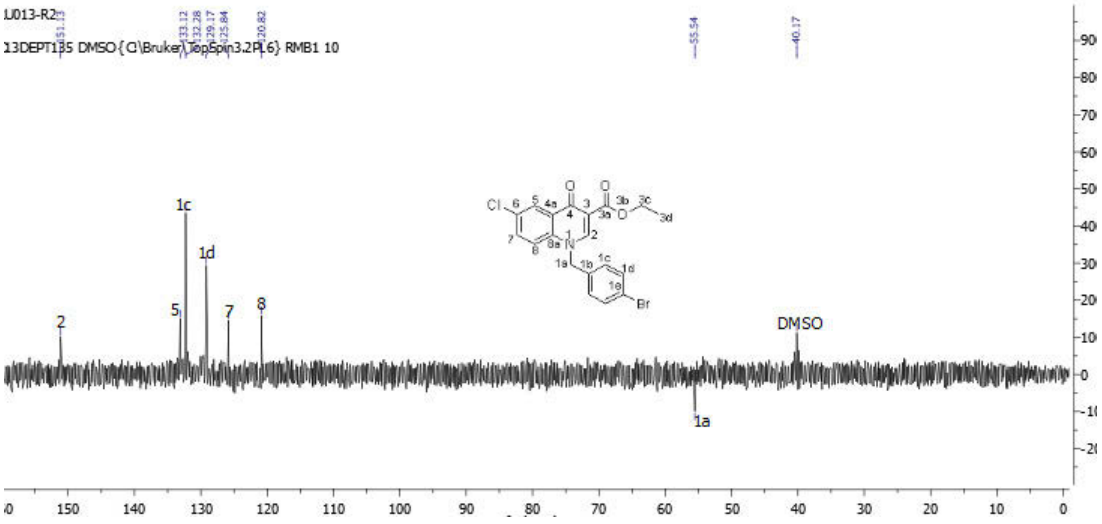

Mass	Calc. Mass	mDa	PPM	DBE	Formula	i-FIT	i-FIT Norm	Fit Conf %	C	H	N	O	Cl	Br
419.9998	420.0002	-0.4	-1.0	11.5	C19 H16 N O3 Cl Br	430.7	2.399	9.08	19	16	1	3	1	1
	420.0002	-0.4	-1.0	3.5	C8 H15 N5 O10 Br	440.3	12.042	0.00	8	15	5	10		1
	419.9992	0.6	1.4	18.5	C20 H6 N O10	454.0	25.711	0.00	20	6	1	10		
	420.0005	-0.7	-1.7	23.5	C21 H2 N5 O6	454.1	25.746	0.00	21	2	5	6		
	419.9984	1.4	3.3	16.5	C20 H11 N3 O3 Br	438.3	9.989	0.00	20	11	3	3		1
	419.9983	1.5	3.6	14.5	C15 H7 N5 O8 Cl	443.2	14.892	0.00	15	7	5	8	1	
	420.0021	-2.3	-5.5	-1.5	C7 H20 N3 O10 Cl Br	438.1	9.763	0.01	7	20	3	10	1	1
	420.0023	-2.5	-6.0	18.5	C20 H7 N3 O6 Cl	442.7	14.371	0.00	20	7	3	6	1	
	420.0024	-2.6	-6.2	20.5	C25 H11 N O Br	439.0	10.669	0.00	25	11	1	1		1

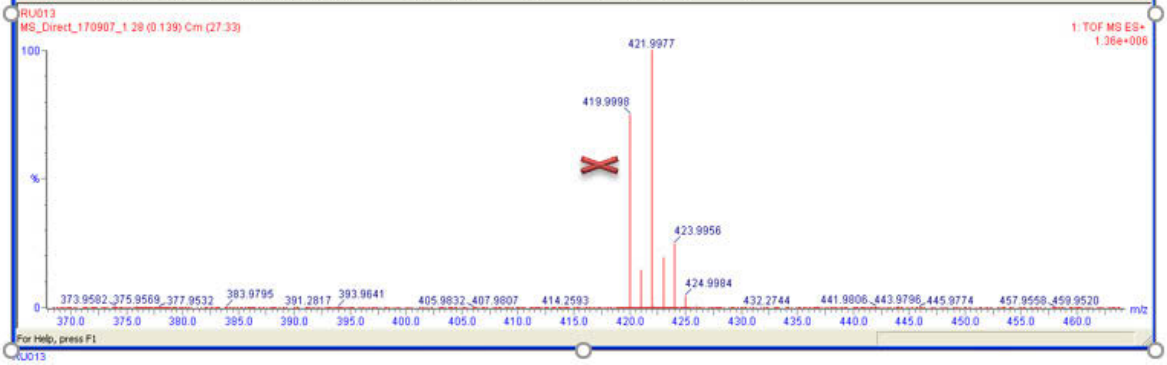

Compound 3c

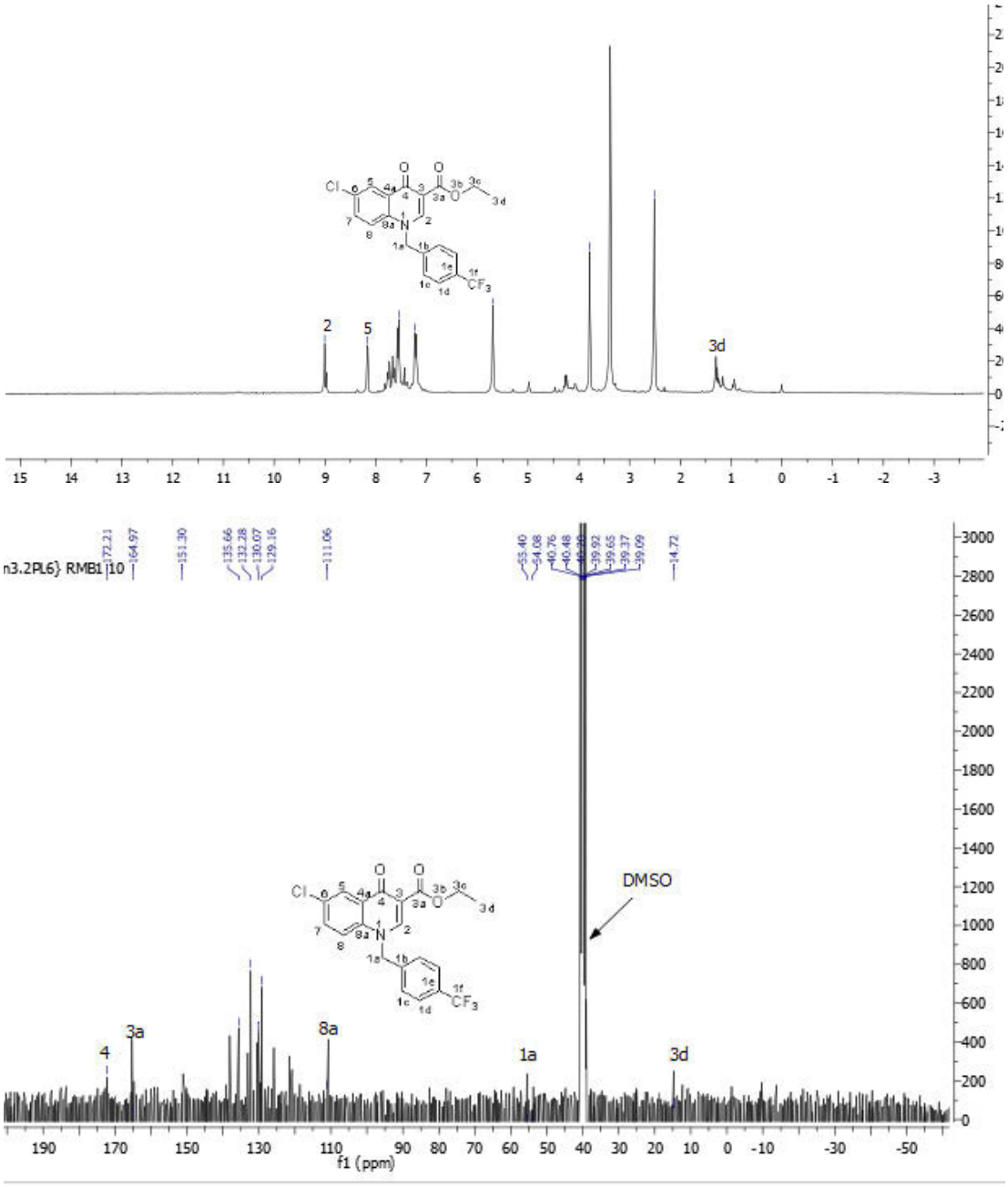

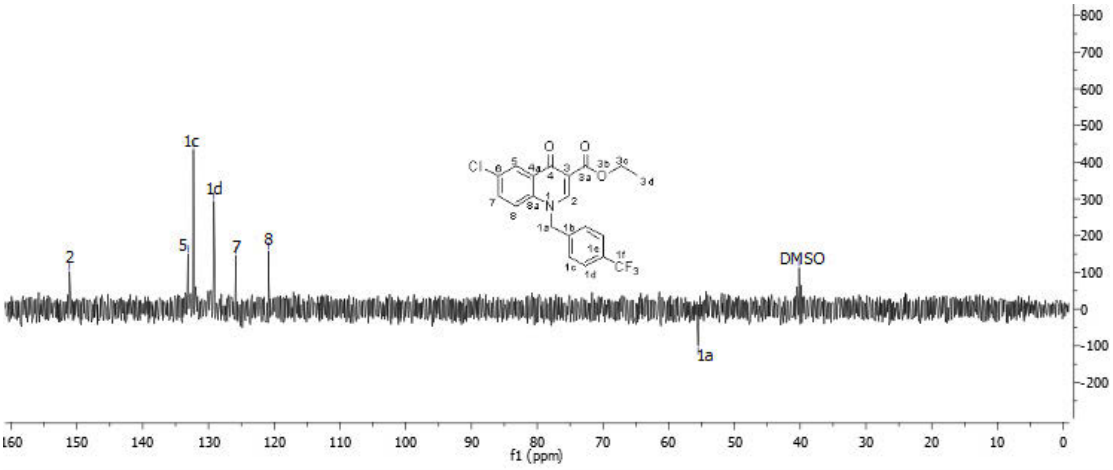
1c
1d
2
5
7
8
DMSO
1a
f1 (ppm)

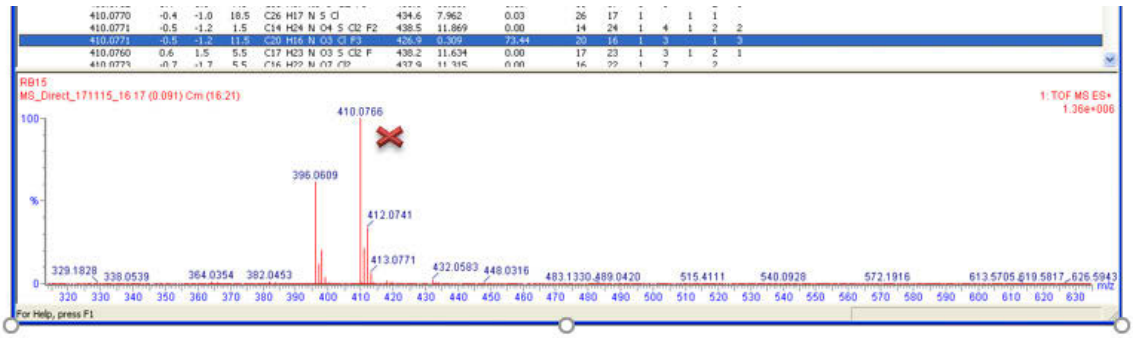
RB15
MS_Direct_171115_16.17 (0.091) Cm (16:21)
1: TOF MS ES+
410.0766
396.0609
412.0741
413.0771
329.1828
338.0539
364.0354
382.0453
432.0583
448.0316
For Help, press F1

Compound 3d

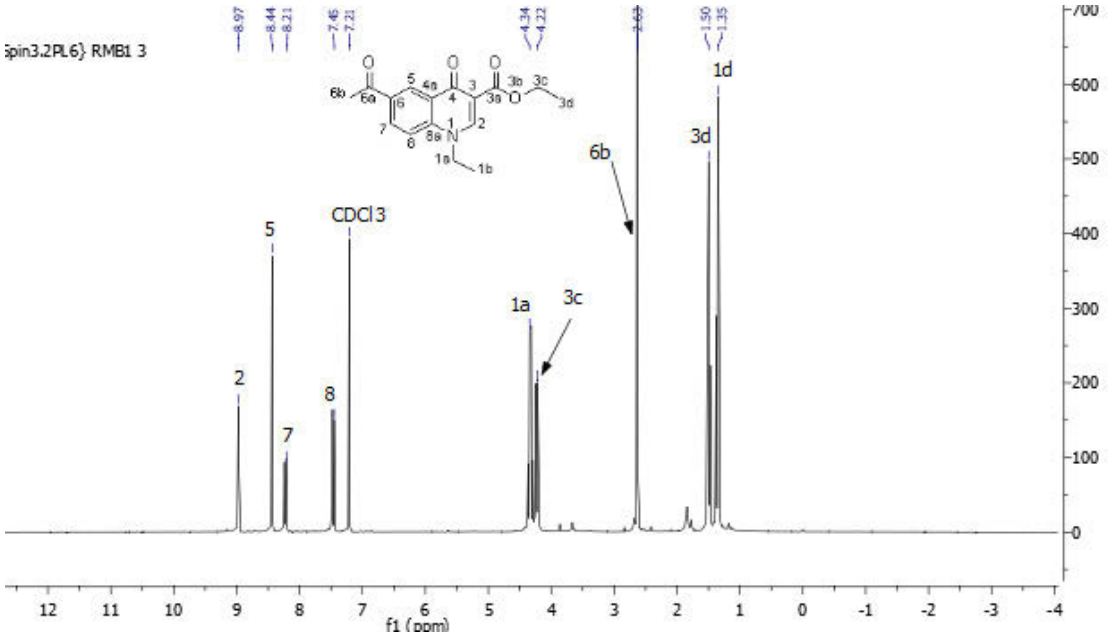
8.97
8.44
8.21
7.46
7.21
4.34
4.22
2.62
1.50
1.35
1d
3d
6b
CDCl3
5
1a
3c
2
8
7
f1 (ppm)

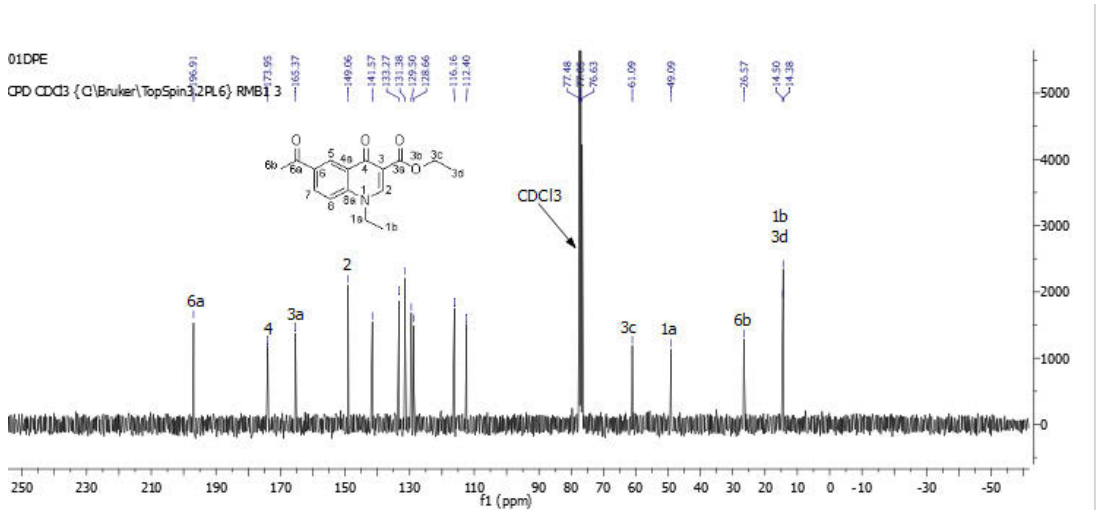

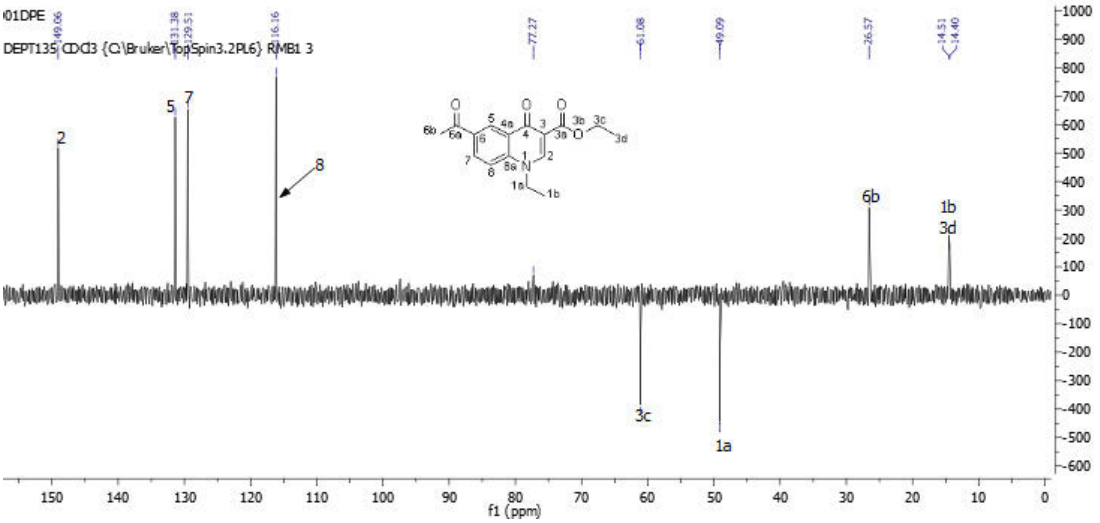

Mass	Calc. Mass	mDa	PPM	DBE	Formula	i-FIT	i-FIT Norm	Fit Conf %	C	H	N	O
288.1234	288.1236	-0.2	-0.7	8.5	C16 H18 N O4	204.7	5.403	0.45	16	18	1	4
	288.1249	-1.5	-5.2	13.5	C17 H14 N5	208.3	8.974	0.01	17	14	5	
	288.1196	3.8	13.2	4.5	C11 H18 N3 O6	205.4	6.103	0.22	11	18	3	6
	288.1308	-7.4	-25.7	4.5	C10 H18 N5 O5	208.0	8.694	0.02	10	18	5	5
	288.1155	7.9	27.4	0.5	C6 H18 N5 O8	212.8	13.455	0.00	6	18	5	8
	288.1137	9.7	33.7	13.5	C18 H14 N3 O	210.2	10.914	0.00	18	14	3	1
	288.1348	-11.4	-39.6	8.5	C15 H18 N3 O3	205.0	5.701	0.33	15	18	3	3
	288.1097	13.7	47.5	9.5	C13 H14 N5 O3	199.3	0.010	98.96	13	14	5	3

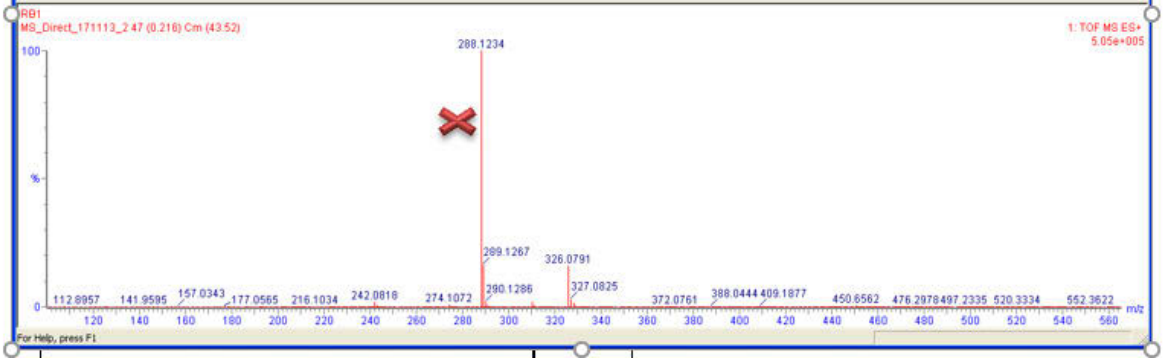

Compound 3e

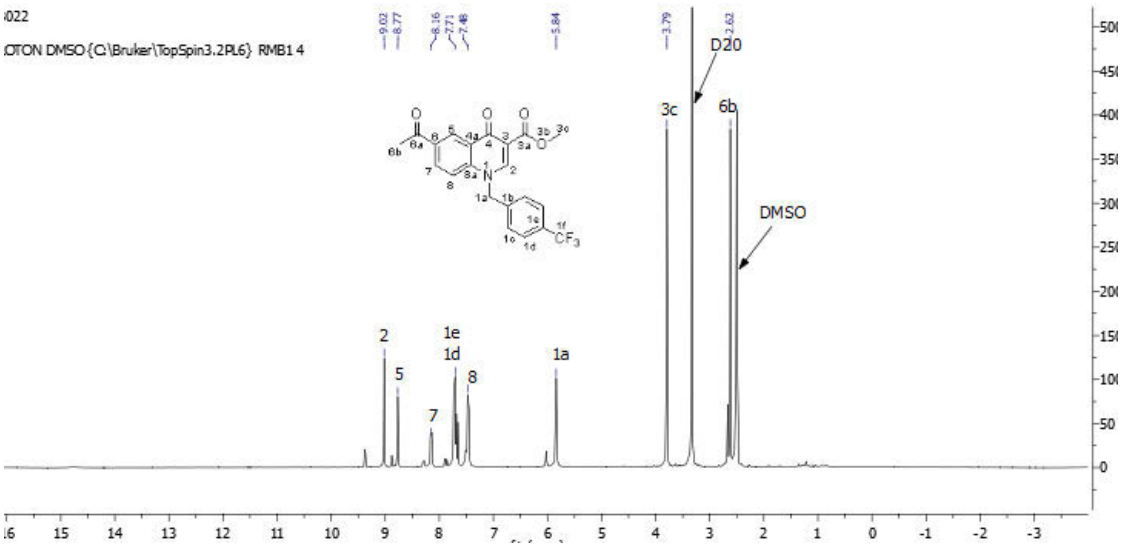
D20
3c
6b
DMSO
2
5
1e
1d
8
7
1a

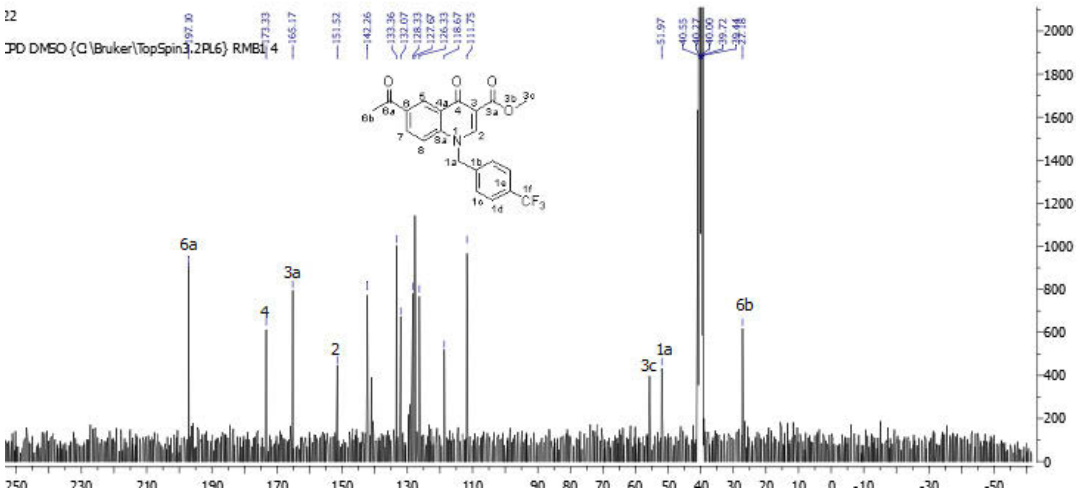
6a
3a
4
2
3c
1a
6b

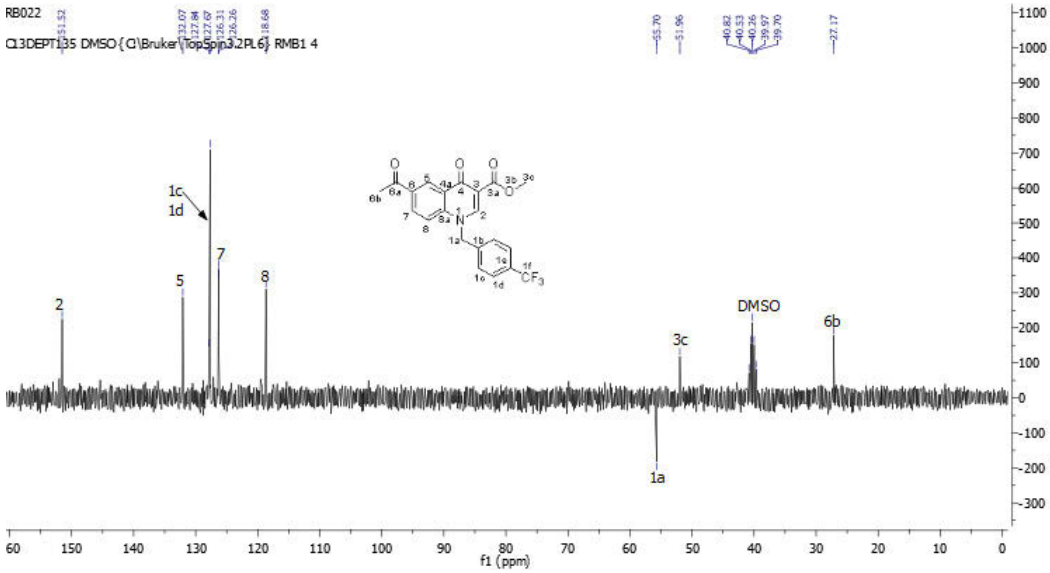
1c
1d
7
5
8
2
DMSO
3c
6b
1a
f1 (ppm)

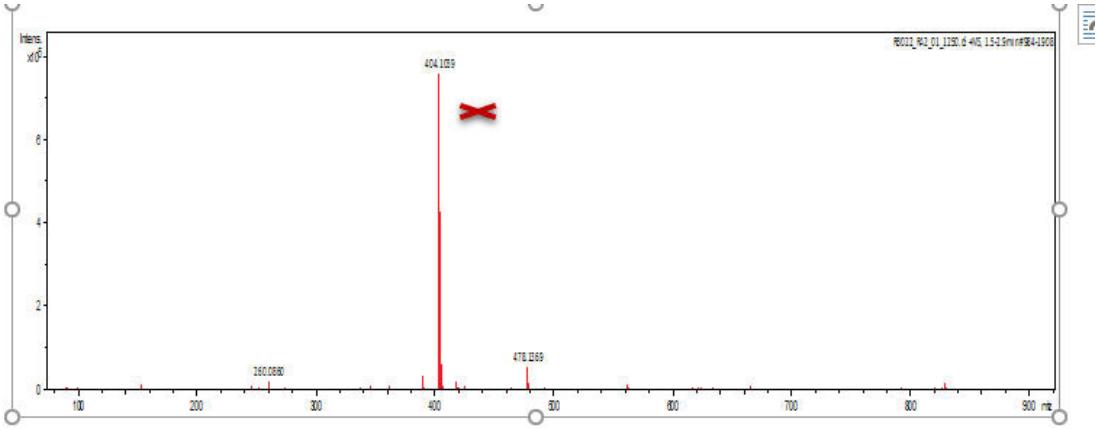
404.1159
478.1369
260.0880

Compound 3f

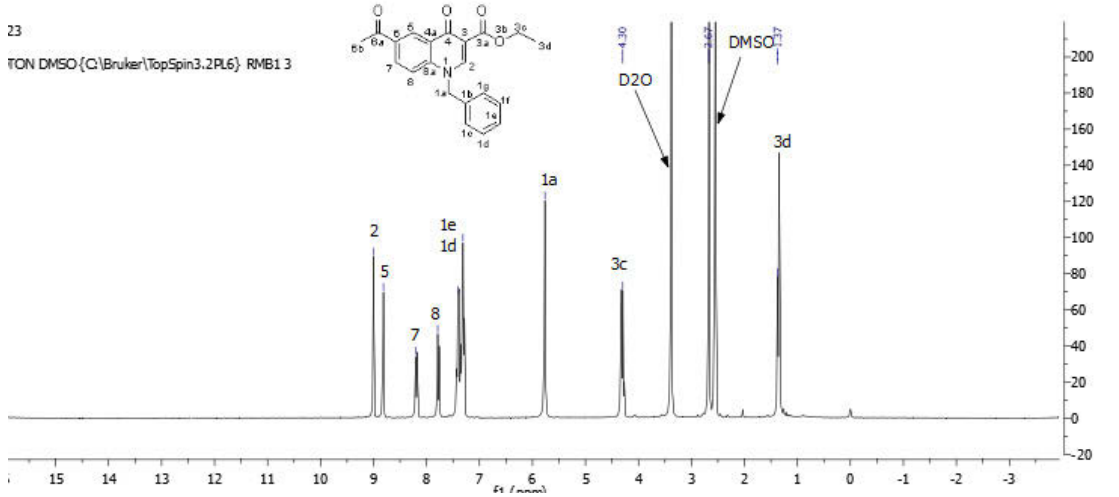
DMSO
D2O
1a
2
5
1e
1d
7
8
3c
3d

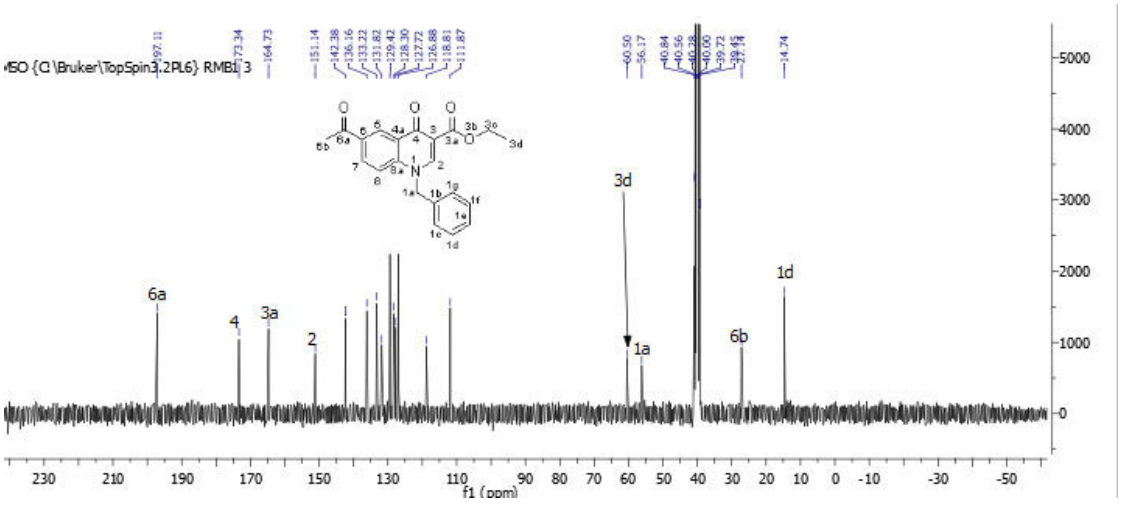
6a
4
3a
2
3d
1a
6b
1d

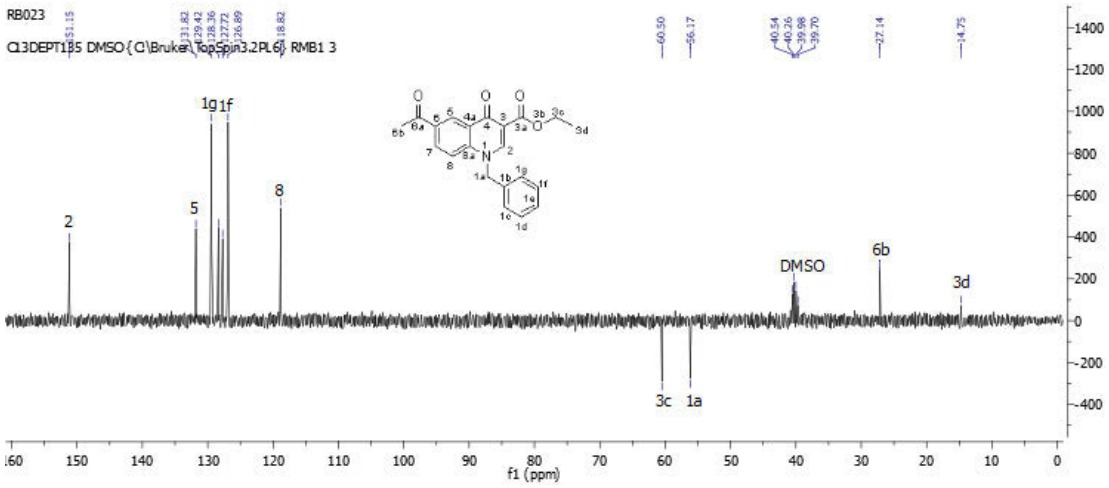
RB023
C13DEPT135 DMSO{C:\Bruker\TopSpin3.2PL6} RMB1 3
1g
1f
2
5
8
DMSO
6b
3d
3c
1a
f1 (ppm)

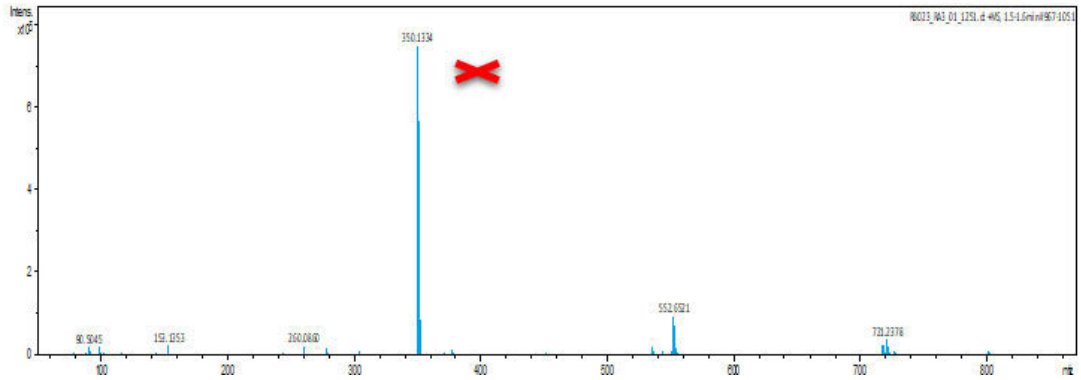
Intens.
350.1334
552.0521
720.2378
m/z

Compound 3g

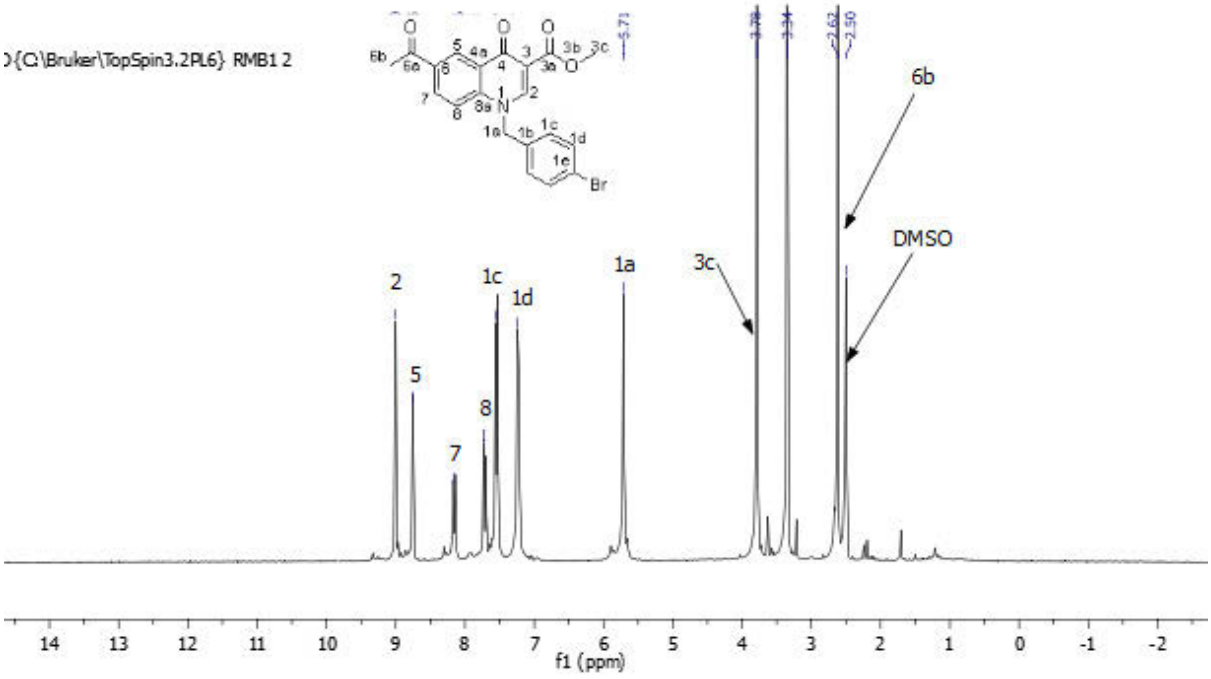
){C:\Bruker\TopSpin3.2PL6} RMB1 2
Br
6b
DMSO
1a
3c
2
1c
1d
5
8
7
f1 (ppm)

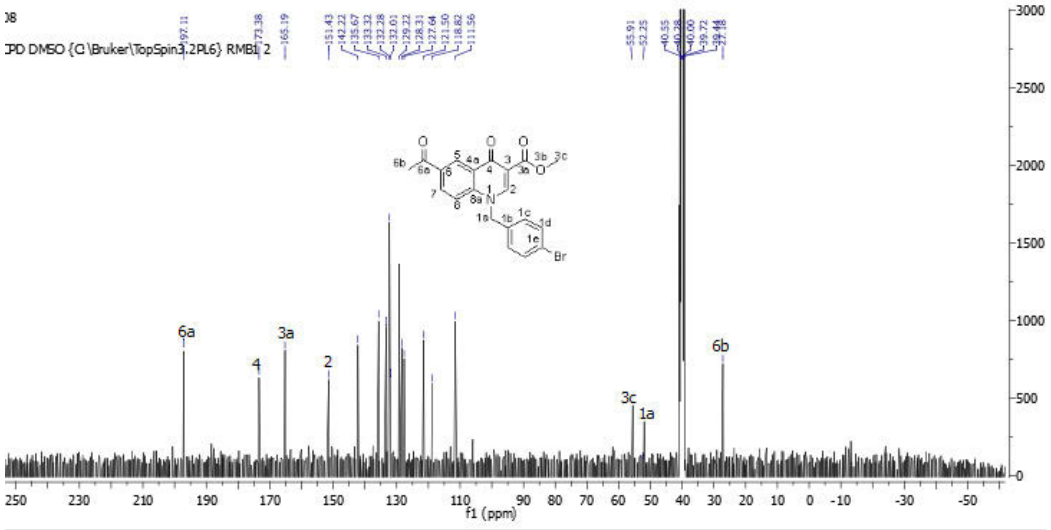
JPD DMSO {C:\Bruker\TopSpin3.2PL6} RMB1 2
6a
3a
4
2
3c
1a
6b
f1 (ppm)

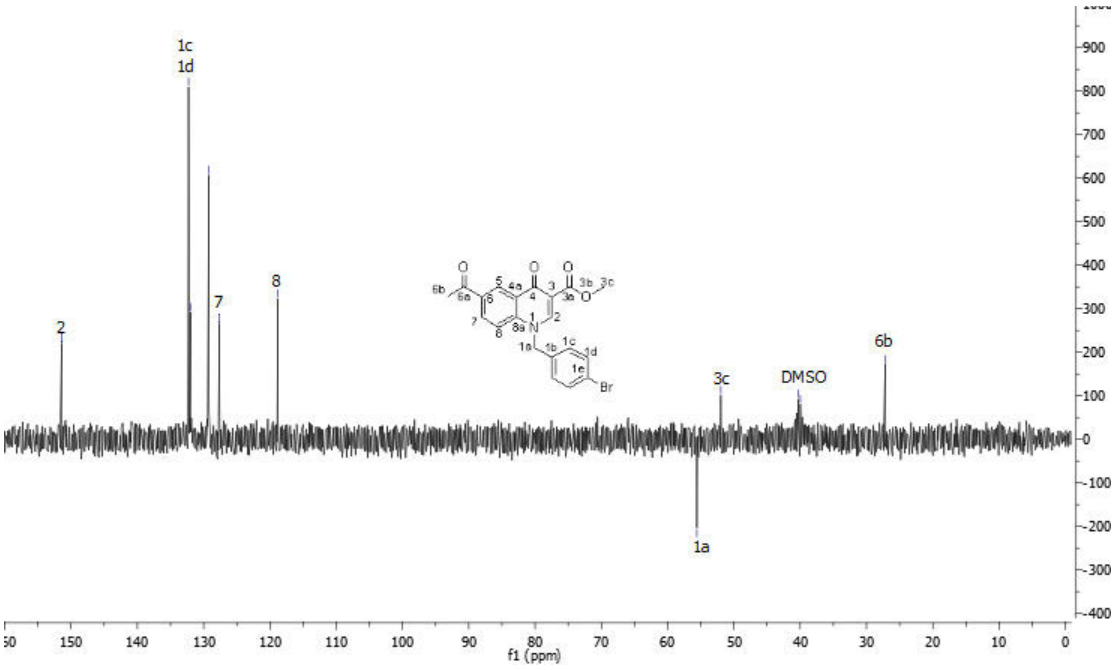
1c
1d
2
7
8
3c
DMSO
6b
1a
f1 (ppm)

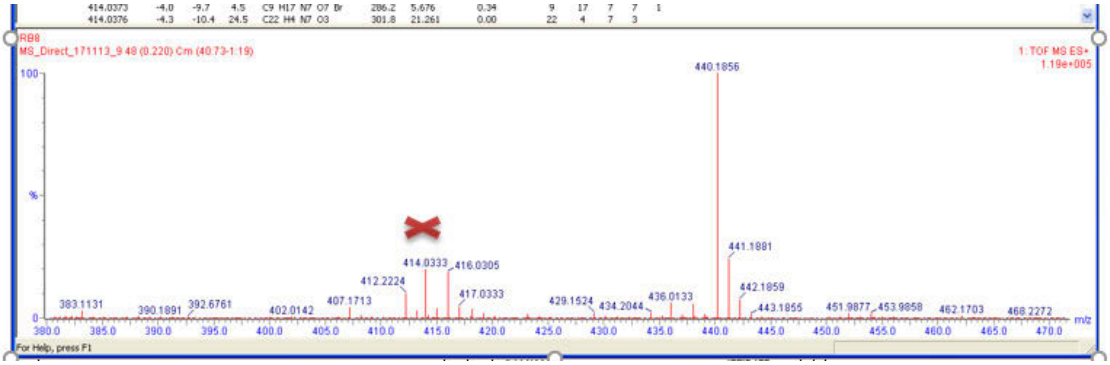
RB8
MS_Direct_171113_9 48 (0.220) Cm (40:73-1:19)
1: TOF MS ES+
1.19e+005
440.1856
441.1881
442.1859
414.0333
416.0305
412.2224
417.0333
383.1131
390.1891
392.6761
402.0142
407.1713
429.1524
434.2044
436.0133
443.1855
451.9877
453.9858
462.1703
468.2272
m/z

Compound 3h

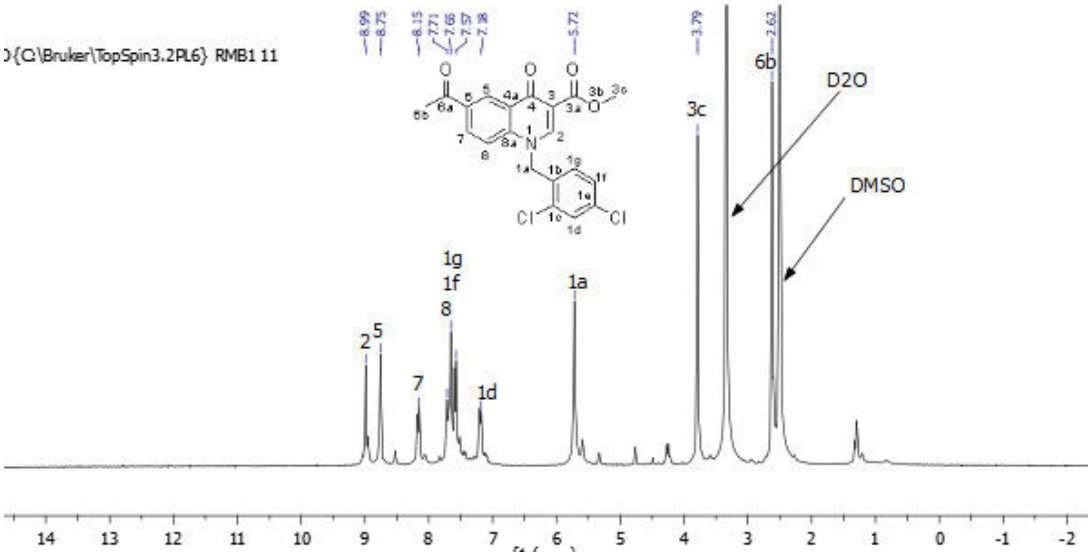
6b
D2O
3c
DMSO
1g
1f
8
2
5
7
1d
1a

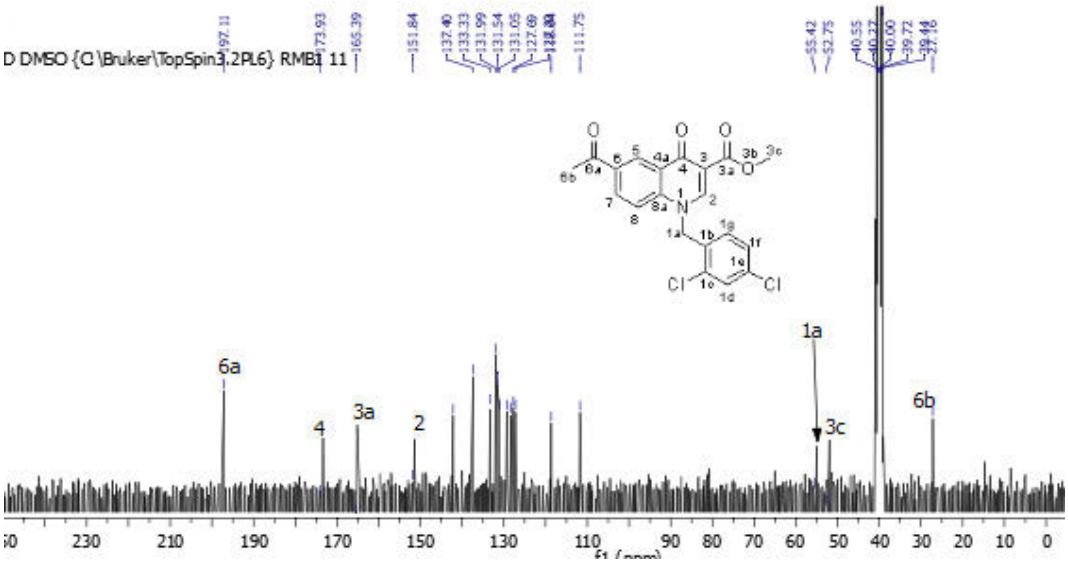
6a
4
3a
2
1a
3c
6b

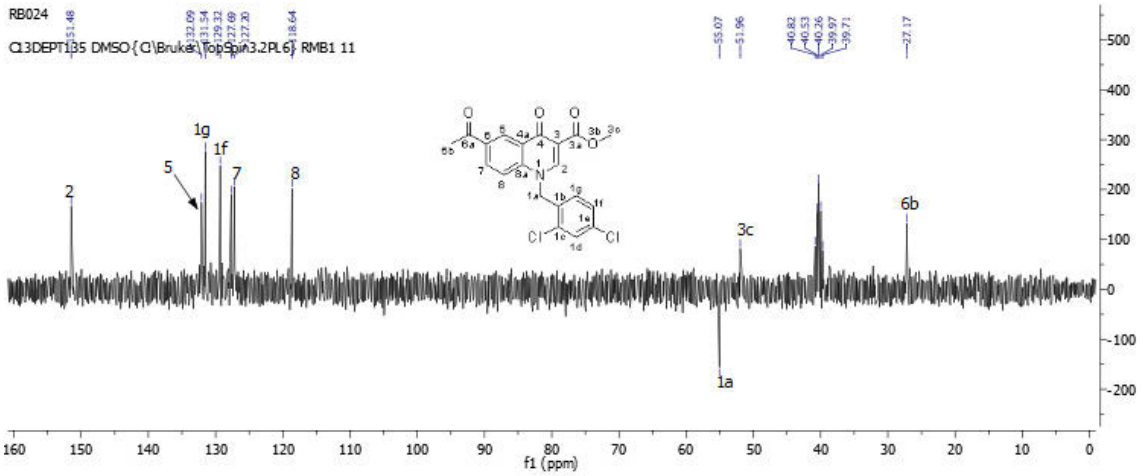
1g
1f
5
7
8
2
3c
6b
1a
f1 (ppm)

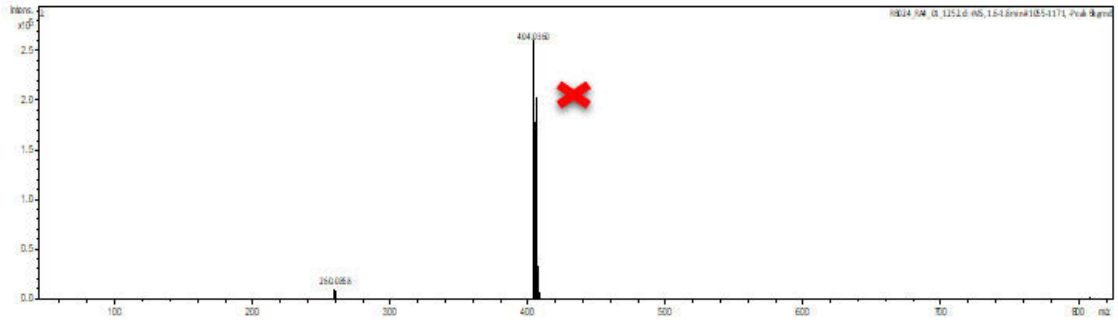

Compound 4a

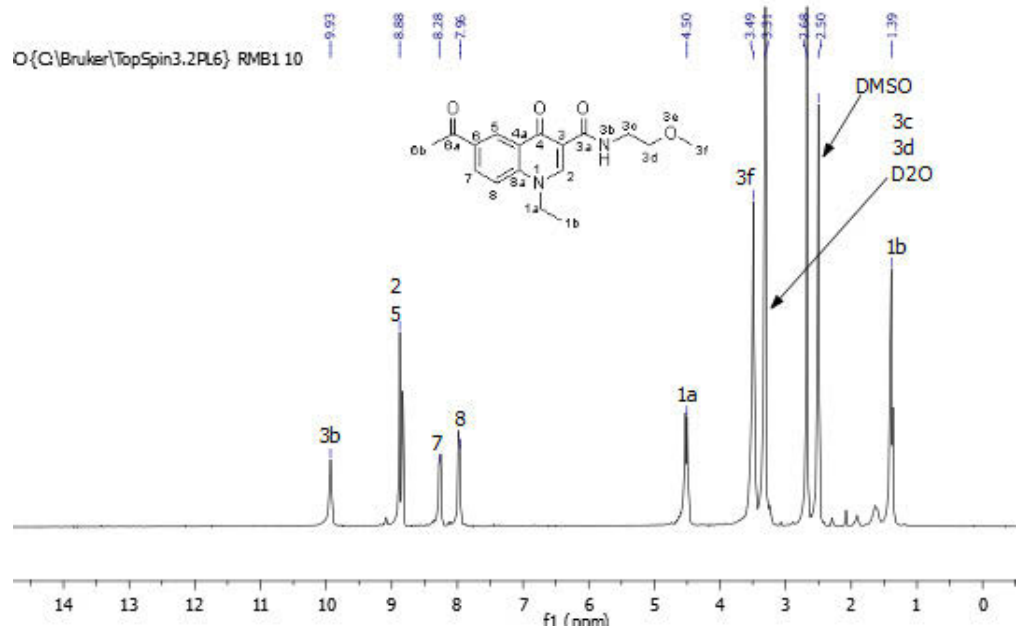
O{C:\Bruker\TopSpin3.2PL6} RMB1 10
9.93
8.88
8.28
7.96
4.50
3.49
3.31
2.68
2.50
1.39
DMSO
3c
3d
D2O
3f
1b
2
5
1a
3b
8
7
f1 (ppm)

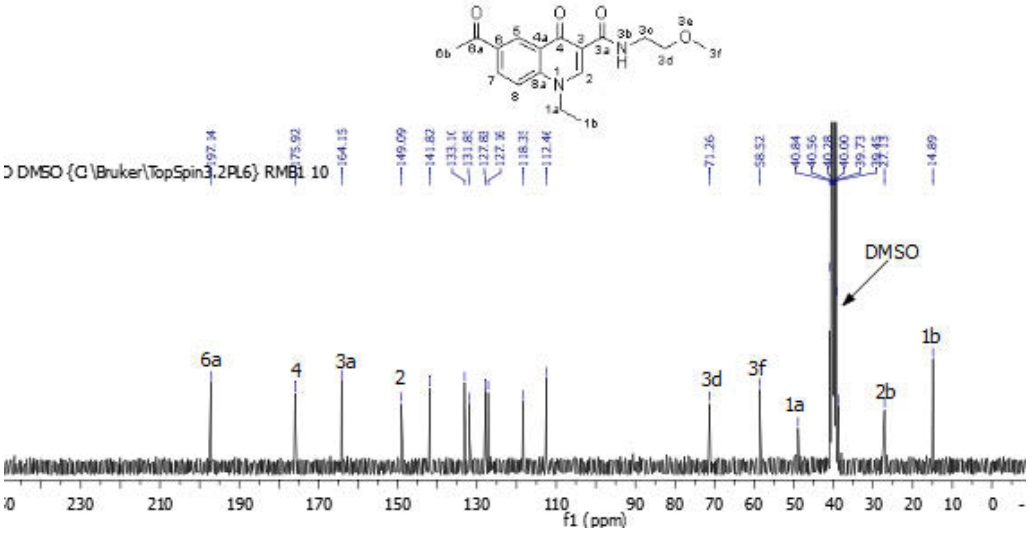
DMSO {C:\Bruker\TopSpin3.2PL6} RMB1 10
197.34
175.92
164.15
149.09
141.82
133.16
131.81
127.81
127.36
118.31
112.44
71.26
58.52
40.84
40.56
40.28
40.00
39.73
39.45
27.15
14.89
DMSO
6a
4
3a
2
3d
3f
1a
2b
1b
f1 (ppm)

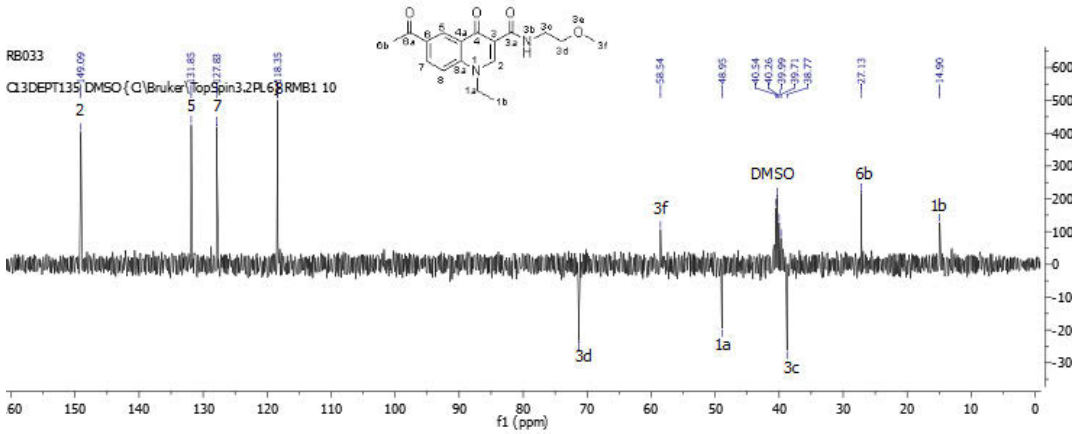
RB033
C13DEPT135 DMSO {C:\Bruker\TopSpin3.2PL6\RMB1 10
2
5
7
DMSO
6b
1b
3f
3d
1a
3c
f1 (ppm)

Compound 4b

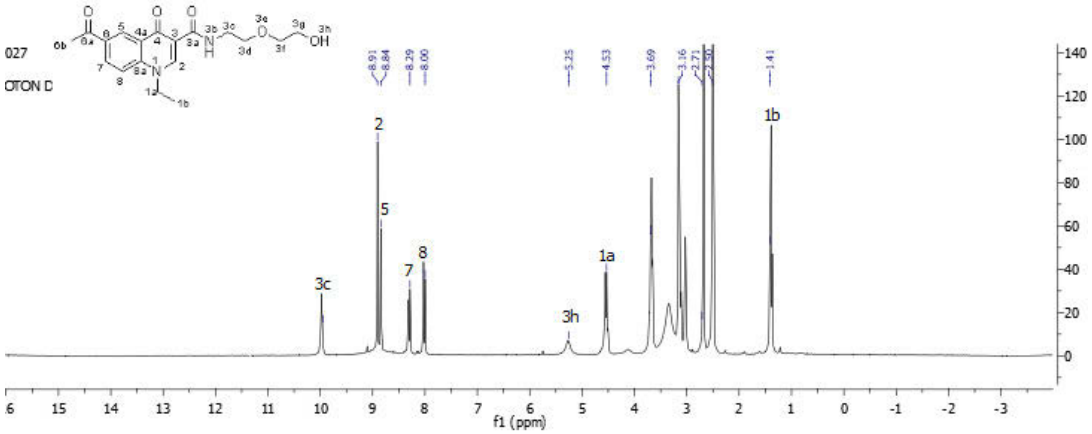
027
OTON D
2
5
7
8
3c
3h
1a
1b
f1 (ppm)

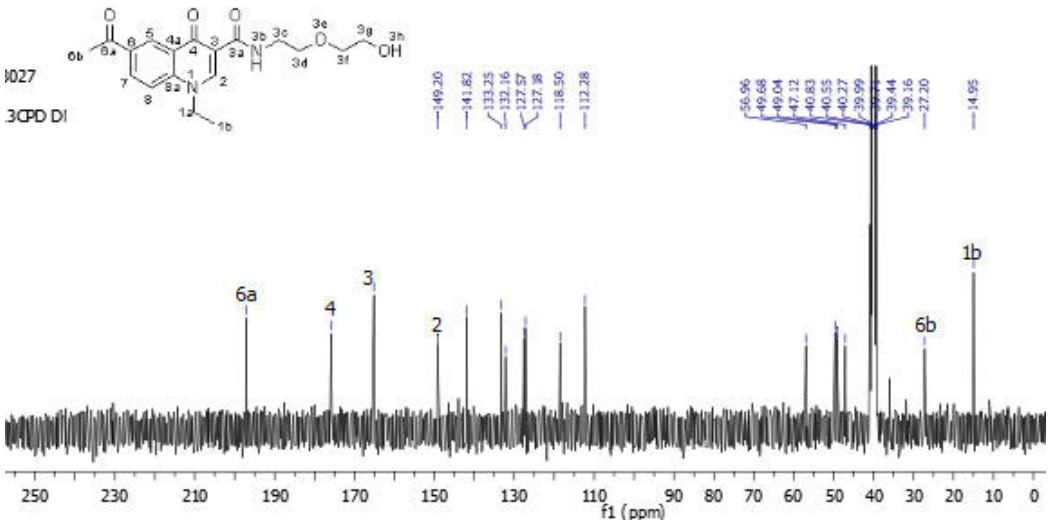
027
3CPD DI
6a
4
3
2
6b
1b
f1 (ppm)

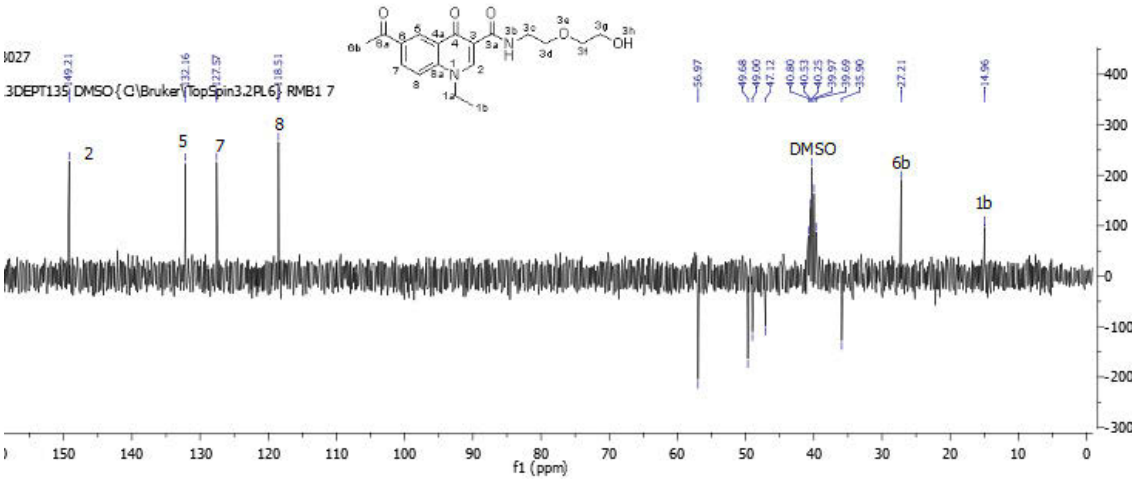

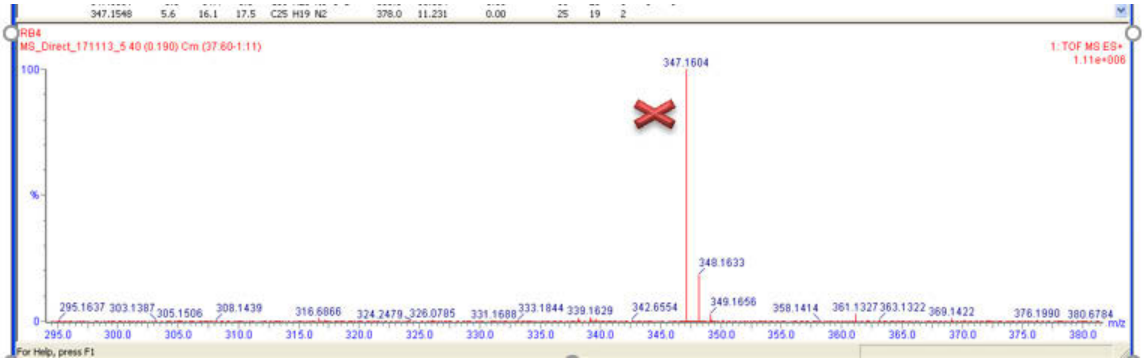

COMPOUND 4c

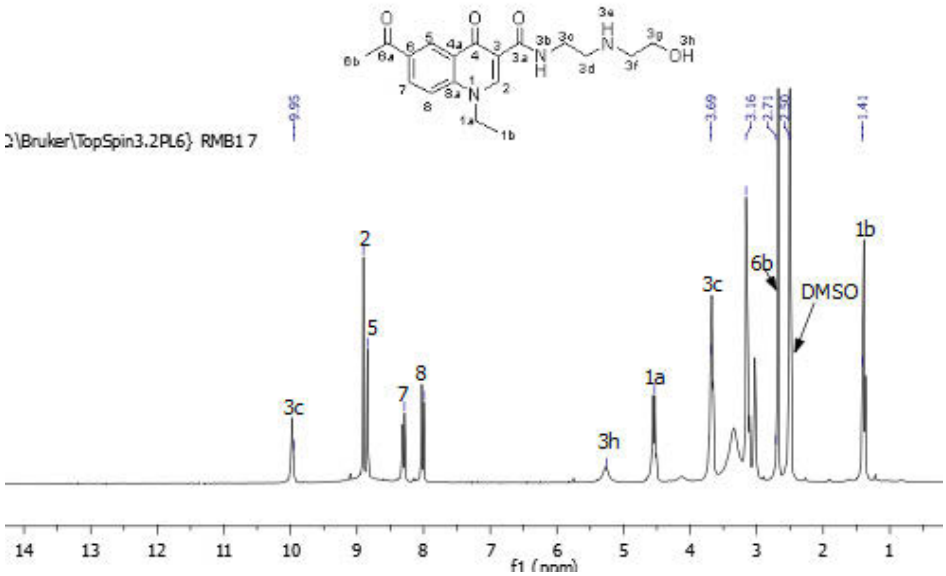

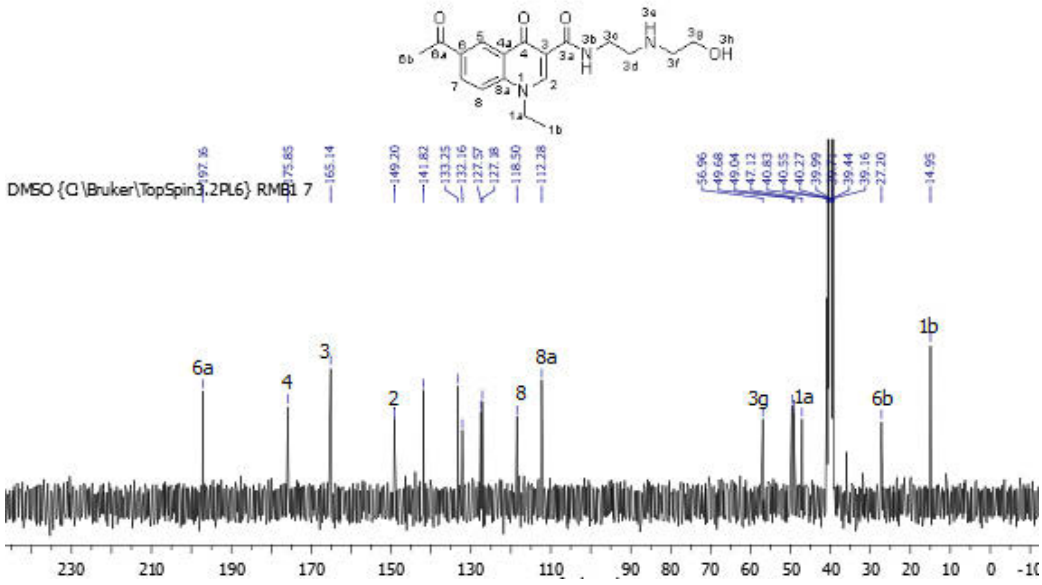
DMSO {C:\Bruker\TopSpin3.2PL6} RMB1 7
6a
4
3
2
8
8a
3g
1a
6b
1b

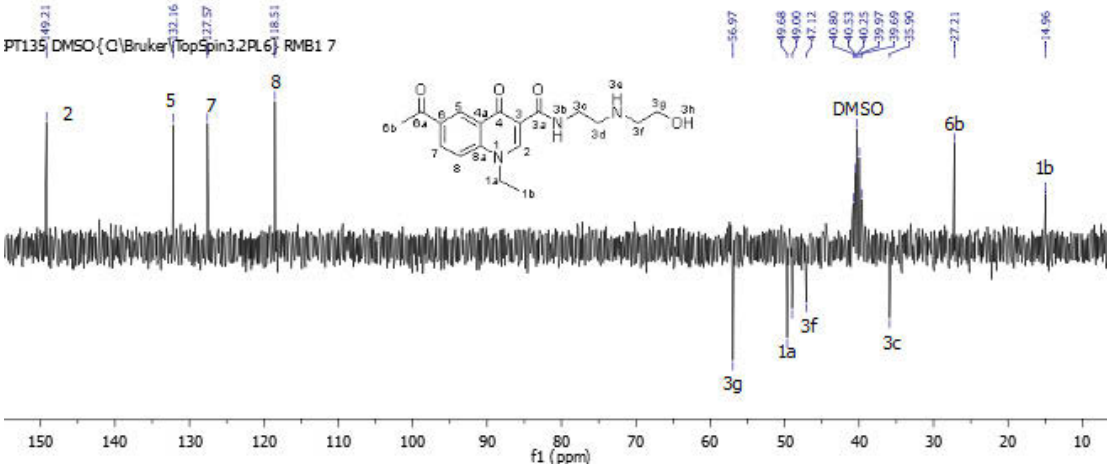
PT135 DMSO {C:\Bruker\TopSpin3.2PL6} RMB1 7
2
5
7
8
DMSO
6b
1b
3g
1a
3f
3c
f1 (ppm)

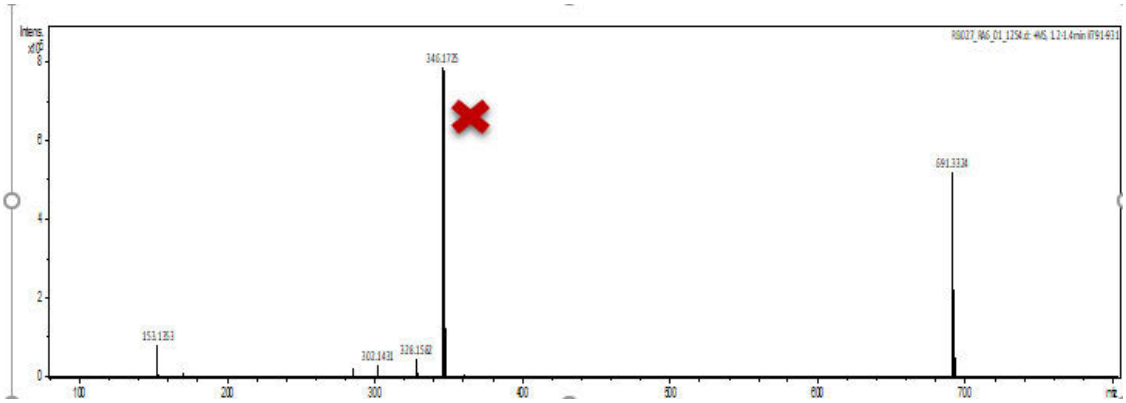
Intens.
346.1725
691.3334
151.1353
302.1431
326.1582
m/z

COMPOUND 4d

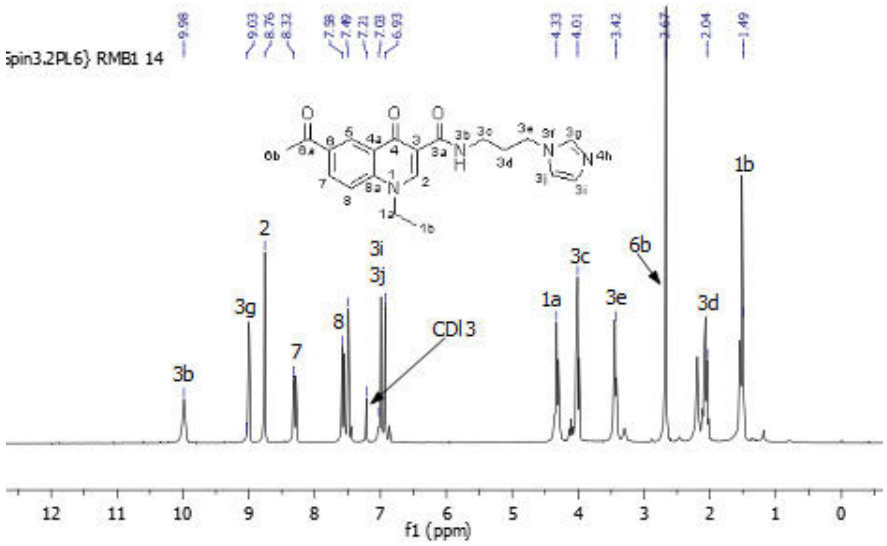
9.98
9.03
8.76
8.32
7.98
7.49
7.21
7.08
6.93
4.33
4.01
3.42
3.67
2.04
1.49
2
3g
7
8
3i
3j
CDl3
3b
1a
3c
3e
6b
3d
1b
f1 (ppm)

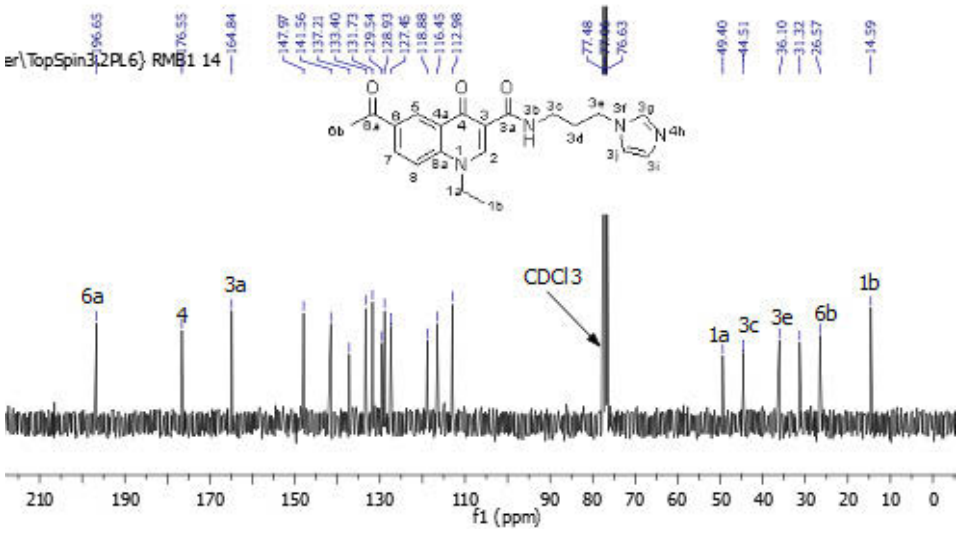
166.65
176.55
164.84
147.97
141.56
137.21
133.40
131.73
129.54
128.93
127.46
118.88
116.45
112.98
77.48
77.06
76.63
49.40
44.51
36.10
31.32
26.57
14.59
6a
4
3a
CDCl3
1a
3c
3e
6b
1b
f1 (ppm)

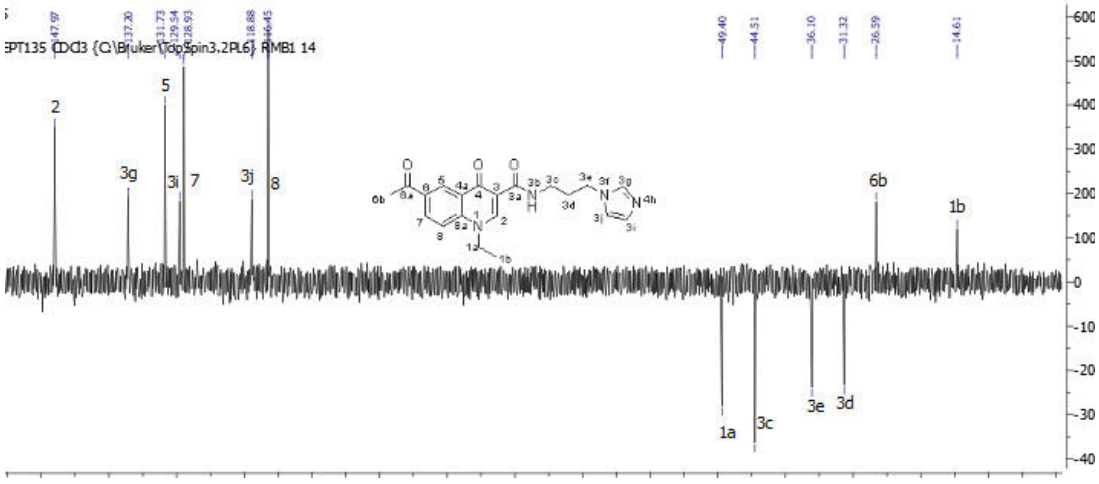
147.97
137.20
131.73
129.54
128.93
118.88
116.45
49.40
44.51
36.10
31.32
26.59
14.61
2
3g
5
3i
7
3j
8
6b
1b
1a
3c
3e
3d

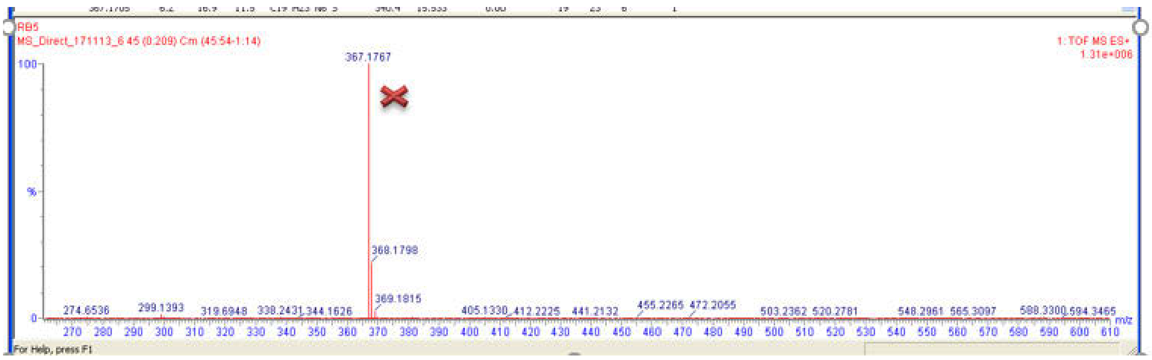
RB5
MS_Direct_171113_6 45 (0.209) Cm (45:54-1:14)
1: TOF MS ES+
1.31e+006
367.1767
368.1798
369.1815
m/z

Compound 4e

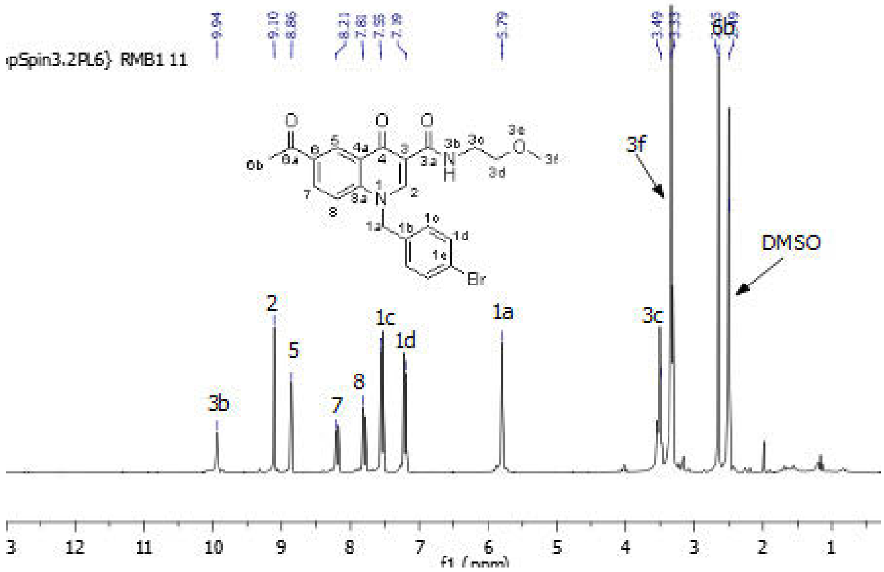
RMB1 11
3f
DMSO
6b
2
5
3b
7
8
1c
1d
1a
3c
f1 (ppm)

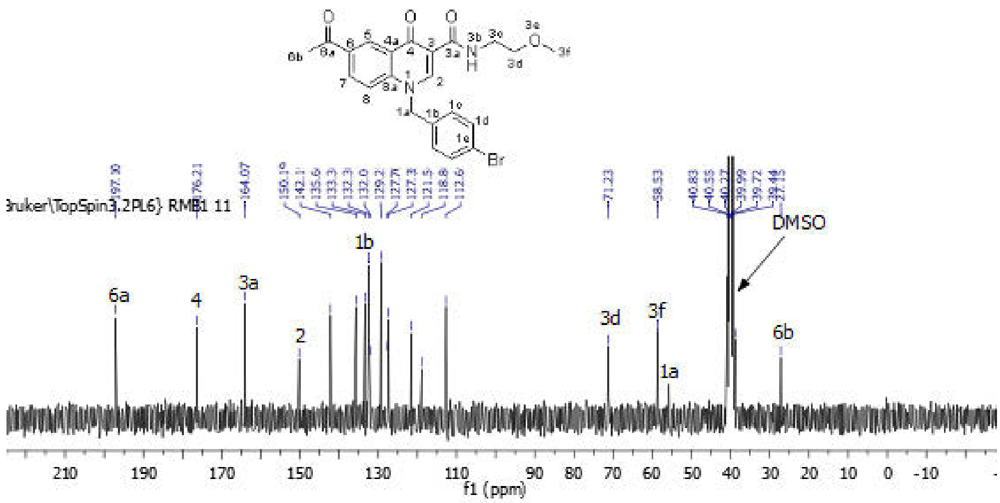
RMB1 11
DMSO
6a
4
3a
2
1b
3d
3f
1a
6b
f1 (ppm)

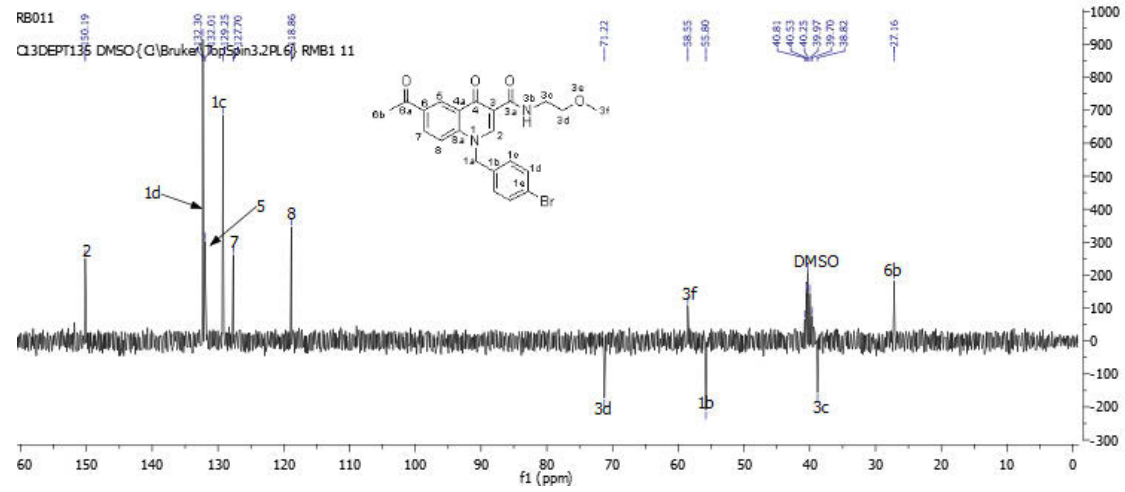
RB011
C13DEPT135 DMSO {C:\Bruker\TopSpin3.2PL6} RMB1 11
1c
1d
5
8
7
2
3f
DMSO
6b
3d
1b
3c
f1 (ppm)

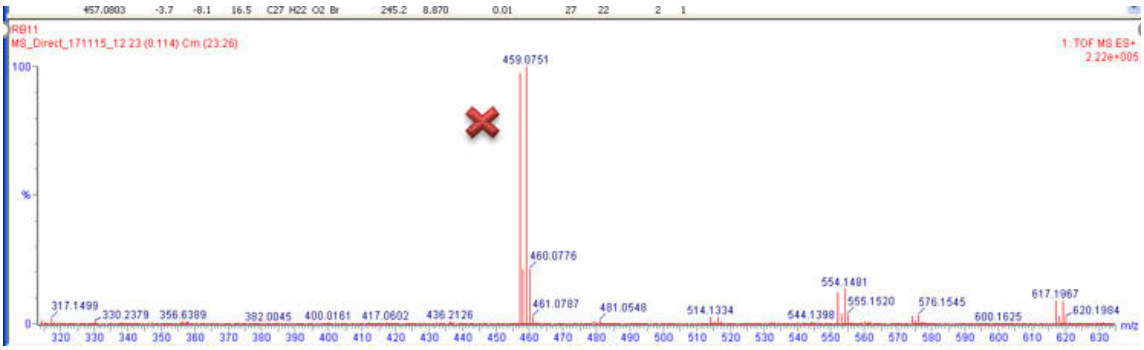
RB11
MS_Direct_171115_12 23 (0.114) Cm (23:26)
1: TOF MS ES+
459.0751
460.0776
461.0787
317.1499
330.2379
356.6389
382.0045
400.0161
417.0602
436.2126
481.0548
514.1334
544.1398
554.1481
555.1520
576.1545
600.1625
617.1967
620.1984
m/z

Compound 4f

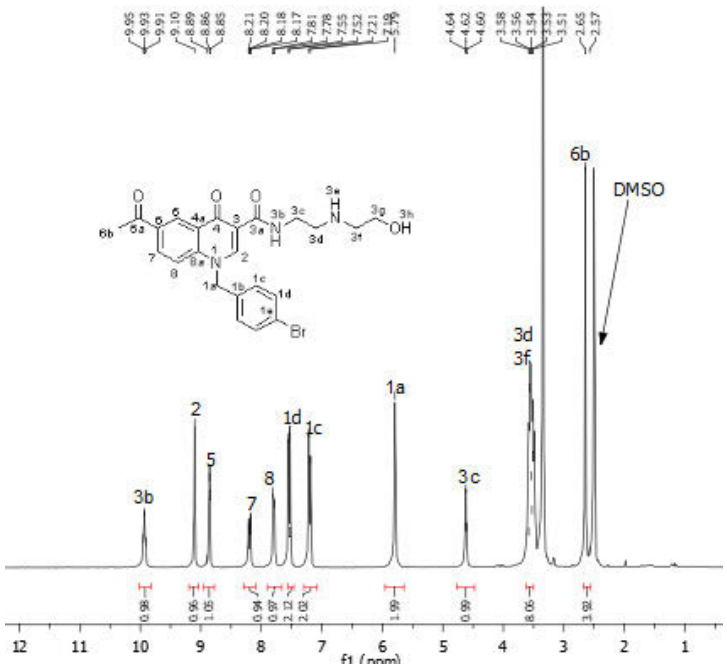
6b
DMSO
3d
3f
1a
2
1d
1c
5
8
7
3b
3c
f1 (ppm)

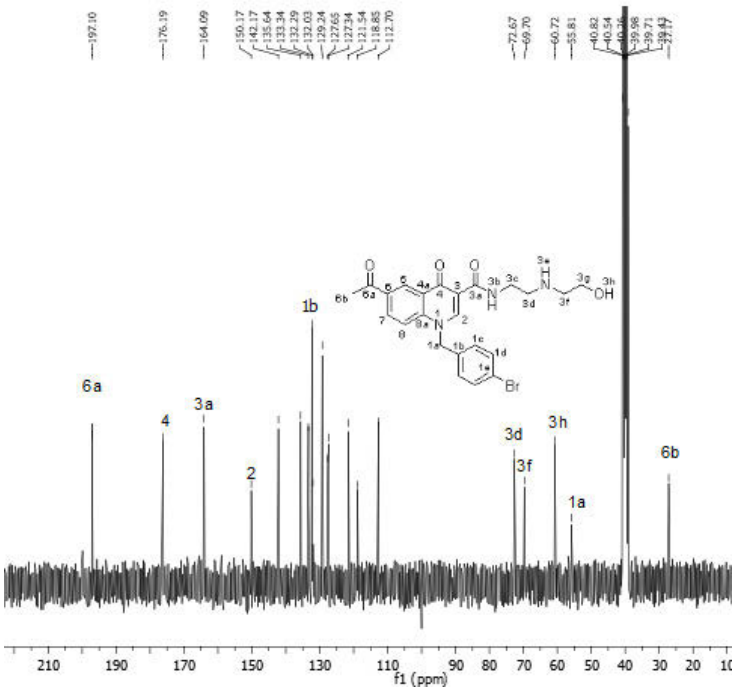
197.10
176.19
164.09
150.17
142.17
135.64
133.34
132.29
132.03
129.24
127.65
127.34
121.54
118.85
112.70
71.67
69.70
60.72
55.81
40.82
40.54
40.26
39.98
39.71
39.43
27.17
1b
6a
4
3a
2
3d
3f
3h
1a
6b
210 190 170 150 130 110 90 80 70 60 50 40 30 20 10
f1 (ppm)

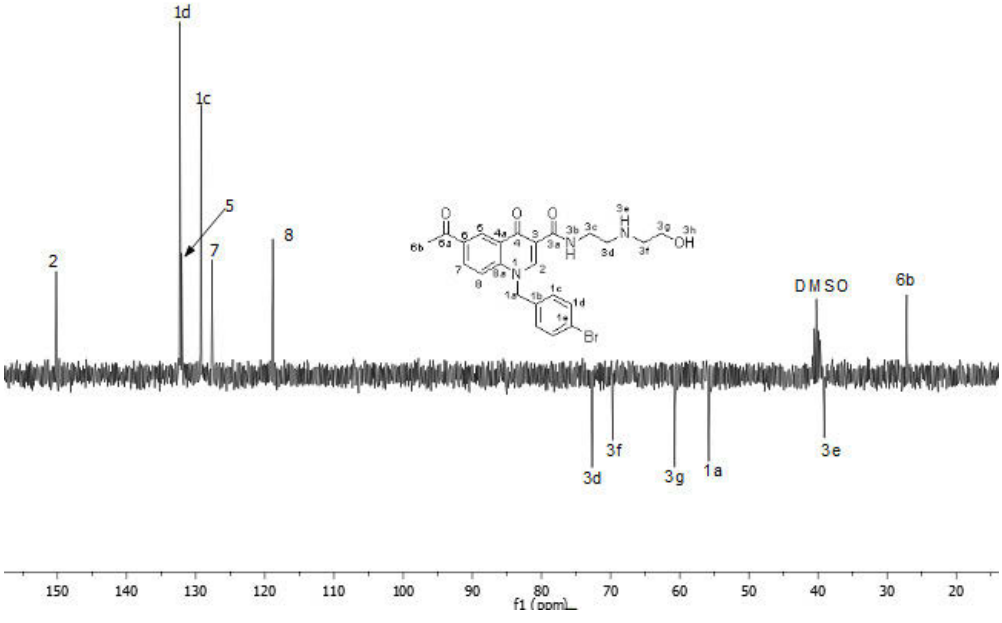
1d
1c
5
7
8
2
DMSO
6b
3d
3f
3g
1a
3e
150 140 130 120 110 100 90 80 70 60 50 40 30 20
f1 (ppm)

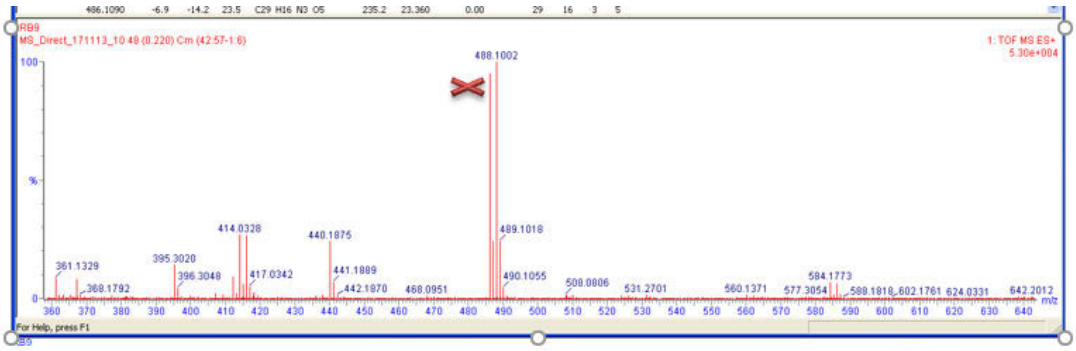
RB9
MS_Direct_171113_10 48 (0.220) Cm (42:57-1:6)
1: TOF MS ES+
5.30e+004
488.1002
489.1018
490.1055
414.0328
440.1875
441.1889
361.1329
395.3020
396.3048
417.0342
442.1870
368.1792
468.0951
508.0806
531.2701
560.1371
577.3054
584.1773
588.1818
602.1761
624.0331
642.2012
m/z
For Help, press F1

Compound 4g, HIT Compound

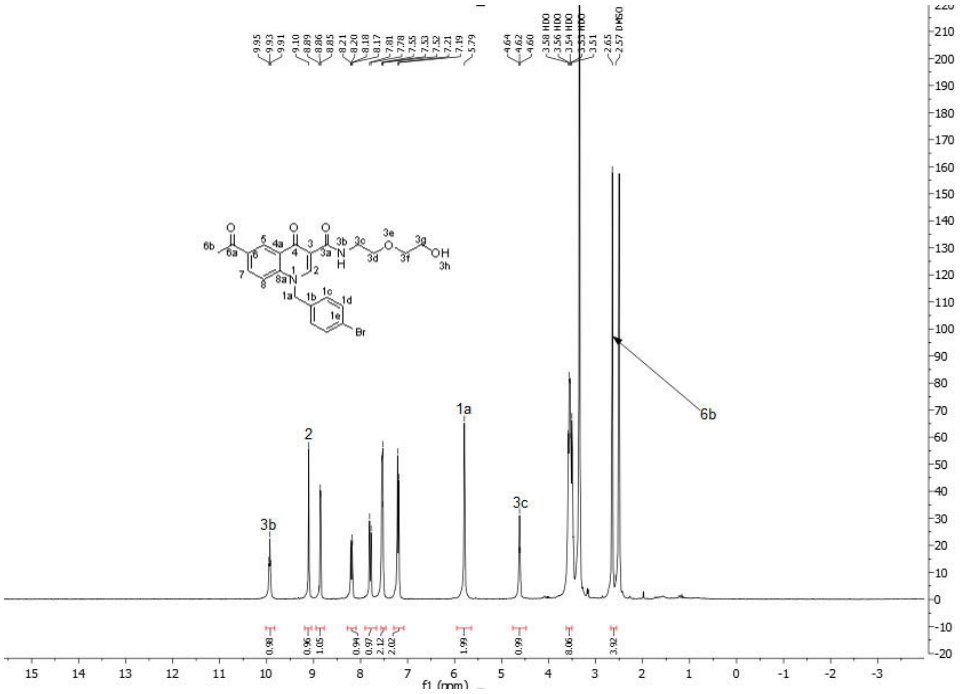

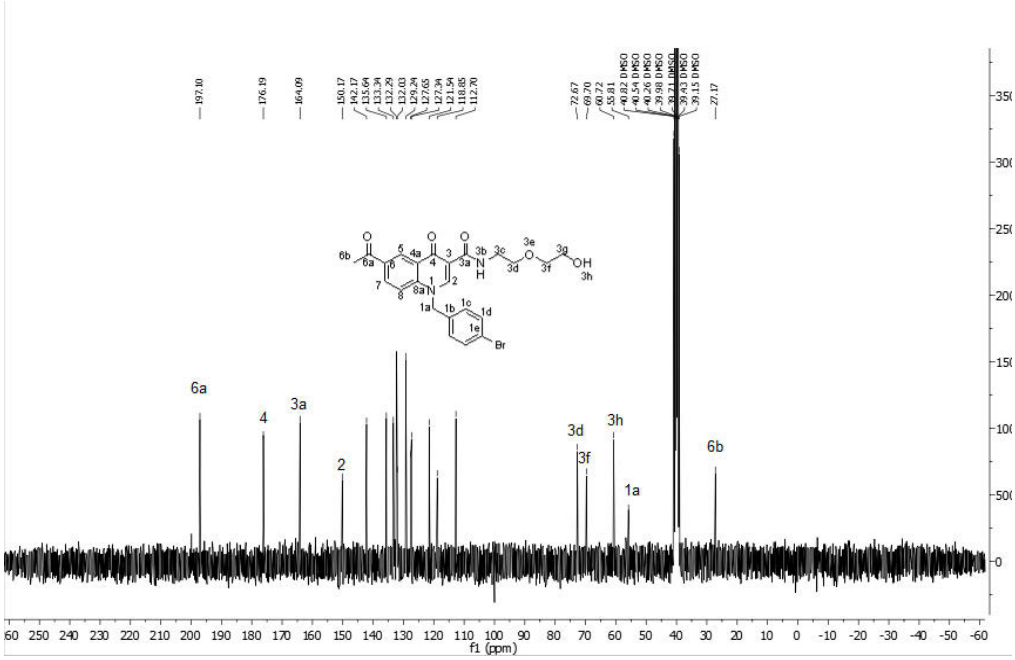

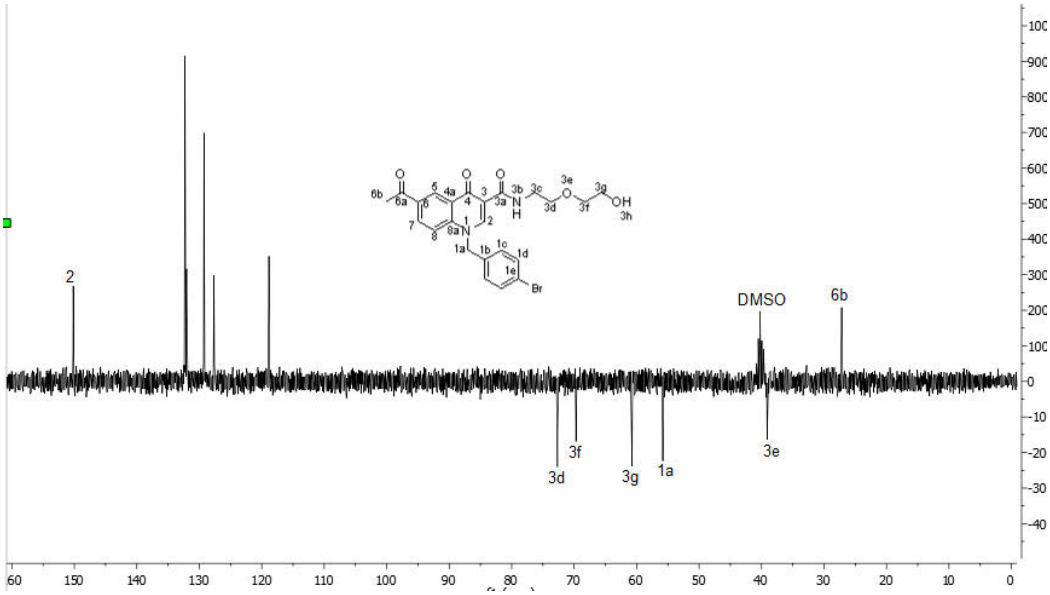
2
DMSO
6b
3d
3f
3g
1a
3e

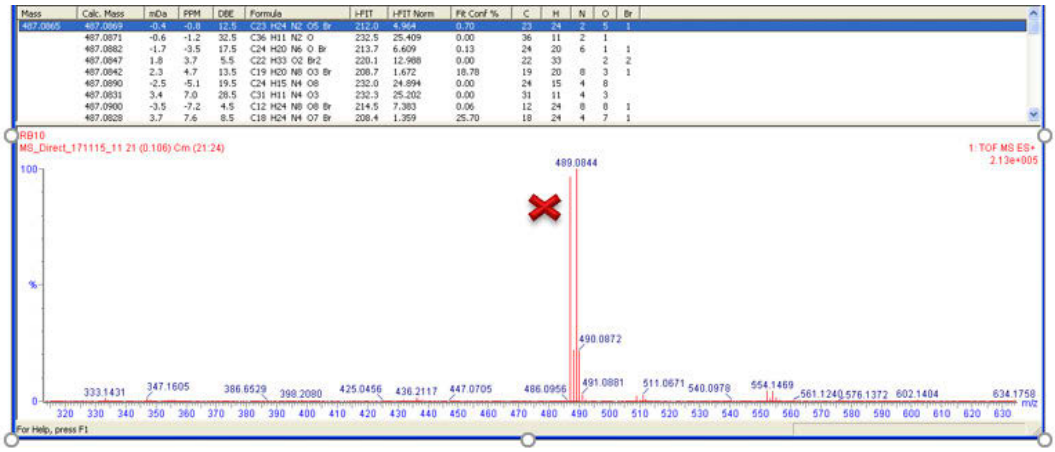
RB10
MS_Direct_171115_11 21 (0.186) Cm (21:24)
1: TOF MS ES+
489.0844
490.0872
491.0881
For Help, press F1

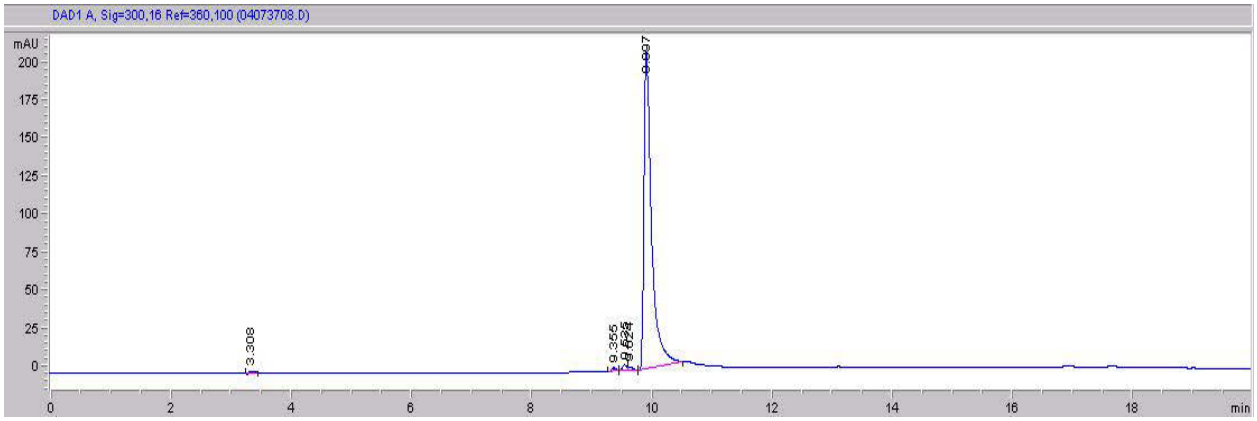
DAD1 A, Sig=300,16 Ref=360,100 (04073708.D)
mAU
3.308
9.355
9.997
min

Compound 4h

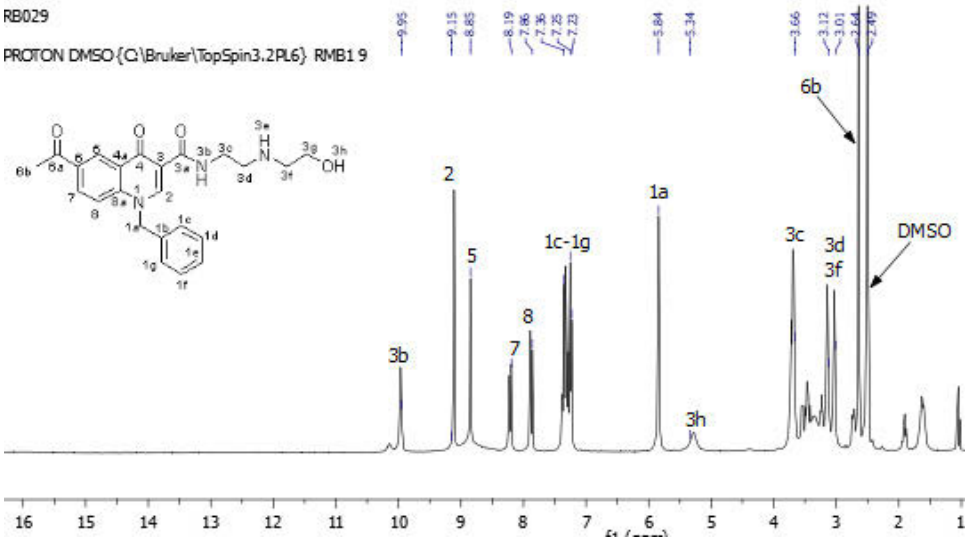
RB029
PROTON DMSO {C:\Bruker\TopSpin3.2PL6} RMB1 9
6b
2
5
1a
1c-1g
8
7
3b
3h
3c
3d
3f
DMSO

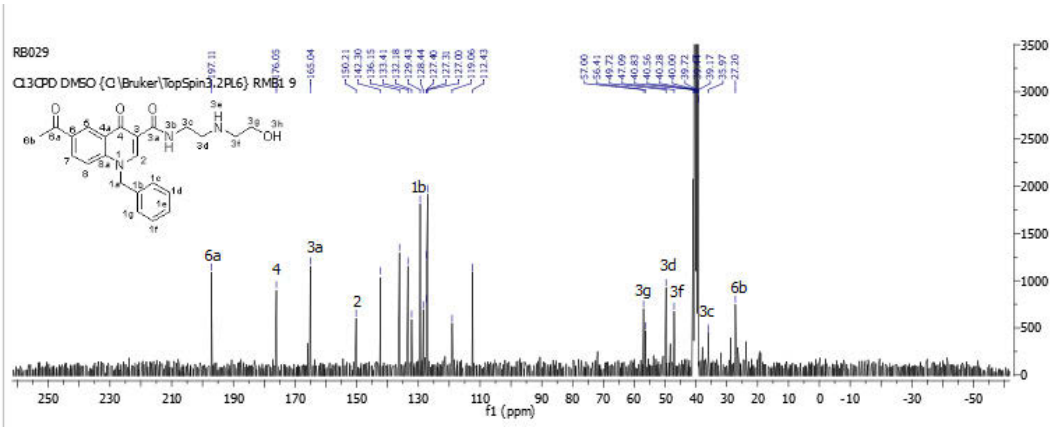
RB029
C13CPD DMSO {C:\Bruker\TopSpin3.2PL6} RMB1 9
1b
6a
4
3a
2
3g
3d
3f
3c
6b
f1 (ppm)

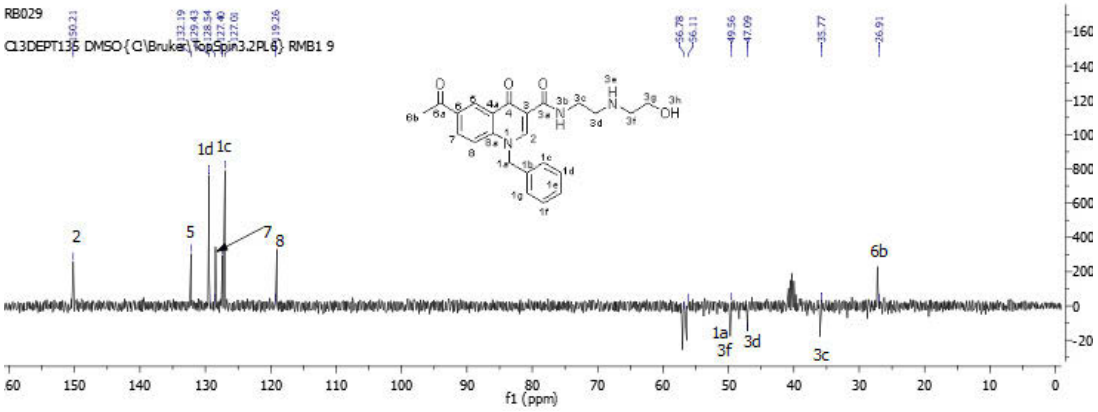
RB029
C13DEPT135 DMSO {C:\Bruker\TopSpin3.2PL6} RMB1 9
1d
1c
2
5
7
8
6b
1a
3f
3d
3c
f1 (ppm)

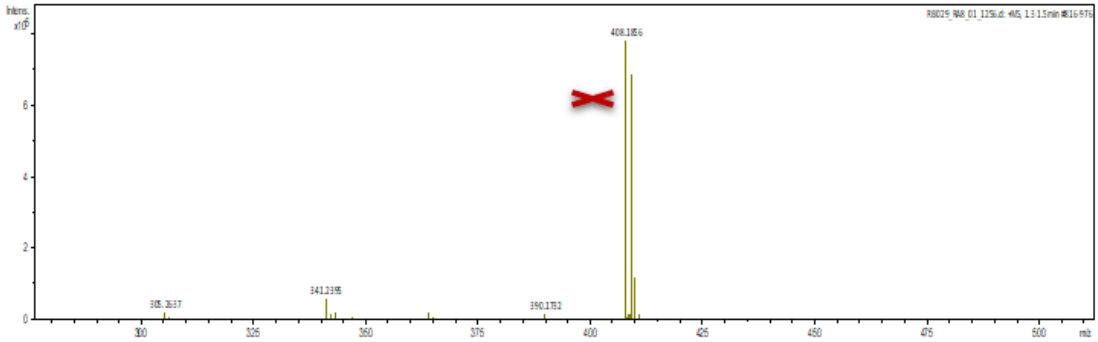

Compound 4i

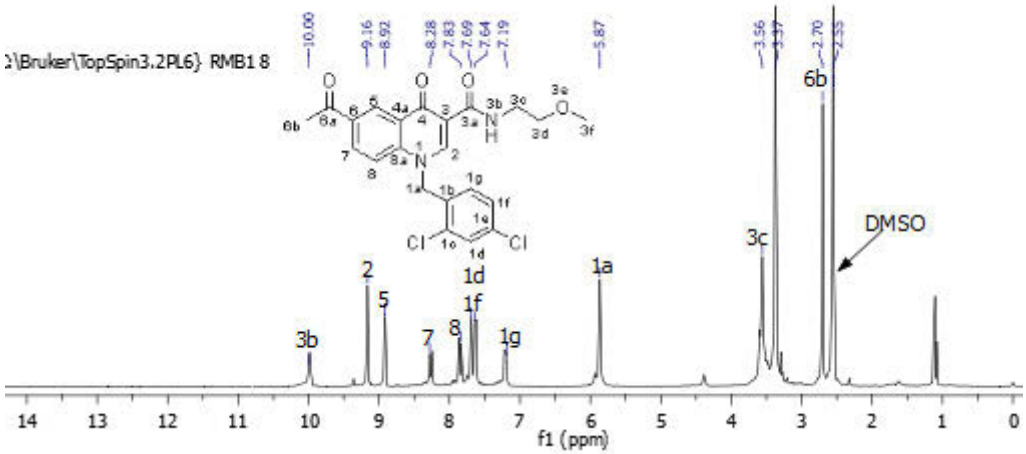
10.00
9.16
8.92
8.28
7.83
7.69
7.64
7.19
5.87
3.56
3.37
2.70
2.55
6b
DMSO
3c
1a
2
5
1d
1f
3b
7
8
1g
f1 (ppm)

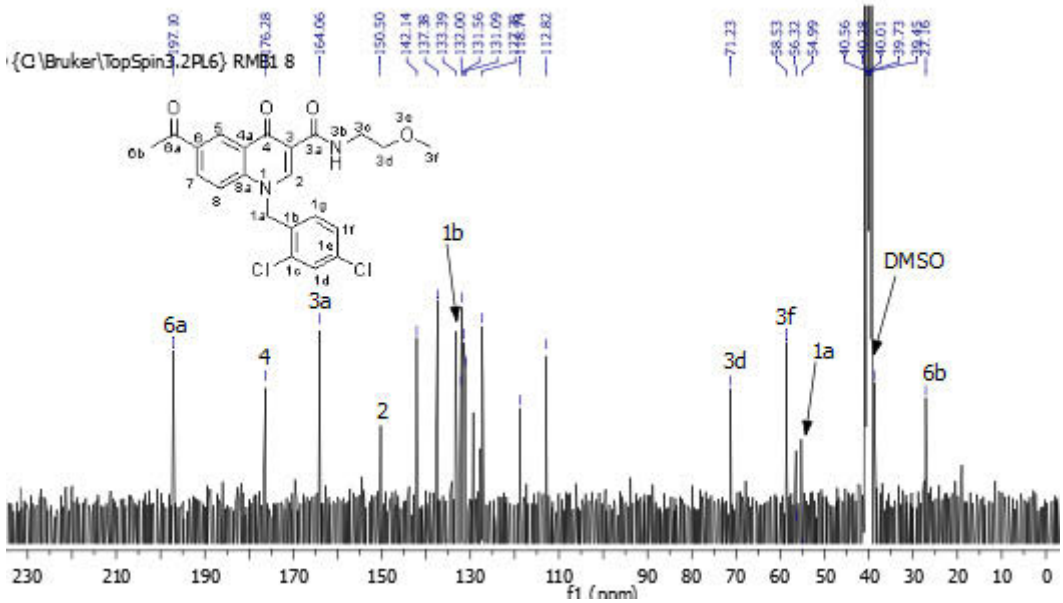
164.06
150.50
142.14
137.38
133.39
132.00
131.56
131.09
112.82
71.23
58.53
56.32
54.99
40.56
40.01
39.73
1b
DMSO
6a
4
3a
3f
3d
1a
6b
2
f1 (ppm)

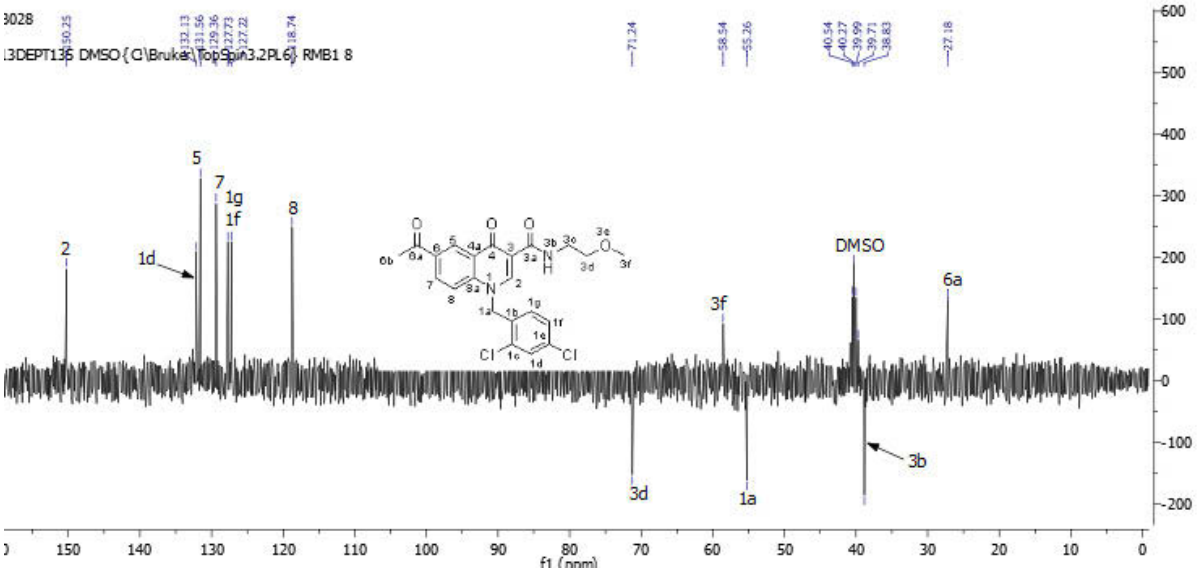
3028
13DEPT135 DMSO (C:\Bruker\TopSpin3.2PL6) RMB1 8
150.25
132.13
131.56
129.36
127.73
127.22
118.74
71.24
58.54
55.26
40.54
40.27
39.99
39.71
38.83
27.18
5
7
1g
1f
8
2
1d
3f
DMSO
6a
3d
1a
3b
f1 (ppm)

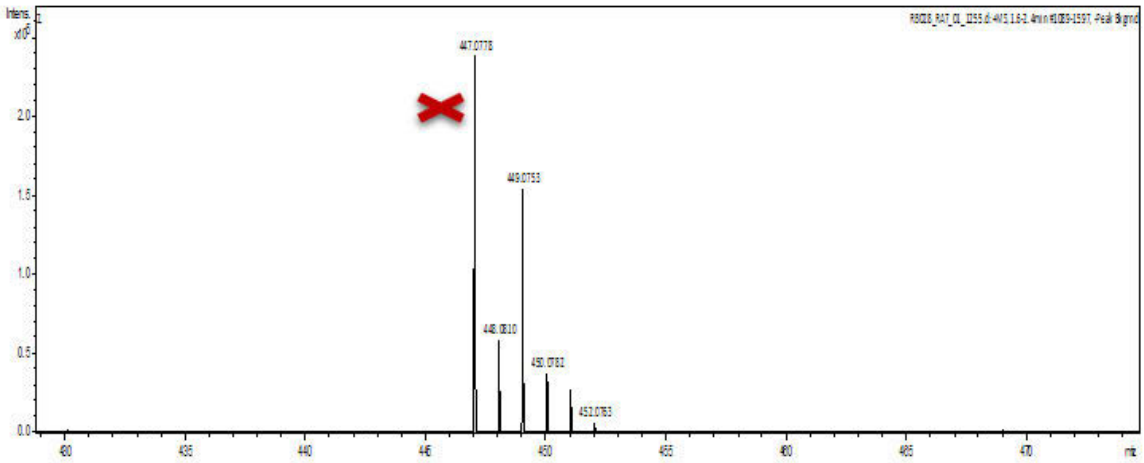
Intens.
x10^5
447.0778
449.0753
448.0810
450.0782
451.0763
m/z

Compound 4J

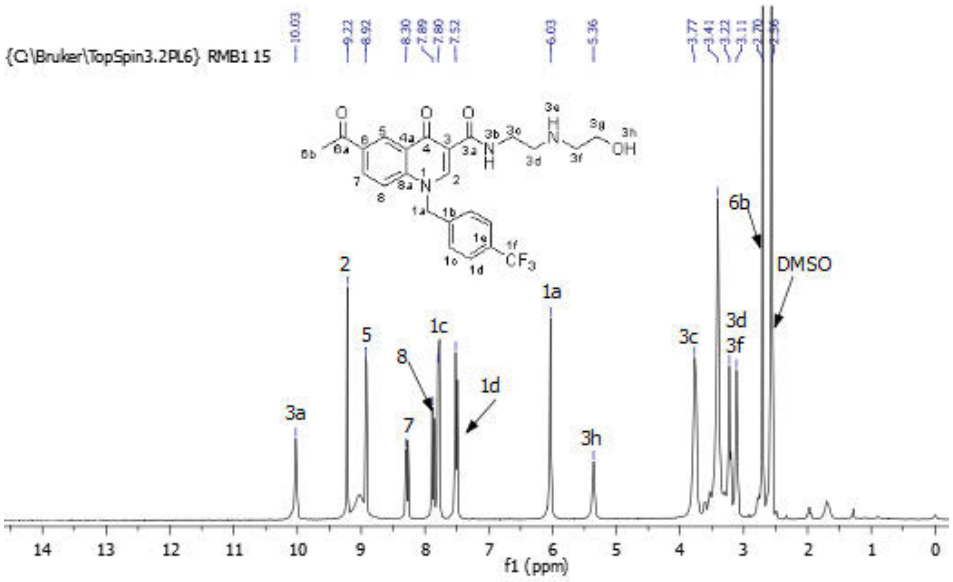
{C:\Bruker\TopSpin3.2PL6} RMB1 15
10.03
9.23
8.92
8.30
7.89
7.80
7.52
6.03
5.36
3.77
3.41
3.22
3.11
2.70
2.56
2
5
8
7
3a
1c
1d
1a
3h
3c
6b
3d
3f
DMSO
f1 (ppm)

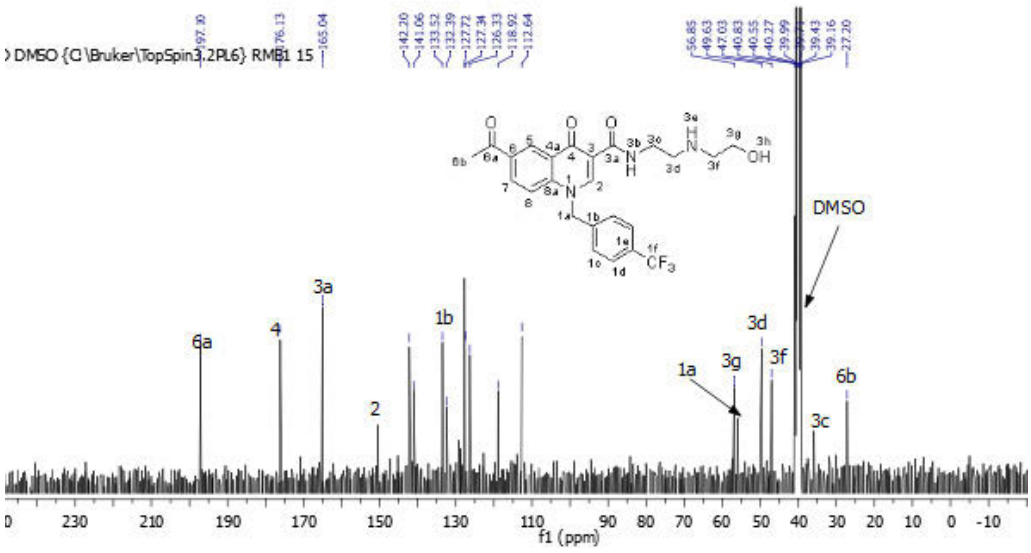
DMSO {C:\Bruker\TopSpin3.2PL6} RMB1 15
6a
4
3a
2
1b
1a
3g
3d
3f
6b
3c
DMSO
f1 (ppm)

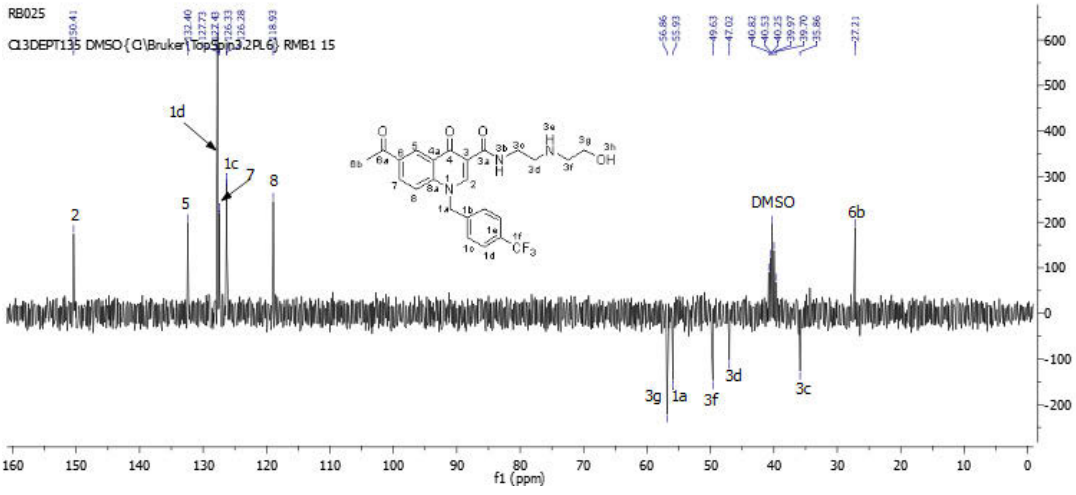
RB025
C13DEPT135 DMSO {C:\Bruker\TopSpin3.2PL6} RMB1 15
1d
1c
7
8
5
2
DMSO
6b
3g
1a
3f
3d
3c
f1 (ppm)

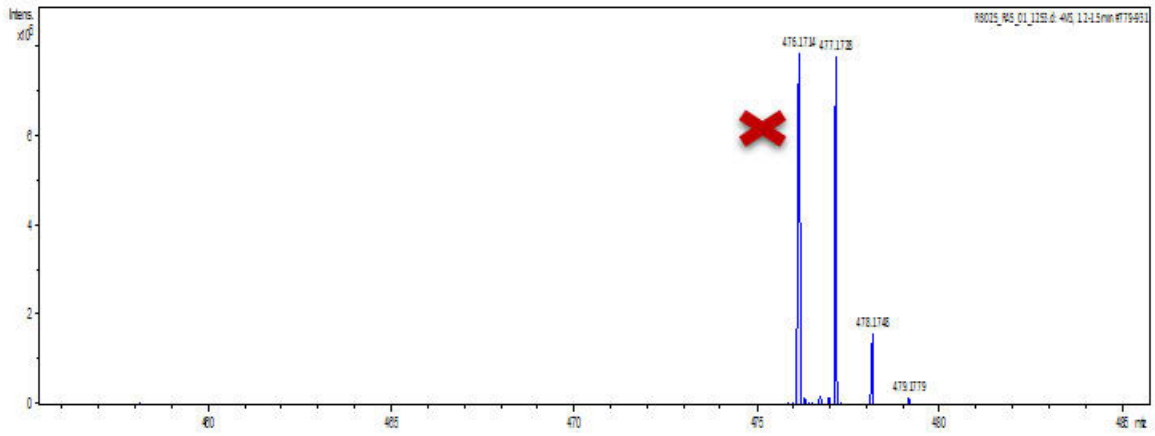

BIOLOGICAL DATA

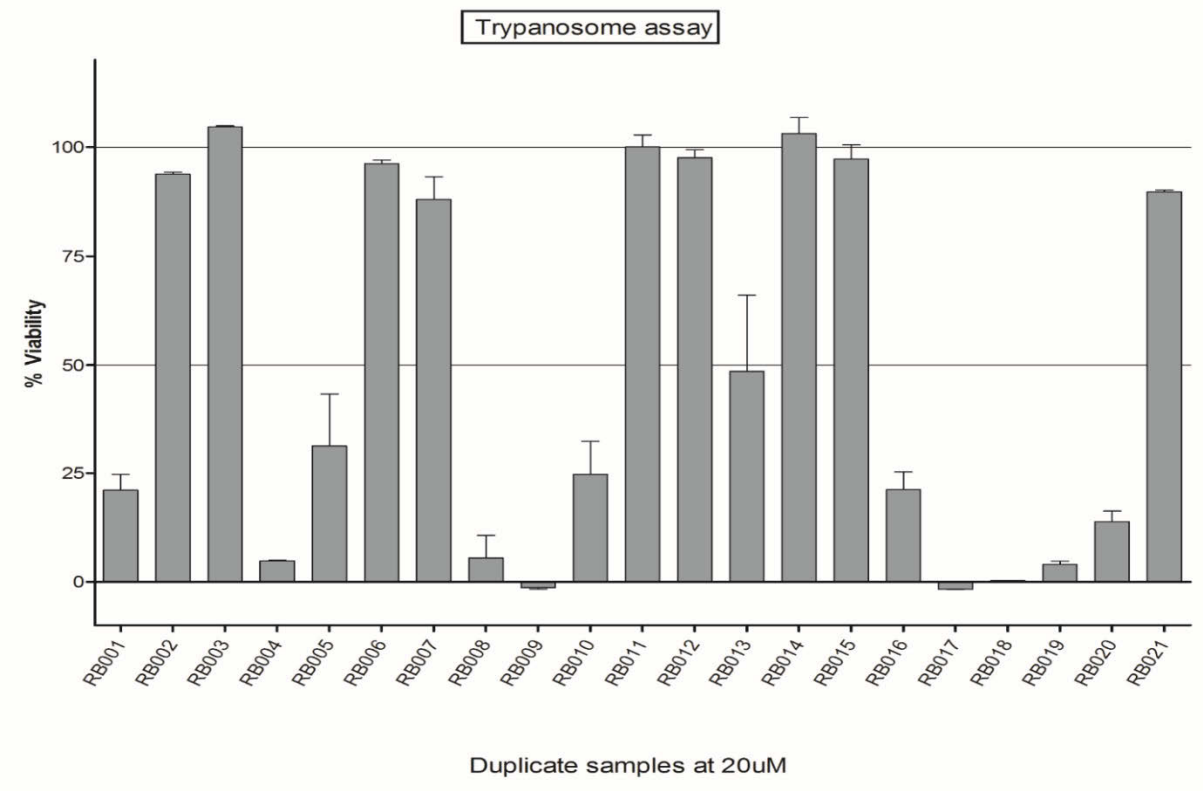

Figure S11a: Compounds inhibitory potential against *T.b. brucei* parasites at 20µM.

Compounds were added to *in vitro* cultures of *T.b. brucei* in 96-well plates at a fixed concentration of 20 µM. After an incubation period of 48 hours, the numbers of parasites surviving drug exposure were determined by adding resazurin. Reduction of resazurin to resorufin by living cells was quantified in a multiwell fluorescence plate reader (Exc_{560}/Em_{590}). The results are expressed as parasite % viability relative to untreated controls.

Compounds were tested in duplicate wells, and a standard deviation (SD) calculated. Only compounds exhibiting less than 20% parasite viability were considered for IC_{50} determination.

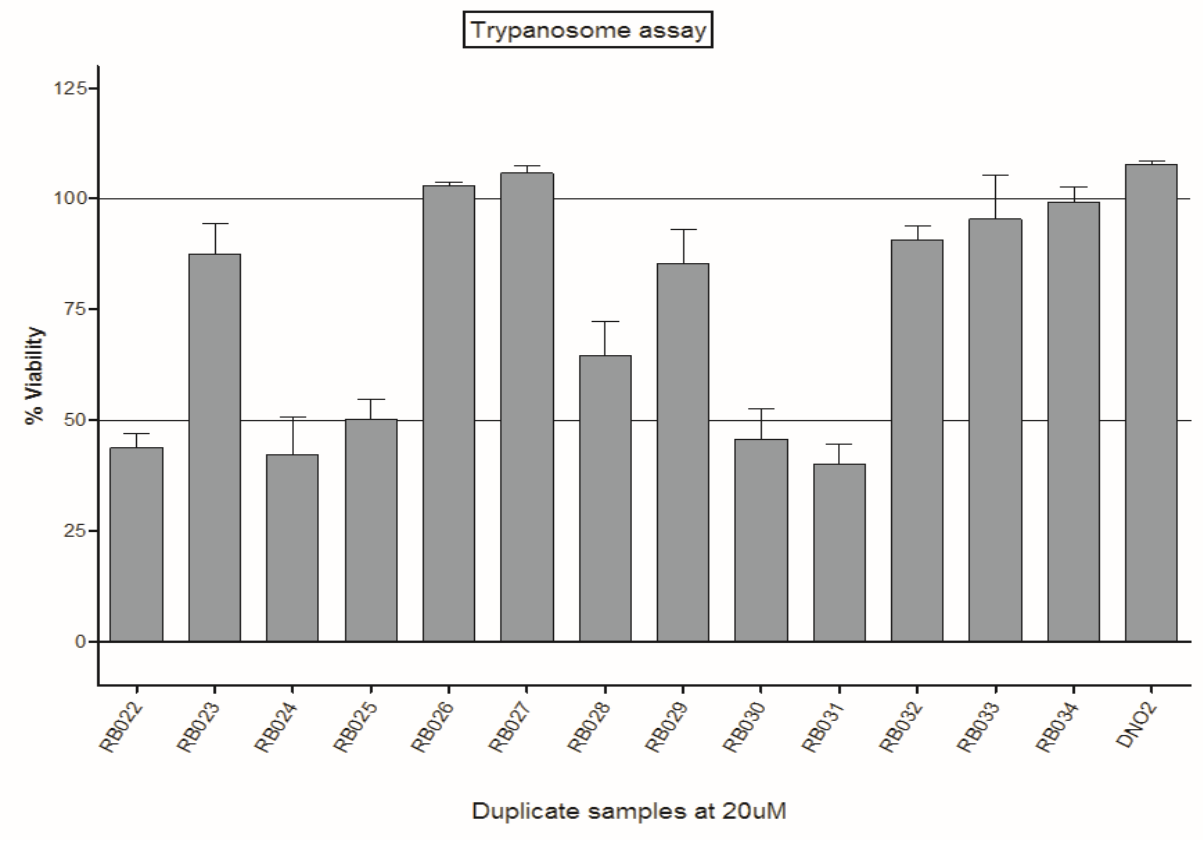

Figure S11b: Compounds inhibitory potential against *T.b. brucei* parasites at 20µM.

Compounds were added to *in vitro* cultures of *T.b. brucei* in 96-well plates at a fixed concentration of 20 µM. After an incubation period of 48 hours, the numbers of parasites surviving drug exposure were determined by adding resazurin. Reduction of resazurin to resorufin by living cells was quantified in a multiwell fluorescence plate reader (Exc_{560}/Em_{590}). The results are expressed as parasite % viability relative to untreated controls. Compounds were tested in duplicate wells, and a standard deviation (SD) calculated. Only compounds exhibiting less than 20% parasite viability were considered for IC_{50} determination.

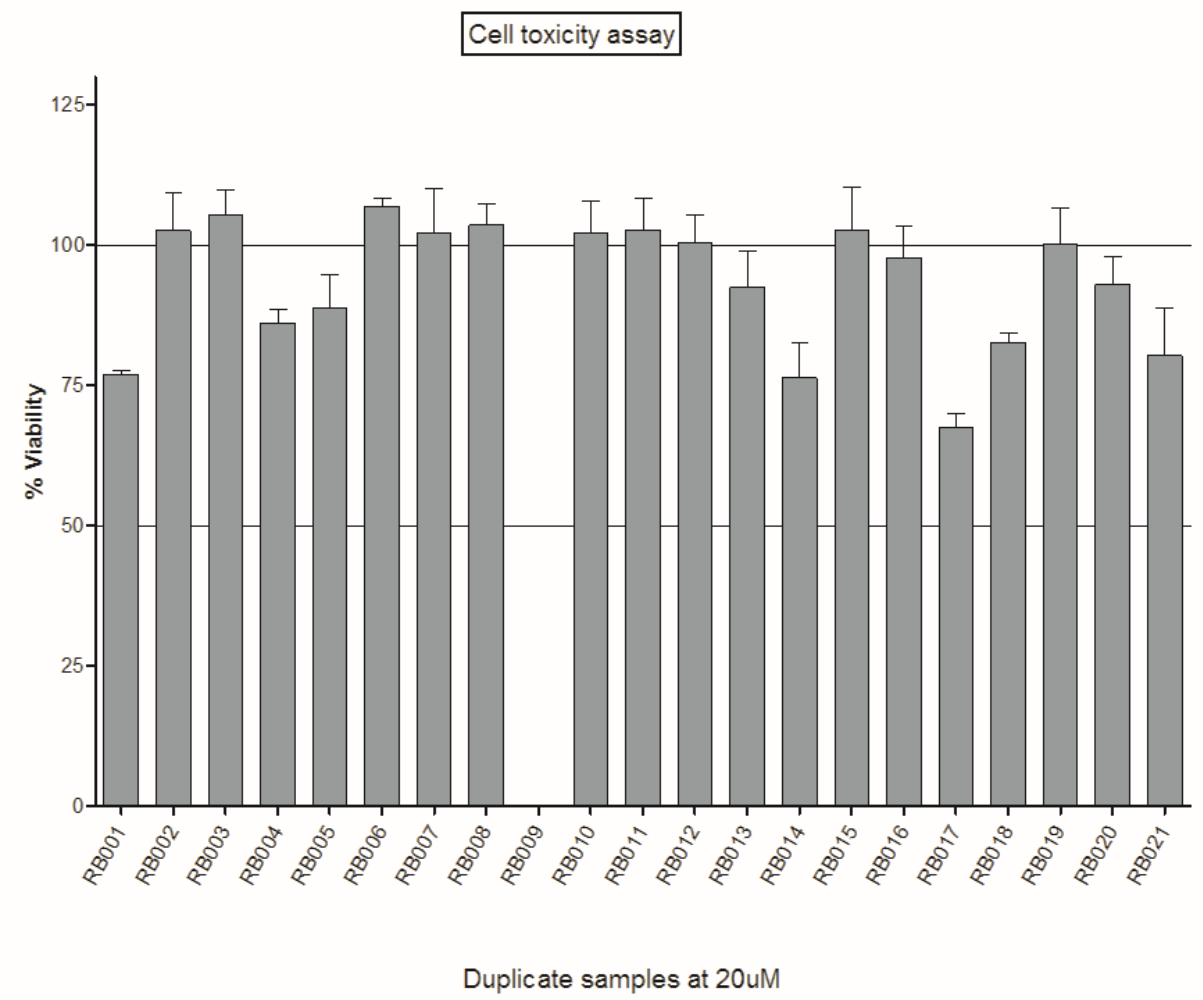

Figure SI2a: Compound cytotoxicity against HeLa cells at 20µM.

Compounds were added to *in vitro* cultures of HeLa (human cervix adenocarcinoma) cells in 96-well plates at a fixed concentration of 20 µM. After an incubation period of 48 hours, the numbers of cells surviving drug exposure are determined by adding resazurin, which was reduced to resorufin by living cells. Resorufin was quantified in a multiwell fluorescence plate reader (Exc_{560}/Em_{590}). The results are express as cell % viability. Compounds were tested in duplicate wells, and a standard deviation (SD) calculated. With the exception of compound **RB009**, this series shows no extensive cytotoxicity against HeLa cells.

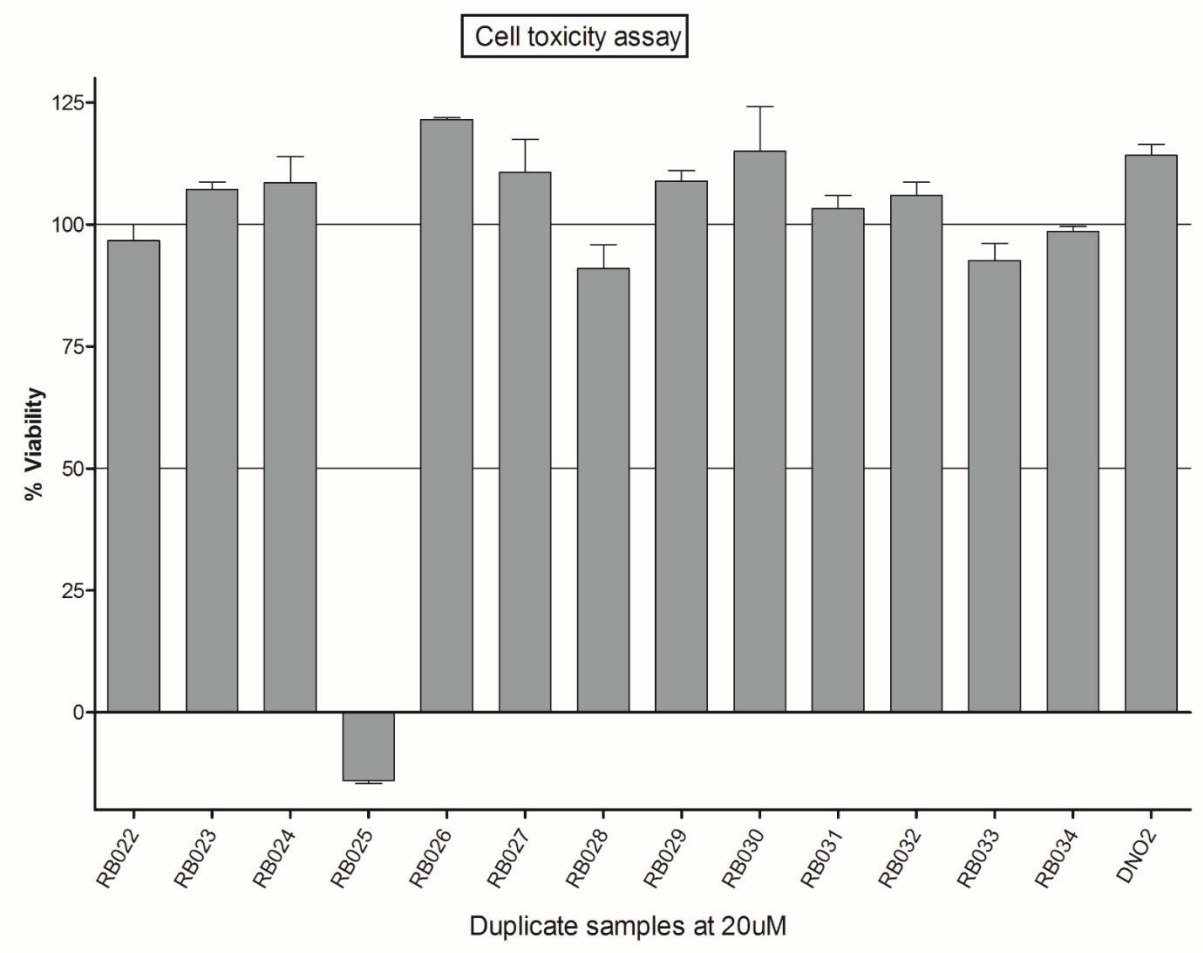

Figure SI2b: Compound cytotoxicity against HeLa cells at 20µM.

Compounds were added to *in vitro* cultures of HeLa (human cervix adenocarcinoma) cells in 96-well plates at a fixed concentration of 20 µM. After an incubation period of 48 hours, the numbers of cells surviving drug exposure are determined by adding resazurin which was reduced to resorufin by living cells. Resorufin is was quantified in a multiwell fluorescence plate reader (Exc_{560}/Em_{590}). The results are express as cell % viability. Compounds were tested in duplicate wells, and a standard deviation (SD) calculated. With the exception of compound **RB025**, this series shows no cytotoxicity against HeLa cells.